

Universidade de Lisboa  
Faculdade de Medicina de Lisboa



# **Intracerebroventricular injection of amyloid $\beta_{1-42}$ peptide in rat behaviour and adult hippocampal neurogenesis**

Sara Raquel Landeira Nabais do Paulo

**Orientador** | Professora Sara Alves Xapelli  
**Co-orientador** | Professora Susana Zeferino Solá da Cruz

Dissertação especialmente elaborada para obtenção do grau de Mestre em Neurociências

2018



Universidade de Lisboa  
Faculdade de Medicina de Lisboa



# **Intracerebroventricular injection of amyloid $\beta_{1-42}$ peptide in rat behaviour and adult hippocampal neurogenesis**

Sara Raquel Landeira Nabais do Paulo

**Orientador** | Professora Sara Alves Xapelli  
**Co-orientador** | Professora Susana Zeferino Solá da Cruz

Dissertação especialmente elaborada para obtenção do grau de Mestre em Neurociências

2018



**A impressão desta dissertação foi aprovada pelo Conselho Científico da Faculdade de  
Medicina de Lisboa em reunião de 19 de junho de 2018**



## Agradecimentos

Em primeiro lugar, gostaria de agradecer à Professora Ana Sebastião pela excelente oportunidade que me concedeu em integrar o seu grupo para realizar a dissertação de mestrado.

À Professora Susana Solá, pela co-orientação, e pela disponibilidade e entusiasmo demonstrados para discutir as ideias e resultados deste projeto.

Um especial e enorme obrigada à minha orientadora, a Professora Sara Xapelli. Por todo o conhecimento que me passou e passa diariamente, científico e não só, pela disponibilidade, paciência e compreensão, por manter sempre uma atitude positiva mesmo nos momentos mais difíceis e por estar sempre lá para me ajudar a melhorar. Por me introduzir ao mundo das neurociências e me fazer querer continuar a seguir este caminho. Pela amizade, por me ter incluído, e me ter feito sentir incluída, num grupo de pessoas maravilhosas que tanto contribuíram para este trabalho e por ser um modelo a seguir, profissional e pessoalmente.

Aos meus colegas e amigos do *Xapelli's Niche* (mesmo às recentes aquisições). Agradeço especialmente ao Rui Rodrigues e à Filipa Ribeiro, por tudo o que me ensinaram e por toda a ajuda com o meu projeto. Rui, obrigada pelo constante entusiasmo, por todas as gargalhadas e boas sortes para a vida, acredita que foram imprescindíveis (ah, e por tantos elogios aos meus chocolates). À Joana Mateus, por toda a ajuda com este trabalho, pela partilha mútua de ideias e desvanios e por todos os momentos *foodie*: já não se fazem *minions* assim. Obrigada a todos pela amizade, dentro e fora do laboratório, por me surpreenderem sempre pela positiva, por me aturarem e compreenderem o meu sentido de humor e o meu ligeiro OCD... Não podia ter pedido melhor, vocês são espetaculares.

À Professora Maria José Diógenes e aos seus alunos, pelo contributo para a parte molecular desta tese. Em especial ao João Gomes, por me ter ensinado e ajudado com os *western blot*, à Sara Tanqueiro e à Rita Belo pela crucial ajuda com as culturas primárias de neurónios. Obrigada aos três pelas ideias e disponibilidade prestada sempre que precisei.

Aos elementos do laboratório da Doutora Luísa Lopes, em especial à Joana Coelho, pela ajuda e pela importante discussão de ideias relacionadas com as experiências de comportamento.

Ao Daniel Costa e à Iolanda Moreira, do biotério, por toda a ajuda e disponibilidade prestadas com o alojamento dos animais, as injeções intraperitoneais, cirurgias e cuidados pós-cirúrgicos.

A todos os elementos do laboratório ASebastião, agradeço o ótimo ambiente e boa disposição proporcionados diariamente e em equipa. Gostaria de agradecer particularmente à Leonor Rodrigues, pelo tempo despendido para me ensinar a análise por ELISA, e ao Francisco Mouro, pela preciosa ajuda com os testes de comportamento. À Joana Freire (*foodie* nº1) e à Leonor, um especial obrigada por serem bem mais do que colegas de trabalho desde o início deste percurso, mas também pela amizade, pelas alegrias e frustrações partilhadas, pela compreensão e pela excelente companhia.

À Liana Shvachiy, primeiro por me ensinar a maior parte dos testes de comportamento, mas mais ainda, por ser muito mais do que uma colega de trabalho ou de casa. Por ser a melhor companheira de viagens, passeios e aventuras. Pela paciência para me aturar todos os dias, pela compreensão, pelos conselhos, partilha de ideias e honestidade. E, como não podia deixar de ser, a ti e à tua mãe, pelas frutas e vegetais biológicos semanais! És sem dúvida uma das pessoas mais espetaculares que conheci até hoje, e com quem tive o gosto de criar ligações de amizade que tenho a certeza que nunca serão dissolvidas. Obrigada por tudo.

Aos meus amigos de Aveiro, em especial à *Mufi* por ser como uma irmã desde que me lembro, e por, apesar de estar longe, manter sempre uma preocupação e uma palavra amiga. Por ser um motivo de orgulho e um exemplo a seguir, do quão importante é ultrapassarmos aquilo que pensamos ser os nossos limites. Ao Tiago Vasconcelos, por ser também como um irmão, por me fazer rir sempre que pode, por partilhar o meu vício por sushi, pelo enorme apoio e por nunca se esquecer de mim (ah, e não esquecendo as sessões gratuitas de fisioterapia). Ao Filipe Pereira (viciado em sushi nº2), pelas conversas filosóficas até de madrugada, por me ouvir e aconselhar. A todos, por serem um dos meus pontos de equilíbrio.

Por último, quero agradecer à minha família, em particular aos meus pais, à minha irmã, à minha tia Bina e aos meus primos, mas também à *minha avó* Olga, porque sem ela nunca me teria tornado na pessoa que sou hoje. À minha querida mãe, um infinito obrigada pelas longas conversas diárias, pela compreensão, pela paciência e apoio incondicionais. No fundo, à minha mãe, ao meu pai e à minha irmã, por serem quem são, com todos os defeitos, feitos e qualidades: não arranjo palavras suficientes para descrever o quão importantes vocês são para mim. À minha maravilhosa tia Bina, também pelas extensas conversas, pela motivação e por acreditar sempre em mim. A todos, sem exceção, por nunca julgarem, por me lembrarem daquilo que realmente importa sempre que estamos juntos e do quão sortuda eu sou por fazer parte desta família. Sem vocês, nada disto seria possível. Um sincero obrigada.



“Success is not final, failure is not fatal. It is the courage to continue that counts.”

Winston Churchill



## Resumo

A forma esporádica da doença de Alzheimer (DA) é atualmente a causa mais comum de demência a nível mundial, estando particularmente associada ao envelhecimento da população. Esta caracteriza-se por um declínio cognitivo progressivo, acompanhado por atrofia cerebral generalizada. Uma vez que o hipocampo é uma das primeiras estruturas a ser afetadas, notáveis défices de memória podem ser observados nas fases iniciais da doença, nomeadamente na memória episódica de longo prazo, agravando-se progressivamente até uma completa dependência dos respetivos cuidadores. Estas alterações estão normalmente associadas a uma acumulação gradual excessiva de depósitos de péptido  $\beta$  amiloide ( $A\beta$ ) no cérebro dos doentes, bem como à deposição de proteína tau hiperfosforilada.

Mais recentemente, a acumulação de oligómeros solúveis de  $A\beta$  em fases pré-clínicas da doença algumas décadas antes das primeiras manifestações sintomáticas, tem sido apontada como fator iniciador da cascata de eventos subjacente à patofisiologia da DA. Apesar da sua crescente incidência, as alternativas para o tratamento da DA são ainda bastante limitadas, e apenas permitem minimizar alguns dos sintomas a curto prazo. Desta forma, uma melhor compreensão dos mecanismos patofisiológicos será essencial para explorar terapêuticas inovadoras e mais eficientes.

A neurogénese pós-natal na zona subgranular (ZSG) do giro dentado (GD) do hipocampo ocorre através de um processo sequencial relativamente conservado entre mamíferos, no qual novos neurónios funcionais são originados a partir de células estaminais/progenitoras neurais (CSPNs) indiferenciadas e com capacidade de autorrenovação. Este processo parece contribuir significativamente para funções dependentes do hipocampo, como plasticidade sináptica e funções cognitivas, particularmente aprendizagem e memória, pelo que tem sido sugerido como um potencial alvo terapêutico da DA. No entanto, estudos *in vivo* e *in vitro*, referentes à forma como a neurogénese poderá ser modulada nesta patologia apresentam resultados altamente controversos, provenientes na sua maioria do uso de modelos da forma familiar da doença. Assim, a maioria dos estudos indica uma diminuição da proliferação e diferenciação, embora um aumento também seja mencionado por alguns autores e, mais raramente, ausência de alterações. Desta forma, o principal objetivo do presente projeto consistiu em caracterizar a neurogénese pós-natal no hipocampo, utilizando um modelo animal que pretende mimetizar as fases iniciais da forma esporádica da DA.

Para o estudo da proliferação e diferenciação celular, ratos Wistar jovens-adultos (9-10 semanas) foram injetados intraperitonealmente com 5-bromo-2'-desoxiuridina (BrdU) (100 mg/kg) durante 3 dias consecutivos, no início do protocolo. Seguidamente, com o objetivo de obter o modelo de doença proposto, realizaram-se cirurgias para a injeção intracerebroventricular (icv) unilateral de uma solução de péptido  $A\beta_{1-42}$  (2.25 mg/ml, 4  $\mu$ l), ou de uma solução veículo (4  $\mu$ l), no caso dos animais controlo. Duas semanas após esta injeção, foram efetuados testes comportamentais, durante a fase noturna e diurna do ciclo circadiano, incluindo o teste do campo aberto (do inglês,

*open-field*), para avaliação da atividade locomotora, e o teste de reconhecimento do novo objeto (*novel object recognition*), para avaliação da memória episódica de longo prazo. Outros paradigmas foram avaliados apenas durante o dia, nomeadamente comportamento do tipo ansioso, pelo labirinto elevado em cruz (*elevated plus maze*), memória de curto prazo, pelo labirinto em Y (*Y-maze*) de alternância espontânea ou alternância forçada, e aprendizagem e memória espaciais, pelo labirinto de Morris (*Morris water maze*). No final do protocolo, os animais foram sacrificados para uma posterior análise celular e molecular, maioritariamente focada no GD. Adicionalmente, o efeito de uma solução de A $\beta$  (20  $\mu$ M) preparada a partir da solução utilizada *in vivo* foi também examinado em culturas primárias de neurónios corticais.

De acordo com o antecipado, a administração de A $\beta$ <sub>1-42</sub> não originou alterações significativas da atividade locomotora, no período noturno ou diurno, nem alterações no comportamento do tipo ansioso, paradigmas que poderiam influenciar o desempenho cognitivo dos animais. Contrariamente à literatura, não foram observados défices de memória a curto prazo, embora no caso do *Y-Maze* de alternância forçada, o desempenho dos ratos controlo parecesse estar comprometido. Relativamente à memória episódica de longo prazo, quando o teste foi realizado durante a noite, os resultados foram semelhantes aos observados no teste *Y-Maze*, isto é, não foram identificados défices nos ratos injetados com A $\beta$  mas sim nos controlos, sugerindo um possível efeito deletério da solução veículo. Por outro lado, quando o teste foi realizado durante o dia, ambos os grupos apresentaram um comprometimento no desempenho da memória, possivelmente associado a uma menor atividade exploratória, no caso do grupo com A $\beta$ . No que respeita à aprendizagem e memória espaciais, funções mais especificamente dependentes do hipocampo, não foram detetadas quaisquer alterações.

A nível molecular, não foi observada qualquer tendência para variações nos níveis de A $\beta$ <sub>1-42</sub> na sua forma solúvel no GD de ratos sacrificados 3 ou 14 dias após as cirurgias, analisado por *ELISA*. Não foi também detetada a presença de depósitos de amiloide no cérebro destes animais, após marcação histológica com vermelho do Congo.

Tem sido demonstrado que a sinalização mediada pelo fator neurotrófico derivado do cérebro (BDNF, do inglês *brain-derived neurotrophic factor*) está comprometida nos neurónios na presença de A $\beta$ , devido à clivagem dos seus recetores tirosina cinase B *full-length* (TrkB-FL), através de um processo dependente da ativação de calpaínas. Assim, os níveis destes recetores bem como do respetivo domínio intracelular (TrkB-ICD) originado pela clivagem, foram utilizados como medida indireta da presença de A $\beta$ . Os resultados obtidos por *western-blot* indicaram a ausência deste mecanismo de neurotoxicidade induzida por A $\beta$ . De facto, não parece haver qualquer tendência para alterações nos níveis de TrkB-FL ou TrkB-ICD no GD, mas também na zona sub-ventricular, analisada por ser uma região mais próxima do local de injeção, 3 ou 14 dias após a mesma. No entanto, o péptido em solução pareceu estar funcionalmente ativo, na medida em que resultados preliminares das experiências realizadas *in vitro* revelaram uma tendência para a clivagem dos

recetores TrkB, ou seja, uma diminuição nos níveis de TrkB-FL, acompanhados por um aumento de TrkB-ICD e pela ativação de calpaínas.

Os marcadores de neurogênese foram analisados no final do protocolo, aproximadamente 30 dias após a primeira injeção de BrdU, com foco apenas na porção dorsal do hipocampo, uma vez que esta parece estar mais intimamente relacionada com funções cognitivas, como memória espacial e discriminação de padrões. Os resultados obtidos nas duas amostras analisadas (A $\beta$ I e II), embora preliminares, são discrepantes. Ainda que na amostra A $\beta$ I não tenha sido observada uma alteração no volume do GD dorsal, na amostra A $\beta$ II observou-se uma tendência para a sua diminuição, consistente com o observado em modelos animais transgênicos e doentes com DA, mesmo em fases pré-clínicas ou iniciais. Relativamente à proliferação celular (BrdU<sup>+</sup>) e à diferenciação em neurónios maduros (BrdU<sup>+</sup>NeuN<sup>+</sup>), não parece haver uma tendência para alterações em qualquer uma das amostras. Em A $\beta$ I, observou-se uma tendência para um aumento da proliferação de neuroblastos e diferenciação em neurónios imaturos (BrdU<sup>+</sup>DCX<sup>+</sup>), embora sem diferenças no número total de neuroblastos/neurónios imaturos (DCX<sup>+</sup>). Contrariamente, em A $\beta$ II, ainda que não parecesse haver uma alteração na proliferação de neuroblastos e diferenciação em neurónios imaturos (BrdU<sup>+</sup>DCX<sup>+</sup>), o número total de neuroblastos/neurónios imaturos (DCX<sup>+</sup>) tendeu a diminuir. Estes resultados divergem maioritariamente daquilo que tem sido reportado em alguns modelos esporádicos da doença, os quais apontam para uma diminuição da proliferação e diferenciação, apesar de, até à data, a neurogênese não ter sido avaliada especificamente no modelo utilizado no presente trabalho.

Não obstante a injeção icv de péptido A $\beta$ <sub>1-42</sub> tenha sido previamente descrita como uma forma de obter um modelo da forma esporádica da DA, nas condições do nosso trabalho não foi possível observar o fenótipo esperado. No futuro, para que seja possível extrapolar acerca do potencial papel da neurogênese na cognição dependente do hipocampo, torna-se necessário aumentar o tamanho da amostra ao nível da análise molecular e celular, assim como proceder à otimização metodológica do protocolo utilizado.

**Palavras-chave** | Doença de Alzheimer; péptido beta amiloide; neurogênese pós-natal; hipocampo; memória.

## Abstract

Sporadic late-onset Alzheimer's disease (AD) is the most common cause of dementia worldwide. It is characterized by a progressive cognitive decline, with a noteworthy episodic long-term memory impairment at early stages that eventually leads to dementia, and is accompanied by a gradual excessive accumulation of amyloid  $\beta$  ( $A\beta$ ) peptide in the brain. Present treatment options for AD are very limited, so understanding its pathophysiology is essential for exploring efficient disease-modifying therapies.

Adult hippocampal neurogenesis occurs in the subgranular zone (SGZ) of the dentate gyrus (DG) through a relatively conserved process across mammalian species, that allows the generation of new functional granule cells (GCs) from undifferentiated neural stem/progenitor cells (NSPCs). This is thought to play a significant role in hippocampus-dependent synaptic plasticity and cognitive abilities, namely learning and memory. However, how neurogenesis is modulated in the different stages of AD remains unclear, as results from *in vitro* and *in vivo* animal studies are controversial, and arise mostly from models of the familial form. Therefore, the focal aim of this project was to characterize a rat model mimicking the initial stages of sporadic AD regarding adult hippocampal neurogenesis.

To study cell proliferation and differentiation, young-adult male Wistar rats were injected intraperitoneally with 5-bromo-2'-deoxyuridine (BrdU) (100 mg/kg) at the beginning of the protocol. Next, with the purpose of obtaining our model of disease, intracerebroventricular (icv) injections of an  $A\beta_{1-42}$  peptide solution (2.25 mg/ml, 4  $\mu$ l) were performed. Behaviour tests were carried out two weeks after the icv injection, including the open field (OF), the novel object recognition (NOR), the elevated plus maze (EPM), the Y-maze spontaneous alternation (SA) and forced alternation (FA), and the Morris water maze (MWM) tests. Animals were sacrificed at the end of the protocol for cellular and molecular analysis, focusing mainly on the DG. Moreover, the effect of the  $A\beta$  peptide solution (20  $\mu$ M) used in the *in vivo* experiments was parallelly examined in primary cortical neuronal cultures.

Our results showed that changes in locomotor activity and anxious behaviour were absent in  $A\beta_{1-42}$  injected rats. However, contrary to our expectations, results showed that  $A\beta_{1-42}$  administration did not impair spatial learning, short-term or long-term memory performance. Furthermore, there was no tendency for a change in the levels of soluble  $A\beta_{1-42}$  in the DG of rats sacrificed at 3 or 14 days post-surgery, and no amyloid deposition was depicted in the brain samples from these animals.

Brain-derived neurotrophic factor (BDNF) signalling has been shown to be compromised in the presence of  $A\beta$  due to the cleavage of its tyrosine kinase B full-length (TrkB-FL) receptors, through a process dependent on calpain activation. Thus, the levels of these receptors as well as the intracellular domain fragment (TrkB-ICD) originated after cleavage were evaluated as an indirect measure of the presence of  $A\beta$ . Levels of TrkB-FL and TrkB-ICD did not tend to change 3 or 14 days

after the injection, indicating absent A $\beta$ -induced neurotoxicity. Importantly, preliminary results from *in vitro* experiments point to TrkB-FL receptor cleavage and calpain activation, suggesting the presence of a functionally active peptide in solution.

Neurogenesis was assessed at the end of the protocol, approximately 30 days after the first BrdU injection. Regarding the dorsal DG volume, one of the two samples showed a trend for reduced volume. Moreover, there does not appear to be any changes in cell proliferation (BrdU<sup>+</sup>) or in mature neuron differentiation (BrdU<sup>+</sup>NeuN<sup>+</sup>). Concerning the total number of neuroblasts and immature neurons (DCX<sup>+</sup>), as well as neuroblast proliferation and immature neuron differentiation (BrdU<sup>+</sup>DCX<sup>+</sup>), further analyses are needed, since results from the two samples demonstrated very distinct trends.

The icv A $\beta_{1-42}$  peptide injection, as performed herein, has been previously described as a model of sporadic AD, yet the expected phenotype was not observed under the conditions of the present work. Increasing the sample size for the cellular and molecular analyses and further methodological optimization are sought in the future.

**Key-words** | Alzheimer's disease; amyloid beta peptide; adult neurogenesis; hippocampus; memory.





## Table of Contents

|   |      |
|---|------|
| Agradecimientos.....  | I    |
| Resumo.....   | V    |
| Abstract.....   | VIII |
| List of figures.....  | XIV  |
| List of tables.....   | XVI  |
| List of abbreviations.....  | XVII |
| <br>  |      |
| 1. Introduction .....   | 1    |
| 1.1. Amyloid $\beta$ as the basis for Alzheimer’s disease pathophysiology .....                       | 1    |
| 1.1.1. Alzheimer’s disease – epidemiology and clinical presentation .....                             | 1    |
| 1.1.2. Pathophysiology of Alzheimer’s disease – amyloid cascade hypothesis.....                       | 3    |
| 1.1.3. Diagnosis and management of Alzheimer’s disease.....   | 6    |
| 1.1.4. Animal models of Alzheimer’s Disease .....   | 7    |
| 1.2. Neurogenesis.....  | 8    |
| 1.2.1. Overview .....   | 8    |
| 1.2.2. The dentate gyrus .....  | 10   |
| 1.2.3. Adult hippocampal neurogenesis.....  | 11   |
| 1.2.4. Adult hippocampal neurogenesis – function and dysfunction.....                                 | 13   |
| 1.2.5. Adult hippocampal neurogenesis and Alzheimer’s disease.....                                    | 16   |
| 1.2.6. Brain-derived neurotrophic factor and Alzheimer’s disease – relevance for<br>neurogenesis..... | 19   |
| 2. Aims.....  | 21   |
| 3. Materials & Methods.....   | 22   |
| 3.1. Ethical Concerns .....   | 22   |
| 3.2. Animals & Housing .....  | 22   |
| 3.3. Timeline for <i>in vivo</i> Experimental Procedures.....   | 22   |
| 3.4. BrdU Administration .....  | 23   |
| 3.5. A $\beta$ <sub>1-42</sub> Peptide Injection.....   | 23   |
| 3.6. Behavioural Analysis .....   | 25   |

|  |    |
|--|----|
| 3.6.1. Open Field (OF) .....   | 26 |
| 3.6.2. Elevated Plus Maze (EPM).....   | 27 |
| 3.6.3. Y-Maze Spontaneous Alternation (SA).....  | 27 |
| 3.6.4. Y-Maze Forced Alternation (FA) .....  | 28 |
| 3.6.5. Novel Object Recognition (NOR).....   | 28 |
| 3.6.6. Morris Water Maze (MWM).....  | 29 |
| 3.7. Animal Sacrifice and Tissue Processing.....   | 30 |
| 3.8. Primary Neuronal Cultures .....   | 31 |
| 3.9. Cellular & Molecular Analysis .....   | 32 |
| 3.9.1. Immunohistochemistry (IHC) .....  | 32 |
| 3.9.2. Histology .....   | 34 |
| 3.9.3. Western Blot (WB).....  | 34 |
| 3.9.4. Enzyme-Linked Immunosorbent Assay (ELISA).....  | 36 |
| 3.10. Statistical Analysis .....   | 37 |
| 4. Results.....  | 38 |
| 4.1. Behaviour characterization.....   | 38 |
| 4.1.1. A $\beta$ <sub>1-42</sub> peptide icv injection did not impact locomotor activity or anxiety-related<br>behaviour.....  | 38 |
| 4.1.2. A $\beta$ <sub>1-42</sub> peptide icv injection did not impair spatial working and short-term memory<br>performance.....  | 41 |
| 4.1.3. A $\beta$ <sub>1-42</sub> peptide injected rats showed distinct episodic long-term memory<br>performance when evaluated during the dark and the light phases of the light/dark cycle..... | 44 |
| 4.1.4. No changes in spatial learning and memory performance were observed after A $\beta$ <sub>1-42</sub><br>peptide injection .....  | 47 |
| 4.2. Cellular and molecular analysis.....  | 49 |
| 4.2.1. Changes in soluble A $\beta$ <sub>1-42</sub> or A $\beta$ <sub>1-42</sub> deposits were not observed 3 or 14 days after<br>icv injection.....   | 49 |
| 4.2.2. Levels of TrkB receptor isoforms in the DG and SVZ did not seem to change 3 or<br>14 days after A $\beta$ <sub>1-42</sub> icv injection .....   | 51 |
| 4.2.3. Primary cortical neuronal cultures incubated with A $\beta$ <sub>1-42</sub> show a tendency for an<br>increase in TrkB receptor cleavage and calpain activity .....                       | 53 |

|   |    |
|---|----|
| 4.2.4. Cell proliferation and neuronal differentiation in the DG after $A\beta_{1-42}$ icv injection..... | 55 |
| 5. Discussion.....  | 62 |
| 6. Conclusions and Future Perspectives .....  | 68 |
| 7. References.....  | 70 |

## List of Figures

|   |    |
|---|----|
| Fig. 1 – Histopathological hallmarks of AD at the hippocampus. ....   | 3  |
| Fig. 2 – Amyloid cascade hypothesis. ....   | 4  |
| Fig. 3 – Main neurogenic niches in the rodent (left) and human (right) brain. ....  | 9  |
| Fig. 4 – Hippocampal structure and main circuits. ....  | 10 |
| Fig. 5 – Putative sequential model of adult neurogenesis in the SGZ of the DG. ....   | 11 |
| Fig. 6 – Putative mechanism for the cleavage of TrkB-FL receptors in the presence of A $\beta$ . .  | 20 |
| Fig. 7 – Timeline for in vivo experimental procedures. ....   | 23 |
| Fig. 8 – Schematic representations of the stereotaxic coordinates used for the icv injection.   | 24 |
| Fig. 9 – Schematic representation of the OF arena. ....   | 26 |
| Fig. 10 – Schematic representation of the EPM apparatus. ....   | 27 |
| Fig. 11 – Schematic representation of the apparatus used in the Y-Maze. ....  | 28 |
| Fig. 12 – Examples of the objects used in the NOR test as familiar and novel ....   | 29 |
| Fig. 13 – Schematic representation of the MWM pool. ....  | 30 |
| Fig. 14 – Schematic representation of the dorsal-ventral DG interface (coronal view). ....  | 33 |
| Fig. 15 – Locomotor and exploratory activity remained unchanged two weeks after A $\beta$ <sub>1-42</sub> peptide injection, as assessed by the OF test. ....           | 39 |
| Fig. 16 – The A $\beta$ <sub>1-42</sub> peptide injection did not affect locomotor activity during the acquisition phase of the MWM test. ....                          | 40 |
| Fig. 17 – Anxiety-related behaviour was not influenced by the A $\beta$ <sub>1-42</sub> peptide injection. ....   | 40 |
| Fig. 18 – Spatial working memory performance did not change after the A $\beta$ <sub>1-42</sub> peptide injection. ....   | 41 |
| Fig. 19 – Rats injected with A $\beta$ <sub>1-42</sub> peptide showed no impairment in short-term reference memory performance, as assessed by the Y-Maze SA test. .... | 43 |
| Fig. 20 – A $\beta$ <sub>1-42</sub> peptide injected rats showed no impairment in episodic long-term memory performance at night. ....                                  | 45 |
| Fig. 21 – A $\beta$ <sub>1-42</sub> peptide injected rats showed impaired episodic long-term memory performance when evaluated during the day. ....                     | 46 |
| Fig. 22 – Spatial learning and memory performance was not changed after A $\beta$ <sub>1-42</sub> peptide injection, as evaluated by the MWM test. ....                 | 48 |

|   |    |
|---|----|
| Fig. 23 – Soluble A $\beta$ <sub>1-42</sub> levels in the DG do not tend to change at 3 or 14 days post A $\beta$ <sub>1-42</sub> injection. ....   | 49 |
| Fig. 24 – A $\beta$ aggregates were absent at 3 or 14 days post A $\beta$ <sub>1-42</sub> injection.....  | 50 |
| Fig. 25 – Levels of TrkB receptor isoforms in the DG were not changed at 3 and 14 days after A $\beta$ <sub>1-42</sub> peptide injection. ....  | 51 |
| Fig. 26 – Levels of TrkB receptor isoforms in the SVZ did not change 3 and 14 days after A $\beta$ <sub>1-42</sub> peptide injection. ....  | 52 |
| Fig. 27 – TrkB receptor cleavage tends to be increased in primary neuronal cultures after incubation with A $\beta$ <sub>1-42</sub> peptide. ....   | 53 |
| Fig. 28 – $\alpha$ -II Spectrin cleavage tends to be increased in primary neuronal cultures incubated with A $\beta$ <sub>1-42</sub> peptide, indicating increased calpain activity. .... | 54 |
| Fig. 29 – Dorsal DG volume estimated from representative coronal sections does not show a tendency to change between the controls and the rats injected with A $\beta$ .....              | 57 |
| Fig. 30 – Cell proliferation in the dorsal DG following A $\beta$ icv injection. ....   | 58 |
| Fig. 31 – Immature neuron differentiation after A $\beta$ injection. ....   | 59 |
| Fig. 32 – Mature neuron differentiation in the dorsal DG after A $\beta$ icv injection. ....  | 61 |

## List of Tables

|   |    |
|---|----|
| Table 1 – Summary of the main changes in neurogenesis in different models of AD. ....                           | 17 |
| Table 2 - Behaviour tests performed for each batch of rats and corresponding time of day..                      | 26 |
| Table 3 – Primary antibodies used to study neurogenesis by immunohistochemistry.....                            | 32 |
| Table 4 - Primary antibodies used to assess TrkB receptor and $\alpha$ -II Spectrin levels by western blot..... | 36 |

## List of Abbreviations

|                            |  |
|----------------------------|--|
| <b>AD</b>                  | Alzheimer's disease                            |
| <b>GABA</b>                | $\gamma$ -aminobutyric acid                    |
| <b>APP</b>                 | Amyloid precursor protein                      |
| <b>AICD</b>                | Amyloid precursor protein intracellular domain |
| <b>A<math>\beta</math></b> | Amyloid $\beta$ peptide                        |
| <b>ANOVA</b>               | Analysis of variance                           |
| <b>BSA</b>                 | Bovine serum albumin                           |
| <b>BDNF</b>                | Brain-derived neurotrophic factor              |
| <b>BrdU</b>                | 5-bromo-2'-deoxyuridine                        |
| <b>CNS</b>                 | Central nervous system                         |
| <b>CSF</b>                 | Cerebrospinal fluid                            |
| <b>CTL</b>                 | Control  |
| <b>CA</b>                  | <i>Cornu ammonis</i>                           |
| <b>DIV</b>                 | Days <i>in vitro</i>                           |
| <b>DG</b>                  | Dentate gyrus                                  |
| <b>DAPI</b>                | 4',6'-diamidino-2-phenylindole                 |
| <b>DCX</b>                 | Doublecortin                                   |
| <b>EPM</b>                 | Elevated plus maze                             |
| <b>EC</b>                  | Entorhinal cortex                              |
| <b>ELISA</b>               | Enzyme-Linked Immunosorbent Assay              |
| <b>FAD</b>                 | Familial Alzheimer's disease                   |
| <b>FA</b>                  | Forced alternation                             |
| <b>GAPDH</b>               | Glyceraldehyde-3-phosphate dehydrogenase       |
| <b>GCs</b>                 | Granule cells                                  |
| <b>GCL</b>                 | Granule cell layer                             |
| <b>HBSS</b>                | Hank's balanced salt solution                  |
| <b>IHC</b>                 | Immunohistochemistry                           |
| <b>IPCs</b>                | Intermediate progenitor cells                  |
| <b>ITI</b>                 | Inter-trial interval                           |
| <b>iMM</b>                 | <i>Instituto de Medicina Molecular</i>         |
| <b>icv</b>                 | Intracerebroventricular(ly)                    |
| <b>LTP</b>                 | Long-term potentiation                         |
| <b>MWM</b>                 | Morris water maze                              |
| <b>Neg</b>                 | Negative                                       |

|                 |   |
|-----------------|---|
| <b>NSCs</b>     | Neural stem cells                             |
| <b>NSPC</b>     | Neural stem/progenitor cell                   |
| <b>NFTs</b>     | Neurofibrillary tangles                       |
| <b>NeuN</b>     | Neuronal nuclei                               |
| <b>NMDAR</b>    | <i>N</i> -methyl-D-aspartate receptor         |
| <b>NOR</b>      | Novel object recognition                      |
| <b>OF</b>       | Open field                                    |
| <b>PFA</b>      | Paraformaldehyde                              |
| <b>PBS</b>      | Phosphate-buffered saline                     |
| <b>PSA-NCAM</b> | Polysialic acid neural cell-adhesion molecule |
| <b>PS1</b>      | Presenilin 1                                  |
| <b>PS2</b>      | Presenilin 2                                  |
| <b>RGL</b>      | Radial glia-like                              |
| <b>RIPA</b>     | Radio Immuno Precipitation Assay              |
| <b>RT</b>       | Room temperature                              |
| <b>SDS</b>      | Sodium dodecyl sulphate                       |
| <b>SBDP</b>     | Spectrin breakdown product                    |
| <b>SA</b>       | Spontaneous alternation                       |
| <b>SEM</b>      | Standard error of the mean                    |
| <b>SGZ</b>      | Subgranular zone                              |
| <b>SVZ</b>      | Subventricular zone                           |
| <b>TBS-T</b>    | Tris buffered saline with Tween 20            |
| <b>TrkB-FL</b>  | Tyrosine kinase B full-length                 |
| <b>TrkB-ICD</b> | Tyrosine kinase B intracellular domain        |
| <b>TrkB-Tc</b>  | Tyrosine kinase B truncated                   |
| <b>VEH</b>      | Vehicle                                       |
| <b>WB</b>       | Western blot                                  |





# 1. Introduction

## 1.1. Amyloid $\beta$ as the basis for Alzheimer's disease pathophysiology

### 1.1.1. Alzheimer's disease – epidemiology and clinical presentation

The first case of Alzheimer's disease (AD) was reported in 1906 by the psychiatrist and neuroanatomist Alois Alzheimer, whom described it as a “peculiar disease process of the cerebral cortex”. He had observed the condition in a 50-year-old woman in 1901, and followed the progression of her symptomatology until 1906, having analysed the brain morphology and histology post-mortem. Although AD was known as such around 1910, the disease was very rare at the time, and so the term was nearly forgotten for more than 50 years <sup>1</sup>.

Currently, AD is the most prevalent neurodegenerative disorder worldwide, being particularly frequent in Western Europe and in the elderly population ( $\geq 65$  years-old). AD is also the most common form of dementia, responsible for about 60-80% of all cases <sup>2-4</sup>. The last study by the World Health Organization in 2015, reported that AD and other dementias were the seventh cause of death globally, and the third cause of death in high income countries <sup>5</sup>. Furthermore, due to population aging, the number of people with AD is estimated to triple by 2050 <sup>4,6</sup>. Besides the major health care costs that have a significant impact on global economy, dementia represents a substantial burden for the families of the patients and caregivers <sup>3,4</sup>. In fact, as the disease progresses, caregivers in the United States were shown to present new and exacerbated health problems, including emotional stress and depression <sup>3</sup>.

The early-onset, familial form of the disease (FAD) accounts for only approximately 5% of the cases and has been mainly linked to the inheritance of autosomal dominant mutations on the genes encoding for amyloid precursor protein (APP) and presenilins 1 and 2 (PS1 and 2), located on chromosomes 21, 14 and 1, respectively <sup>7-10</sup>. Most of the cases of AD have unknown etiology, occurring as the late-onset sporadic form, with onset above the age of 65 years <sup>4,7</sup>. Although dementia cannot be referred to as a regular part of aging, advanced age is indeed the greatest risk factor for AD, with 32% of all people with age 85 or higher being estimated to develop the disease. Having a family history of dementia, especially in the first degree, also increases the likelihood of having AD early on. Another determinant of the risk for AD is the apolipoprotein E genotype, a protein which transports cholesterol and other lipids through the bloodstream. Carrying the APOE-e4 allelic form has been associated with increased risk of AD, even though most patients do not carry this allele. In contrast, having the e2 or e3 forms relates with a lower predisposition for AD. Other variables that associate with increased risk of AD include: stroke, hypertension, diabetes, hyperlipidaemia, traumatic brain injury, and having less years of formal education <sup>3,10</sup>.

Preceding the onset of symptoms, neurodegenerative changes associated with AD are proposed to start at a preclinical stage, developing over the course of various decades<sup>3,11</sup>. Clinically, the disease is characterized by a cognitive, behavioural and functional decline, that slowly progresses over an average of 8 years since the time of diagnosis, although substantial variability can be observed between patients<sup>10,11</sup>. At the initial phases, AD patients usually show short-term and semantic memory loss, as well as a noteworthy hippocampal-dependent episodic memory impairment regarding more recent events<sup>10-12</sup>. During mild to moderate stages of the disease, procedural memory, and episodic memory of past years also start to be affected<sup>11-13</sup>. As the disease progresses, compromised language function becomes more evident, as do deficits in attention, logical reasoning, planning and visuospatial orientation. Depression and apathy, delusions and aggressiveness may also prevail at this stage. At severe stages of dementia, practically all cognitive functions become severely deteriorated, and patients become completely dependent on their caregivers, as they lose basic motor functions including walking, speech, swallowing and bladder/bowel control<sup>10,11</sup>. Because currently available treatments are unable to stop neurodegeneration, the disease is eventually fatal, being aspiration pneumonia, myocardial infarction and septicaemia the most common causes of death<sup>3,10,11</sup>.

AD is typically associated with generalized cerebral atrophy, predominantly affecting the parietal, temporal and frontal cortices, the limbic system and the subcortical nuclei, with subsequent ventriculomegaly<sup>9,10</sup>. Furthermore, significant neuronal loss is present, and there is a gradual accumulation of excess extracellular amyloid  $\beta$  (A $\beta$ ) peptide deposits, termed senile or neuritic plaques, accompanied by the formation of intracellular neurofibrillary tangles (NFTs), resulting from hyperphosphorylation of microtubule-associated protein tau. These are considered the classical histopathological hallmarks of AD (Fig. 1)<sup>9,10,14</sup>. While the formation of senile plaques usually begins in some regions of the neocortex, in the hippocampus, and the entorhinal cortex (EC), NFTs originate first in the entorhinal-perirhinal and hippocampal region, only reaching the neocortex at later stages of the disease<sup>15-18</sup>. Additionally, amyloid deposition in the walls of blood vessels in the central nervous system (CNS), termed cerebral amyloid angiopathy, and intracellular formation of granulovacuolar degeneration with Hirano bodies, can be denoted in the brain of individuals suffering from AD (Fig. 1)<sup>19-22</sup>.

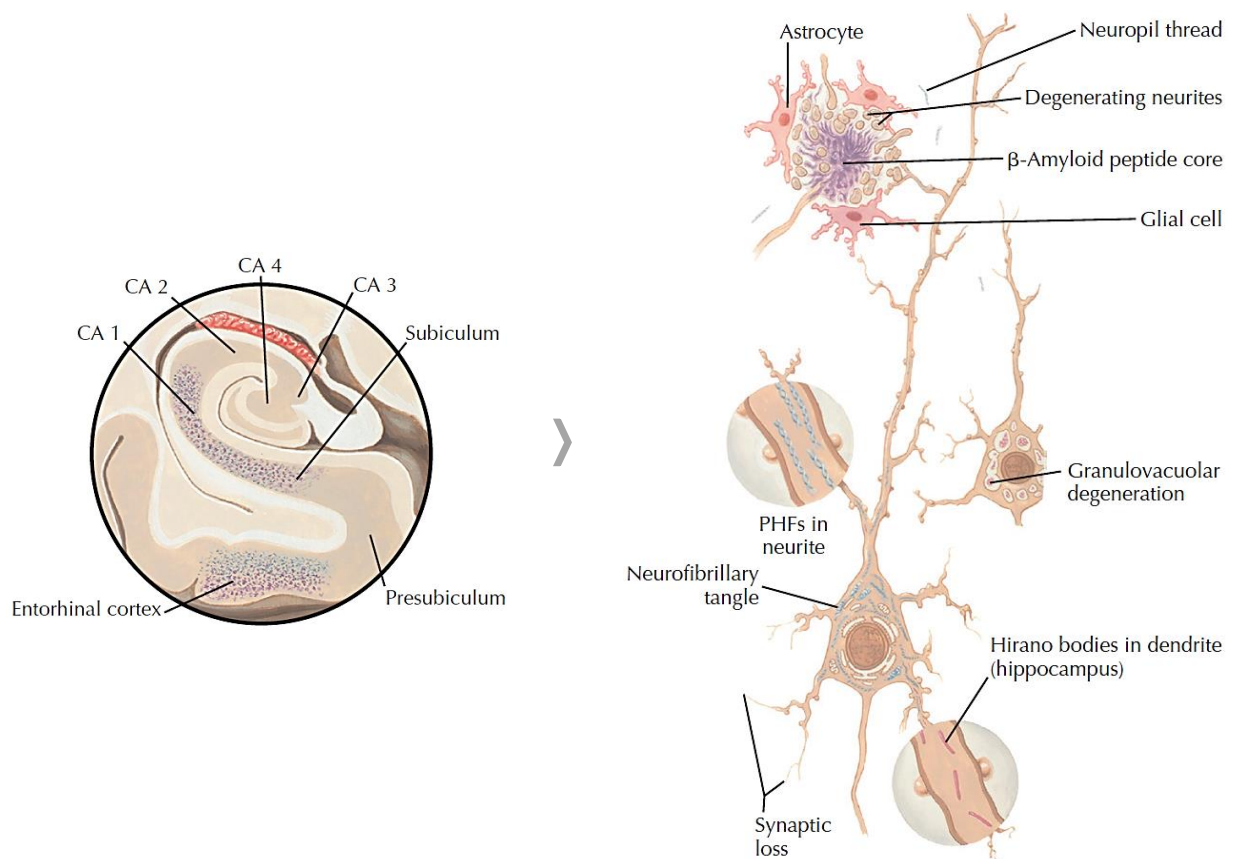


**Fig. 1 – Histopathological hallmarks of AD.** The hippocampal formation, namely the *cornu ammonis* 1 (CA1) region, subiculum, and entorhinal cortex, is one of the structures to be primarily affected by the formation of senile plaques, neurofibrillary tangles, and neuronal loss (left). Senile plaques are composed of dystrophic neurite processes, A $\beta$  peptide, microglial cells and astrocytes, while neurofibrillary tangles contain paired helical filaments (PHFs) of hyperphosphorylated tau protein (right). Adapted from Yuval, 2012 <sup>10</sup>.

### 1.1.2. Pathophysiology of Alzheimer’s disease – amyloid cascade hypothesis

Several hypotheses try to clarify the pathophysiology underlying AD, and although none seems to individually explain the whole clinical condition, the amyloid cascade hypothesis continues to have the most acceptance among researchers, after being proposed for the first time in 1991 <sup>23,24</sup>. According to this hypothesis, the neurodegenerative and functional changes associated with AD are thought to be initially triggered by the deposition of A $\beta$  in the brain (Fig. 2) <sup>24,25</sup>. More recently, discussion regarding this hypothesis points to soluble A $\beta$  oligomers rather than deposits as the initiators for the cascade, likely during the preclinical stage of the disease <sup>14,23</sup>.

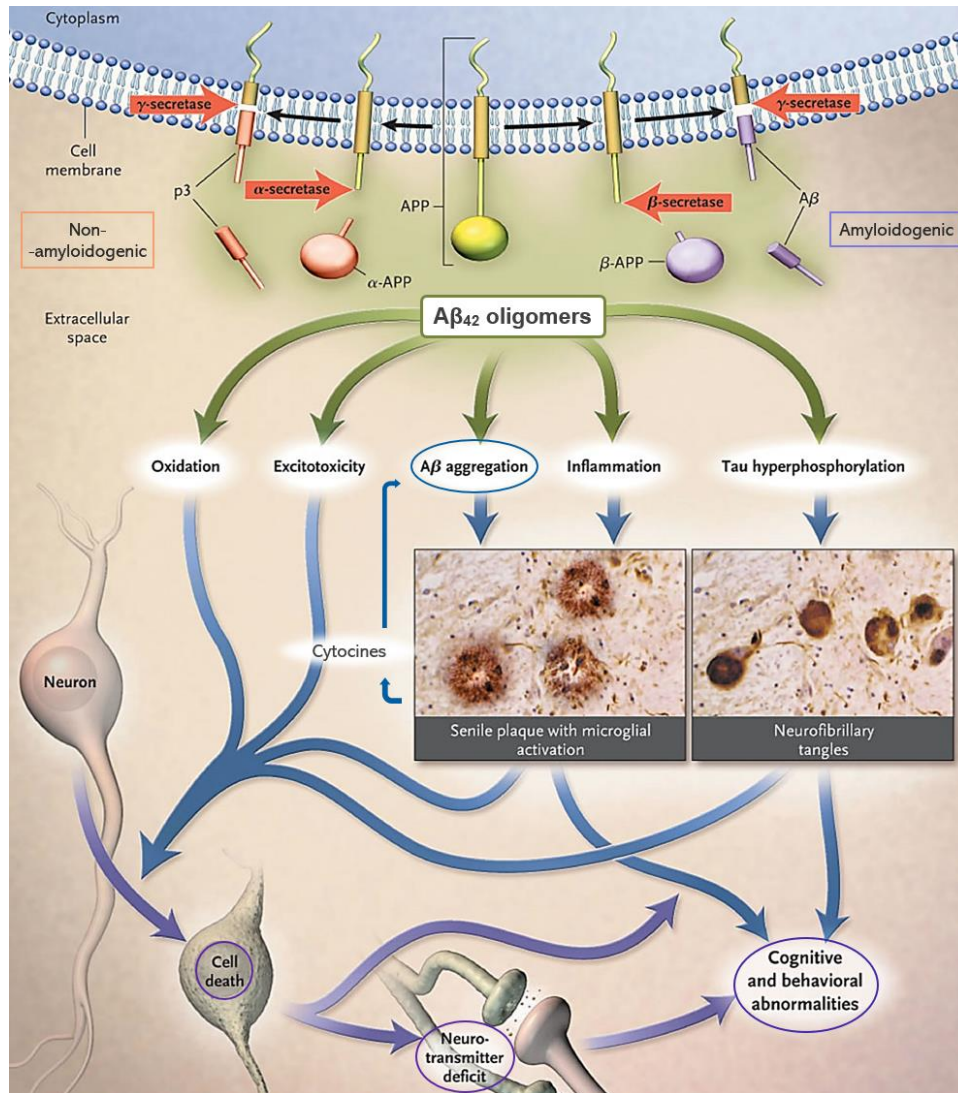


**Fig. 2 – Amyloid cascade hypothesis.** Adapted from Cummings, 2004 <sup>25</sup>.

$A\beta$  is a 38-42 amino acid fragment produced in virtually all neurons, from the sequential cleavage of APP <sup>22</sup>. This integral membrane glycoprotein possesses a cytoplasmic (C-terminal) and an extracellular (N-terminal) domain, and can be processed either by a non-amyloidogenic or an amyloidogenic pathway (Fig. 2) <sup>9,25</sup>. The non-amyloidogenic pathway begins with the proteolytic cleavage of APP by the metalloenzyme  $\alpha$ -secretase, releasing the soluble N-terminal domain sAPP $\alpha$  <sup>22,26</sup>. The C-terminal fragment of APP is then cleaved by  $\gamma$ -secretase enzymatic complex, with PS1 and 2 composing the two active catalytic sites, originating the p3 fragment ( $A\beta$  17-40/42) and releasing the APP intracellular domain (AICD) fragment into the cytoplasm <sup>10,22</sup>. Following the amyloidogenic pathway, APP is first cleaved by  $\beta$ -secretase enzymatic complex, resulting once again in the release of a soluble N-terminal domain sAPP $\beta$ . Further cleavage of the remaining transmembrane fragment by  $\gamma$ -secretase leads to the formation of the  $A\beta_{1-38/42}$  peptide and release of the AICD fragment inside the cell. Although the physiological functions of the elements involved in these pathways remains largely uncertain, APP seems to play a significant role in neuronal

plasticity and formation of synapses, and some neuroprotective and neurotrophic actions have also been attributed to sAPP $\alpha/\beta$  and AICD<sup>22,26</sup>. A number of physiological roles have also been suggested for  $\alpha$ -,  $\beta$ - and  $\gamma$ -secretase enzymes<sup>26,27</sup>.

Both pathways described are present in healthy individuals and AD patients, being A $\beta_{1-40}$  peptide the major form of A $\beta$  generated through the amyloidogenic pathway in healthy individuals (around 80-90%), followed by A $\beta_{1-42}$  (about 5-10%)<sup>9,22,28</sup>. Therefore, studies suggest that pathological changes associated with AD arise from an imbalance between the production and clearance of A $\beta$  which favours the amyloidogenic pathway, as well as an increase in the ratio between A $\beta_{1-42}$  and A $\beta_{1-40}$ . This leads to an excessive accumulation of the peptide at an intracellular and extracellular level, with distinct physical properties and aggregation states<sup>22,28,29</sup>. A $\beta_{1-42}$  peptide is more hydrophobic than A $\beta_{1-40}$ , and therefore tends to aggregate at a higher rate into soluble oligomers, which appear to be the most toxic form of A $\beta$ <sup>26,28,29</sup>. These oligomers spontaneously acquire an anti-parallel  $\beta$ -sheet conformation, folding into insoluble fibrils that accumulate and eventually form diffuse and neuritic plaques<sup>10,23,26</sup>.

A series of neurotoxic mechanisms have been shown to be pathologically induced by A $\beta$  oligomerization (Fig. 2). These changes include tau hyperphosphorylation with subsequent microtubule destabilization and disrupted cytoskeleton structure, culminating in the formation of intracellular NFT, with loss of neuronal and synaptic function<sup>10,23,30</sup>. Tau phosphorylation has been demonstrated to occur downstream of A $\beta$  oligomerization, yet the underlying mechanism is still unknown<sup>31,32</sup>. It has been hypothesized that oxidative damage plays an important role in NFT formation, which is another key component of the amyloid cascade<sup>9,33</sup>. When an excessive production of toxic A $\beta_{1-42}$  oligomers occurs, they start being released by neurons and are able to bind receptors on neighbouring astrocytes, namely the nicotinic acetylcholine receptor  $\alpha$ -7nAChR<sup>23</sup>. This induces the release of glutamate from astrocytes that can, in turn, activate astrocytic *N*-methyl-D-aspartate receptors (NMDARs) and trigger Ca<sup>2+</sup>-mediated excitotoxicity, mitochondrial dysfunction and exacerbated oxidative damage<sup>22,23,30</sup>. Notably, signalling by various neurotransmitters has been reported to be compromised in AD, with cholinergic function being the first to be blatantly affected. Other neuro-chemical systems that appear to be gradually damaged include the serotonergic, noradrenergic and  $\gamma$ -aminobutyric acid (GABA)ergic<sup>10,30</sup>. Moreover, A $\beta$  deposition has been shown to promote a neuroinflammatory response through activation of microglia that produce proinflammatory cytokines, further stimulating the A $\beta_{1-42}$  oligomers in a vicious cycle<sup>23,30</sup>. Along with disease progression, these pathological changes eventually result in disrupted synaptic transmission, cell death and cognitive decline<sup>10,23,31</sup>.

### 1.1.3. Diagnosis and management of Alzheimer's disease

As for most dementias, a definitive diagnosis of AD can only be achieved post-mortem upon confirmation of histopathological features<sup>10</sup>. Today, diagnosis still relies mostly on the ability of clinicians to perform a cautious and comprehensive assessment<sup>3,34</sup>. For this, physicians should require a detailed medical and family history, and evaluate the major cognitive domains of the patients, as well as their physical and neurological function<sup>3,10</sup>. Additionally, analysis of a few biomarkers has been implemented in some of nowadays clinical practice<sup>35,36</sup>. The pattern and extent of cerebral atrophy, as well as vascular changes, including vascular amyloid deposition, can be highlighted by magnetic resonance imaging (MRI) or, alternatively, by high-resolution computed tomography (CT)<sup>34,35</sup>. Concerning A $\beta$  deposition, *in vivo* detection of fibrillary aggregates may be achieved nowadays by Pittsburgh compound B PET (PiB PET) techniques, using high-affinity ligands<sup>14,35</sup>. Notably, identification of biomarkers in the cerebral spinal fluid (CSF) of patients constitutes a relevant part of AD diagnosis, allowing evaluation of A $\beta$ <sub>1-42</sub>, A $\beta$ <sub>1-40</sub>, total tau (t-tau) and phosphorylated tau (p-tau) levels, which correlate with the major hallmarks of the disease<sup>14,35</sup>. Lower levels of soluble A $\beta$ <sub>1-42</sub> as well as a decreased A $\beta$ <sub>1-42</sub>/A $\beta$ <sub>1-40</sub> ratio in the CSF are expected in individuals suffering from AD, as the peptide tends to deposit in senile plaques along disease progression, contrary to t-tau and p-tau levels, which are expected to increase<sup>35,36</sup>.

Achieving an early diagnosis of AD poses a major challenge due to the absence of symptomatic manifestations in preclinical stages of the disease, that only become prominent in later stages. In the last years, several efforts have been made in order to find new biomarkers that potentially allow an earlier and definitive diagnosis<sup>14,36,37</sup>. In this regard, many studies have been focusing on finding more sensitive measures for A $\beta$  quantification as its levels seem to be altered decades before the onset of symptoms<sup>34,37,38</sup>. Recently, the analysis of A $\beta$  plasma levels has gained some attention<sup>37-39</sup>. An example is the detection of low plasma levels of A $\beta$ <sub>1-42</sub> by high-performance immunoprecipitation coupled with mass spectrometry, which may provide a novel cost-effective, accurate method for routine screening and prediction of dementia onset in preclinical/prodromal stages<sup>39</sup>.

Despite the increasing volume of drugs being researched and tested in clinical trials, present treatment options for AD are very limited, only providing symptomatic relief and/or modestly and temporarily slowing down disease progression. These include acetylcholinesterase inhibitors and NMDAR antagonists<sup>3,23,30</sup>. Again, a major portion of studies regarding research of new drug treatments is being directed at amyloid, namely focusing on modulating A $\beta$  synthesis, transport, aggregation and clearance, but also through amyloid based immunotherapy<sup>23,26,40</sup>. Other potential targets being studied include tau protein, neurotransmitters and their receptors, oxidative stress, neurogenesis and inflammation, and a combination of multiple-target ligands<sup>23,30,40</sup>.

#### 1.1.4. Animal models of Alzheimer's Disease

Since AD does not spontaneously occur in the most widely used laboratory animal species, as mice and rats, a variety of *in vivo* animal models of the disease have been used and developed for preclinical studies in the past two decades, extensively based on the amyloid cascade hypothesis<sup>41,42</sup>. These models have allowed not only to investigate the pathophysiological mechanisms underlying AD, but also to unravel novel diagnostic biomarkers, and to develop new therapeutic strategies<sup>41</sup>. Several model organisms like the *Drosophila melanogaster* and the zebrafish are currently used to study AD, yet rodents are the major tools for preclinical research in AD<sup>43,44</sup>.

Nowadays, transgenic mice constitute the most commonly used models of AD. These mice are usually genetically altered to overexpress several mutations that have been associated with FAD, specially targeting APP, PS and tau, either individually or in different combinations<sup>41,43</sup>. One of the advantages of these models is a progressive development of pathophysiological changes that, at least in part, resembles what is observed in different stages of human AD<sup>41</sup>. Although transgenic rat models are less common, mainly due to a reduced availability of genome altering tools, they are also used to study AD<sup>45,46</sup>. In fact, the physiology and genetic background of rats is more closely related to humans when compared to mice. Moreover, rats display more complex and well characterized behaviour performance<sup>45,47-49</sup>. Plus, some procedures like neurosurgery and brain imaging are more easily performed in rats due to a larger body size<sup>45</sup>. Notwithstanding, genetic manipulation of an organism can lead to compensatory mechanisms, introducing possible confounding variables in research studies<sup>41</sup>. In addition, while transgenic mice have provided valuable insights into the pathophysiological mechanisms of AD, they only represent the familial form of the human disease, responsible for approximately 5% of all cases<sup>50</sup>.

Sporadic models of AD have been increasingly described, usually obtained by intracerebroventricular (icv) or intrahippocampal administration of A $\beta$ <sup>41</sup>. Although these models may have a more acute or chronic effect depending on the protocol of injection, they do not mimic the gradual disease development that occurs in humans. On the other hand, these models may reproduce the initial stages of AD, prior to A $\beta$  plaque deposition. Additionally, advantages of using sporadic models include: studying the effects of specific A $\beta$  species with distinct aggregation states, and at defined concentrations, on particular pathways promoting the dysfunctions associated with AD; and eliminating the confounding consequences of genetic manipulation<sup>41,51</sup>.

Overall, although these models might not thoroughly recapitulate all the clinical changes associated with human AD, some key features can be denoted both in transgenic and sporadic models, namely histopathological alterations, compromised synaptic transmission and neuroplasticity, and notable memory impairments<sup>41</sup>. Furthermore, combining the evidences obtained both from transgenic and sporadic models may be a way of overthrowing the limitations of different models.



## 1.2. Neurogenesis

### 1.2.1. Overview

The process of neurogenesis can be defined altogether as the sequential generation of new neurons from specific precursor cells <sup>52,53</sup>. During embryonic and postnatal development, neurogenesis is crucial for the appropriate and structured formation and maturation of the nervous system, through a step-wise process shared across several vertebrate species <sup>54-56</sup>. A particular parallelism can be noticed between humans and rodents, although the time course of these changes are considerably different <sup>54,57</sup>. The formation of the CNS begins with the differentiation of the ectoderm into a structure called the neural tube <sup>54,58</sup>. Neurogenesis per se starts with the formation of the neocortex from the neural tube, which latter gives rise to the brain and spinal cord <sup>58,59</sup>. During prenatal and early postnatal period, neuroepithelial cells originate precursor cells that migrate to specific target locations, where they will differentiate and mature into neurons and glial cells. Following growth of axons and dendritic branching, synaptogenesis occurs <sup>56,58</sup>. Because there is an overproduction of neurons throughout these periods, the process is regulated by apoptosis and selective elimination of synapses (synaptic pruning), allowing maintenance of only the most relevant connections to form a functional neuronal circuitry <sup>57,58</sup>.

Maturation of the human brain continues for 20-25 years after birth, however, and contrary to previous scientific beliefs, neurogenesis does not appear to cease after development <sup>60</sup>. The first evidences of adult neurogenesis were observed in 1965, in a study that found the presence of a germinal pool of undifferentiated cells in the dentate gyrus (DG) of the rat hippocampus <sup>61</sup>. In fact, it has been increasingly shown that adult neurogenesis is maintained throughout the whole lifespan of many mammalian species, namely rodents, humans and other primates <sup>62-64</sup>. However, the controversy regarding human studies remains, as different authors suggest contradictory results, showing either maintained or decreased levels of neurogenesis, and even absent neurogenesis during adulthood and aging <sup>65-67</sup>. This process occurs in brain regions termed neurogenic niches, considered to be specialized microenvironments surrounding and sustaining self-renewal of multipotent neural stem cells (NSCs), and promoting their migration and differentiation into neurons and glial cells <sup>68</sup>. Numerous other components make up these niches, including an extracellular matrix, progenitor and endothelial cells, astrocytes, microglia, oligodendrocytes, and blood vessels <sup>69,70</sup>. These microenvironments have a dynamic and plastic nature, and are regulated by a variety of extrinsic and intrinsic factors or pathways, thought to provide not only maintenance of the pool of undifferentiated NSCs, but also to modulate and adjust the production of new cells on demand <sup>52,53,69</sup>.

The subventricular zone (SVZ) of the lateral ventricles and the subgranular zone (SGZ) in the DG of the hippocampus constitute the two major neurogenic niches in the adult mammalian brain <sup>71</sup>. In rodents, progenitor cells from the SVZ largely migrate through the rostral medial stream (RMS) to the olfactory bulb (OB) (Fig. 3), where they originate new neurons that have been shown to play a substantial role in odour discrimination and establishment of olfactory memories <sup>52</sup>. Whether migration of neuronal progenitors to the OB occurs in humans remains controversial, although a less keen sense of smell might suggest the absence or decrease of this process <sup>72</sup>. On the other hand, neurogenesis in the human striatum appears to be more prominent than in other mammals, and although the origin of these neurons has not yet been clarified, it is hypothesized that they could arise from the migration of progenitors from the SVZ to this region (Fig. 3) <sup>69,72</sup>.

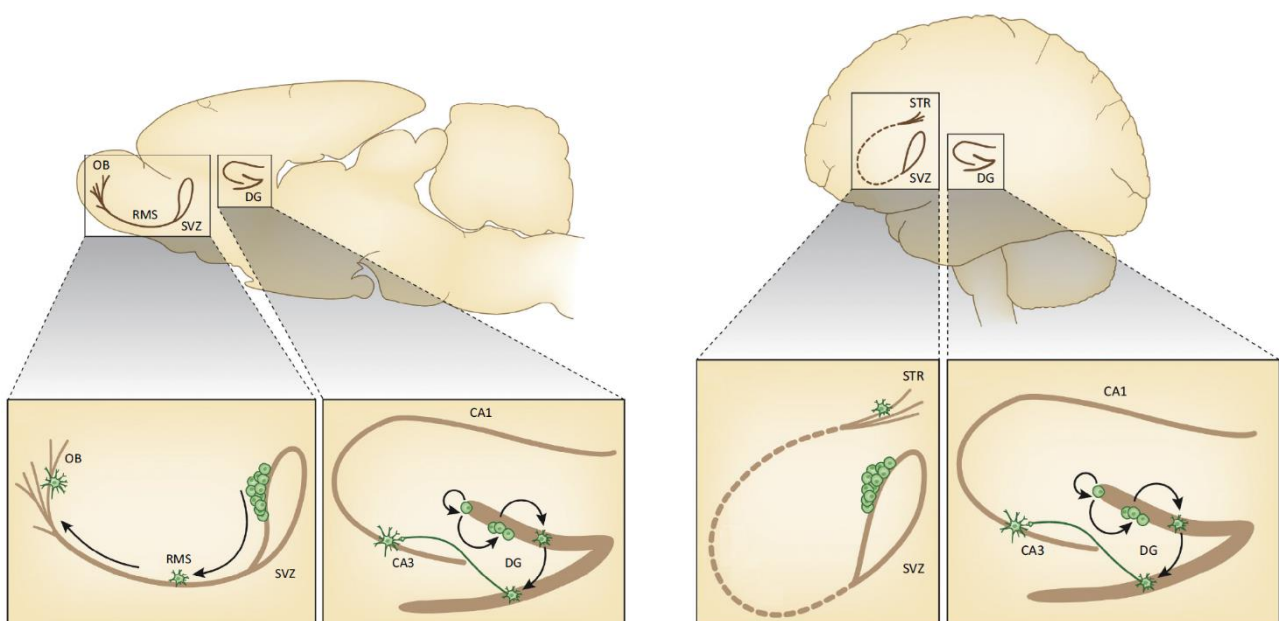


**Fig. 3 – Main neurogenic niches in the rodent (left) and human (right) brain.** STR: Striatum. Adapted from Borsini et al, 2015 <sup>73</sup>.

When considering the hippocampus, the extent and basic underlying mechanisms of neurogenesis in the DG seem to be comparable to other mammalian species so far, especially rodents <sup>72</sup>. This supports the use of mice and rats as a good model to study the normal process of adult hippocampal neurogenesis, as well as possible changes that may be related with neurological and psychiatric disorders. Additionally, less commonly explored neurogenic sites have been proposed in structures such as the neocortex, hypothalamus, amygdala, *substantia nigra*, cerebellum and spinal cord, thus suggesting the relevance of these mechanisms of neurogenesis-based structural plasticity throughout the mammalian CNS <sup>74,75</sup>.

### 1.2.2. The dentate gyrus

The DG is a part of the hippocampal formation, along with the CA1, CA2 and CA3 regions, the subicular complex (subiculum, presubiculum and parasubiculum), and the EC <sup>76</sup>. Information in the hippocampus is processed through a classical trisynaptic network (Fig. 4), where the EC projects to the DG and CA1 subfield via the perforant pathway. The axons from granule cells (GCs) of the DG in turn connect to the CA3 pyramidal cells, forming the mossy fiber pathway. Next, CA3 neurons project to CA1 through the Schaffer collaterals, followed by connection of CA1 pyramidal cells to the subiculum and EC, and from the subiculum to the EC. Recurrent connections within the DG and CA3 can also be observed <sup>76-78</sup>. Moreover, the hippocampus connects to most neocortical association areas via the EC, as well as to numerous subcortical regions <sup>78</sup>.

The DG constitutes a V-shaped structure around the CA3 subfield, composed of three cell layers. The outermost one, termed molecular layer, primarily contains axons from the EC connecting with dendrites of GCs, but also GABAergic interneurons and extrinsic input afferent fibers. Cell bodies of GCs, the main excitatory neurons of the DG, are densely packed below the molecular layer, forming the granule cell layer (GCL), that can be divided into the suprapyramidal and infrapyramidal blades, depending on its location above or below the CA3 region, respectively. Neurogenesis occurs in the SGZ, located right underneath the GCL, where precursor cells reside. The deepest layer is the polymorphic cell layer, or hilus, containing axons of GCs plus glutamatergic and GABAergic interneurons <sup>76,77,79</sup>.

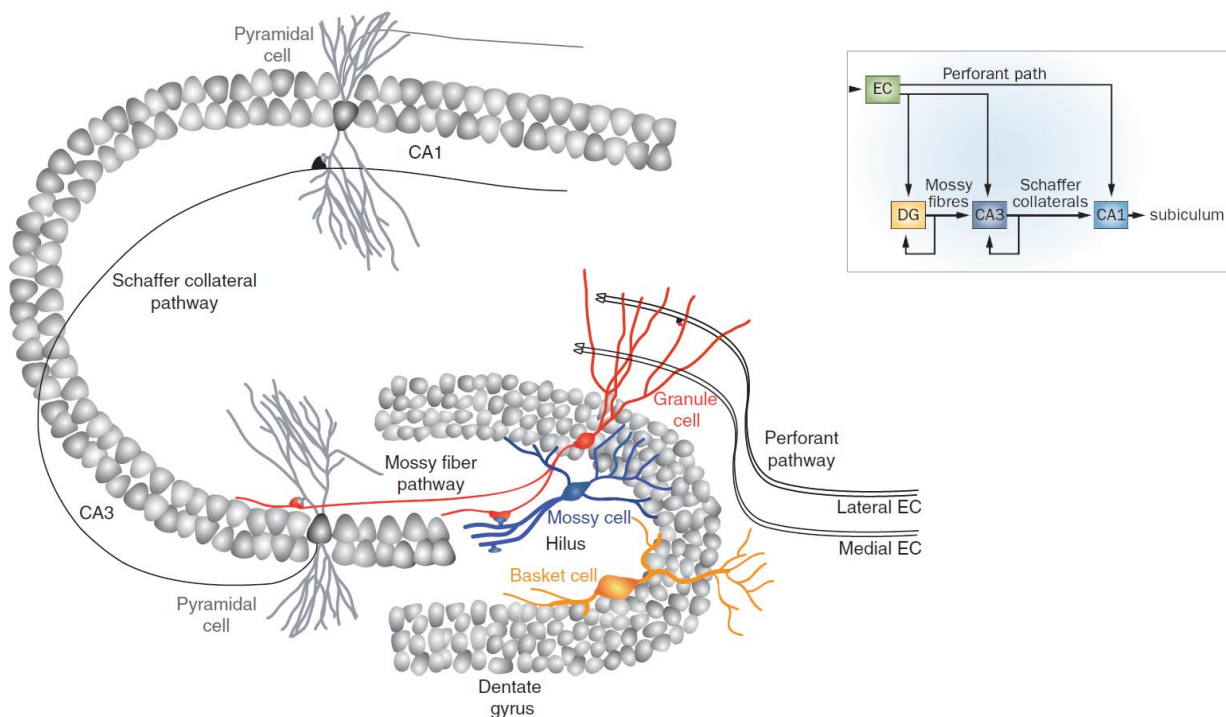


**Fig. 4 – Hippocampal structure and main circuits.** Adapted from Toni and Schinder, 2016, Bartsch and Butler, 2013 <sup>77,78</sup>.

### 1.2.3. Adult hippocampal neurogenesis

The formation of highly functional new neurons can be observed in the human DG, with a turnover of approximately 0.004% neurons per day, considering that around one third of all hippocampal neurons have the ability to be exchanged<sup>80</sup>. New adult-born neurons in the DG take approximately 7-8 weeks to form and fully mature and, to date, GCs are the only type of neuron that has been shown to derive from adult neurogenesis<sup>70,77</sup>. Most knowledge of neurogenesis, namely the properties of NSCs and progenitors comes from *in vitro* and *ex vivo* studies, yet increasing evidence from *in vivo* studies, with the use of new methodologies has allowed the proposition of a sequential mechanism underlying adult neurogenesis in the mammalian hippocampus (Fig. 5)<sup>77,81,82</sup>.

Radial glia-like (RGL; type 1) cells appear to be at the starting point of adult neurogenesis in the DG<sup>70,82</sup>. While their soma is located in the SGZ, processes usually branch through the GCL and the molecular layer<sup>83</sup>. These cells show properties of NSCs, possessing the ability to self-renew through symmetrical divisions, and to differentiate into neurons, astrocytes and oligodendrocytes (multipotency), although the latter does not seem to be generated under physiological conditions<sup>82</sup>. Moreover, whether self-renewal ability is unlimited or restricted to a certain number of cell divisions remains unclear<sup>84</sup>. Most RGL cells are believed to be arrested in the G<sub>0</sub> phase of the cell-cycle, remaining in a quiescent state, and hence having a low proliferative rate<sup>52,82</sup>. Molecularly, they are characterized by expression of intermediate filaments glial acidic fibrillary protein (GFAP) and nestin, and transcription factor sox2<sup>70</sup>.

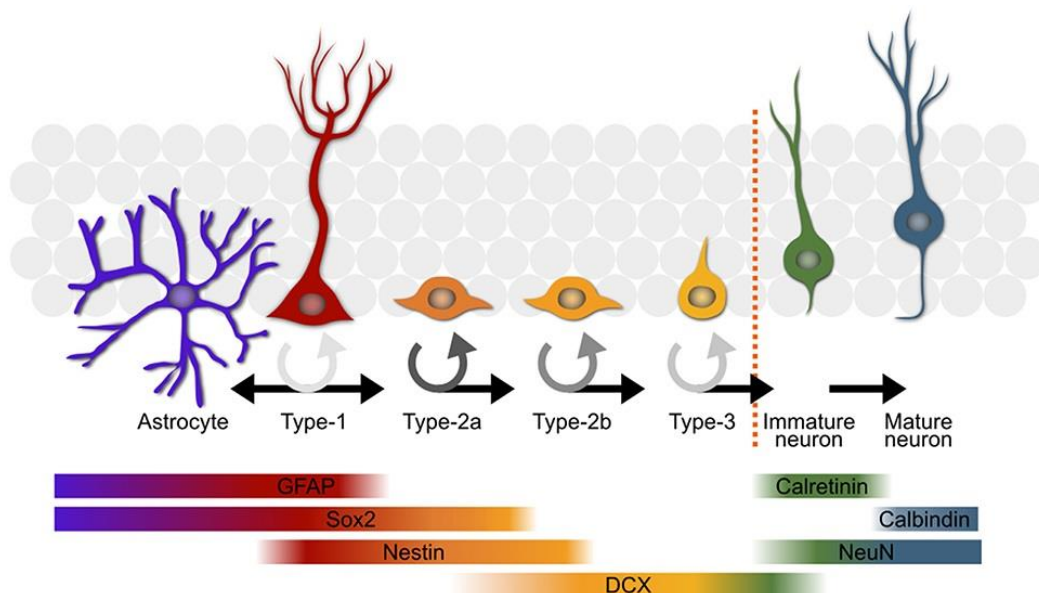


**Fig. 5 – Putative sequential model of adult neurogenesis in the SGZ of the DG.** Different cellular stages express distinct molecules that can be labelled by immunohistochemistry. Adapted from Overall et al, 2016<sup>85</sup>.

Once activated, RGL cells originate fast proliferating nonradial intermediate progenitor cells (IPCs; type 2 cells), with short processes oriented parallelly to the GCL, that allow the expansion of the pool of undifferentiated cells <sup>70,83</sup>. IPCs can be distinguished in type 2a and type 2b cells. While the first subtype still expresses glial markers, including nestin and sox2, the latter starts expressing early neuronal markers, like microtubule-associate protein doublecortin (DCX) and polysialic acid neural cell-adhesion molecule (PSA-NCAM), being therefore hypothesized that cell fate may be determined at this transition point <sup>70,77</sup>. It is also at this point that these new cells receive their first depolarizing (excitatory) GABAergic inputs from diffuse ambient GABA <sup>86</sup>. Next, IPCs give rise to neuroblasts (type 3 cells), which lack any glial markers, and are fully committed to the neuronal lineage, expressing DCX, PSA-NCAM, and transcription factors NeuroD and Prox1 <sup>70,83</sup>. These cells are still proliferating to some extent, and show a heterogenous morphology, with their processes gradually changing from a horizontal to a vertical orientation <sup>83</sup>.

Following expansion of the cell pool, neuroblasts differentiate into immature GCs in an early survival phase, marking the exit of the cell-cycle <sup>70</sup>. As for embryonic development, most new-born cells are eliminated by apoptosis at this stage, before any functional maturation occurs <sup>70,83</sup>. Early GCs selected for long-term survival continue expressing DCX and PSA-NCAM, and start expressing post-mitotic markers calcium-binding calretinin and neuronal nuclei (NeuN) <sup>70</sup>. During the initial days, immature neurons remain in the SGZ. As they start acquiring a polarized shape, bipolar neurites begin to extend into the GCL <sup>77</sup>. First, axons start to elongate in direction to the CA3 region, where they compete to form their first efferent connections, along with dendrite extension through the molecular layer, to form afferent connections from the EC. The soma of adult-born GCs migrates to the GCL, which will induce cells to be structurally integrated into the DG network <sup>70,77</sup>.

Later in the post-mitotic maturation phase, calretinin is replaced by calbindin, another calcium-binding protein <sup>70,83</sup>. As expression of voltage-dependent Na<sup>+</sup> and K<sup>+</sup> channels, as well as GABA and glutamate receptors increases, GABAergic inputs become progressively hyperpolarizing (inhibitory), corresponding to the onset of functional glutamatergic dendritic spine formation, together allowing cell membranes to change from a high input resistance state, to a more regular state resembling mature GCs <sup>70,77</sup>. New-born cells take several months to become fully mature glutamatergic dentate GCs, with continued dendritic branching and increase in spine density <sup>77</sup>. During the first weeks of this period, immature GCs display unique characteristics of activity-dependent enhanced synaptic plasticity, as they have lower activation thresholds and greater amplitudes for long-term potentiation (LTP) <sup>70,77,83</sup>. These properties might serve as a feedback mechanism that favours the enduring integration of new cells, but are also proposed to play a significant role in the proper function of the DG, namely regarding learning and memory, as will be further discussed in the next section <sup>70,77</sup>.

#### 1.2.4. Adult hippocampal neurogenesis – function and dysfunction

The role of the hippocampal formation has been extensively described in regard to learning and memory, playing an important part in acquisition of new memories, consolidation from short-term to long-term memory, and retrieval of previously consolidated memories <sup>87,88</sup>. The main contribution of the hippocampus and its connections is related to declarative (or explicit) memory, which refers to memories that can be recalled consciously, and can be further divided in episodic and semantic. Whereas episodic memory comprehends memory of personal experiences and events, along with the associated temporal and spatial context, semantic memory represents the knowledge of the external world, independent of context. In contrast, non-declarative (or implicit) memory refers to unconscious memory of skills and habits, and correlates better with the function of brain structures as the striatum and the cerebellum <sup>78,89</sup>. Interestingly, studies from patients with amnesia associated to brain lesions indicate that the left and right hippocampal formations could have distinct contributions, with the former being more commonly related to episodic memory, and the latter to spatial memory processing <sup>90</sup>.

It has been increasingly suggested that the involvement of the DG and formation of new adult-born neurons is crucial to general hippocampal function <sup>52,70,91</sup>. Indeed, attending to the continuous formation of highly functional new-born GCs in the DG, it appears that adult hippocampal neurogenesis and its role in neuroplasticity in the mammalian brain has been favoured from an evolutionary perspective <sup>92</sup>. Also, although only a small portion of these cells receives inputs from the EC, a noteworthy amplification of neuronal output can be observed through the DG-CA3 pathway, since a single GC can communicate with twelve CA3 neurons, which in turn connect with a substantial number of surrounding pyramidal cells and interneurons <sup>87</sup>. This way, spatial and visual information coming from several cortical and sensory regions, via distinct layers of the EC, is perceived and encoded by the DG, building a full spatial representation <sup>89</sup>.

The dorsal (in rodents, posterior in primates) and ventral (in rodents, anterior in primates), and even intermediate zones of the hippocampus can be functionally discriminated. In fact, these areas appear to have distinct anatomical, electrophysiological and molecular properties. Concerning behaviour, while the dorsal portion seems to be implicated in more cognitive tasks, namely contextual and spatial learning and memory, the ventral portion is suggested to be more associated with anxious and mood-related behaviours <sup>88,93</sup>. A possible segregation between the supra- and infrapyramidal layers of the DG is also worth mentioning. Particularly, enhanced plasticity in the suprapyramidal layer has been suggested due to a more complex GC morphology in relation to the infrapyramidal one, as well as increased adult neurogenesis, at baseline and in response to stimuli, like stress <sup>93,94</sup>. Additionally, hyperexcitability has been found in the infrapyramidal layer when compared with the suprapyramidal layer <sup>95</sup>. Notably, it has been recently proposed that these

subregional segregations of the hippocampus might be linked to the presence of distinct subpopulations of newly-generated neurons, contributing to different functional roles <sup>93</sup>.

The DG has been extensively implicated in pattern separation, which allows processing and storing of identical spatial contexts or locations, while avoiding overlapping or interference between similar memories. Likewise, this structure is suggested to play an important part in episodic memory, granting a way to selectively separate events in time <sup>91,96</sup>. Specifically, based mostly on evidence from studies using rodents, adult hippocampal neurogenesis seems to be required for contextual discrimination, spatial memory and pattern separation <sup>87,89,93</sup>. In this context, enhancing hippocampal neurogenesis has been shown to improve the performance in novelty recognition and pattern separation tasks <sup>89</sup>. In addition, the characteristic electrophysiological features of immature GCs was demonstrated to be essential for these tasks <sup>89,97</sup>. As an example of the contribution of adult neurogenesis for spatial learning, reducing neurogenesis by ablation of cells expressing nestin was shown to impair rodent performance in the Morris water maze test, and suggested a specific role of neurogenesis in allocentric-guided spatial navigation, but not egocentric <sup>89,98</sup>. Similarly, studies both depleting or promoting neurogenesis revealed, respectively, deficits or improvement in tasks evaluating reversal learning, indicating that new neurons are important for executive function through retrieval of formerly consolidated memories <sup>89</sup>. Of note, a possible role of neurogenesis in encoding the temporal factor of episodic memory has also been proposed, yet further studies are needed in this regard <sup>89,91</sup>.

Another projected function of adult hippocampal neurogenesis respects to memory clearance. Modulating the formation of new GCs is thought to maintain a balance between learning and forgetting: while upregulation of neurogenesis would optimize acquisition of new memories without interference with previously consolidated ones, downregulation would favour endurance of older memories rather than acquisition of new ones <sup>87</sup>.

The remarkable neuroplasticity of the hippocampal circuitry grants the ability to individually adapt in response to endogenous and exogenous stimuli, and can be reflected at several levels <sup>88</sup>. Just as changes in adult hippocampal neurogenesis influence a number of physiological and pathological processes and behaviours, the formation of new neurons is also activity-dependent, and can be modulated by many intrinsic and extrinsic factors <sup>52,70,81</sup>. This interplay is in the basis of the contribution of adult neurogenesis to hippocampal plasticity <sup>70</sup>. Regulation of neurogenesis at the cellular and molecular level includes actions of growth and neurotrophic factors, cytokines, hormones, transcription factors, neurotransmitters and epigenetic regulators. Adult neurogenesis is also activity and environmentally regulated by physiological stimuli like learning, physical exercise, metabolism, environmental enrichment, stress and aging <sup>81,82,99</sup>.

How adult hippocampal neurogenesis is modulated throughout aging is still a subject of debate<sup>65,66,100</sup>. In the aging rodent brain, an accentuated decrease in the rate of proliferation and in the number of progenitors, neuroblasts and immature neurons has been reported<sup>89,100</sup>. Concerning humans, a recent study suggests undetectable levels of hippocampal neurogenesis in adult and aged subjects, when assessing proliferation and immature neuron markers<sup>65</sup>. Conversely, different authors have described a less pronounced decline in hippocampal neurogenesis throughout adulthood and aging, with a recent study indicating that progenitor and immature neuron number is maintained, while the pool of quiescent precursor cells is specifically reduced in the anterior DG, accompanied by a decrease in angiogenesis and neuroplasticity<sup>66,80,101</sup>. Nonetheless, memory impairment and cognitive decline preferentially targeting spatial, episodic, and working memory occurs during regular aging<sup>89</sup>. As the DG appears to be the earliest structure to be affected, this cognitive decline is speculated to be associated with changes in neurogenesis<sup>89,100</sup>. Interestingly, neurogenesis in old age can still be regulated by a few stimuli, namely physical exercise, drugs and chronic stress<sup>100</sup>.

On the other hand, a noticeable degree of neuroplasticity conferred, in part, by adult neurogenesis, makes the hippocampal formation highly susceptible to detrimental conditions<sup>88</sup>. Some pathological stimuli demonstrated to inflect neurogenesis include seizures, traumatic brain injury, stroke/ischemia, drug abuse, chronic stress and psychological and neurodegenerative disorders<sup>81,82</sup>. Protein misfolding and abnormal aggregation, gradual loss of neuronal structure and/or function, and subsequent neuronal death are some of the features shared among neurodegenerative diseases like Alzheimer's, Parkinson's and Huntington's disease<sup>50,102</sup>. In recent years, compromised adult neurogenesis has also been suggested as a common characteristic in these disorders, although results both from animal models and post-mortem human samples have inconclusive, and sometimes contradicting, results<sup>50,102,103</sup>.

The extent to which a subject is influenced by a disease affecting cognitive function is thought to be dependent on its cognitive reserve. Having a high cognitive reserve can arise from increased brain volume, neuronal count, number of synapses or other quantitative features (brain reserve), and it is anticipated to correlate with a more efficient adaptability or ability of an individual to compensate for disease in the CNS or age-associated changes<sup>104</sup>. The concept of neurogenic reserve, first proposed by Kempermann in 2009, refers to the contribution of adult hippocampal neurogenesis to this process. This way, promoting neurogenesis at a young age would allow hippocampal circuitry to better adapt to new experiences and disease processes at old age, helping to build a cognitive reserve, and vice-versa<sup>105</sup>. Evidence supporting this hypothesis suggests that engagement in social and cognitively stimulating activities, a higher level of education and regular physical exercise, which are also modulators of adult neurogenesis, delay the onset of dementia symptoms, reduce the risk of AD, and promote healthy aging<sup>3,104</sup>.



### 1.2.5. Adult hippocampal neurogenesis and Alzheimer's disease

Although an impairment in adult hippocampal neurogenesis has been implicated in different neurodegenerative disorders, the consequences of AD concerning hippocampal neurogenesis in humans are unclear, and results from animal studies remain largely controversial<sup>50,106,107</sup>.

Remarkably, some key molecular players in the formation of A $\beta$  have been shown to regulate the process of adult neurogenesis<sup>68,106</sup>. As an example, enhancing  $\alpha$ -secretase activity in transgenic mice was shown to significantly promote proliferation of NPCs and neuronal differentiation, as well as the length of dendrites in immature neurons<sup>108</sup>. Although sAPP $\alpha$  appears to be physiologically involved in the positive regulation of cell proliferation, survival, adhesion and migration, as well as synaptogenesis and neurite growth, its role has not yet been well established in the adult rodent or human DG<sup>109,110</sup>. Similarly, the role of  $\beta$ -secretase in hippocampal neurogenesis remains unknown<sup>106</sup>. On the other hand, increasing the expression of AICD in mice appears to have a negative modulatory effect upon adult neurogenesis in the DG, namely by reducing neural stem/progenitor cell (NSPC) proliferation and survival in an A $\beta$ -independent manner<sup>109,111</sup>.

*In vitro*, A $\beta_{1-42}$  peptide and aggregated forms lead to impaired proliferation and neuronal differentiation, but also reduced survival of cultured human and rodent NSPCs, namely mediated by disruption of intracellular calcium homeostasis, and calpain and caspase activation<sup>112,113</sup>. Corroborating these experiments, a recent study disclosed that A $\beta_{1-42}$  oligomers promote senescence of mice NSPCs, and compromise proliferation and differentiation in culture<sup>114</sup>. Dissident from these evidences, increased neuronal differentiation of cultured rat and mice NSPCs was observed in the presence of A $\beta_{1-42}$  oligomers, while there was no change in proliferation or survival<sup>115</sup>. Notably, the toxic effect of A $\beta$  on neurogenesis has also been described as dependent on its aggregation state. Whereas monomeric and fibrillary A $\beta_{1-42}$  were shown to have a detrimental action upon cultured mice NSPCs, oligomeric forms promoted their proliferation, neuronal differentiation and migration<sup>116</sup>.

Most evidence on the role of PS1, full-length APP and A $\beta$  has been provided from the use of transgenic mouse models encompassing mutations associated with FAD. Despite the discrepancies, most studies reveal a decrease in hippocampal neurogenesis (Table 1)<sup>106,107,117</sup>.

In this regard, impaired survival, proliferation and neuronal differentiation was observed in transgenic mice carrying solely PS1 mutations<sup>118,119</sup>. Similarly, mice expressing the APP Swedish mutation (APP<sup>swe</sup>), show reduced proliferation and survival, and compromised morphological development of the DG<sup>112,120</sup>. In transgenic mice models combining APP and PS1 mutations (APP<sup>swe</sup>/PS1 $\Delta$ E9), a gradual decrease in proliferation, differentiation and maturation has been reported along with intracellular and extracellular built-up of A $\beta$ <sup>121,122</sup>. Interestingly, potentiating hippocampal neurogenesis in this model was shown to improve differentiation and survival of new neurons, and simultaneously restore recognition memory performance<sup>123</sup>. Moreover, a recent study

revealed that ablation of neurogenesis in APP/PS1 transgenic mice correlated with deficits in contextual conditioning and pattern separation <sup>124</sup>. Another mouse model that has increasingly been used to study FAD is the triple transgenic (3xTg-AD) containing APP, PS1 and tau mutations. In this model, a significant decrease in proliferation was linked to the progressive deposition of A $\beta$  <sup>125</sup>. Additional changes in downregulation of proliferation, differentiation, dendritic morphology and number of synapses in immature neurons have also been observed when using this model <sup>126</sup>. Notably, compromised neurogenesis accompanied by A $\beta$  deposition has been suggested in more complex models like the 5XFAD, which includes three different APP and two PS1 mutations <sup>127</sup>.

Notwithstanding, studies have also shown an increase in adult neurogenesis. Namely, mice expressing APP<sup>swe</sup> and Indiana (APP<sup>swe,ind</sup>) mutations reveal enhanced NSPC proliferation and neuronal differentiation, pre- and post-A $\beta$  deposition <sup>128,129</sup>. Likewise, in APP/PS1 transgenic mice, enhanced proliferation and neuronal differentiation was observed, concomitant with aggravation of A $\beta$  pathology <sup>130</sup>. Moreover, only a few authors report absent changes in neurogenesis in transgenic mouse models of AD <sup>107,131,132</sup>.

**Table 1 – Summary of the main changes in neurogenesis in different models of AD.**

| Effect on neurogenesis         | Findings   | Model       |  | References |
|--------------------------------|--|-------------|--|------------|
| Decrease                       | Survival   | Familial AD | PS1P117L   | 118        |
|                                | Proliferation; differentiation                       |             | PS1 $\Delta$ E9,M146L                                    | 119        |
|                                | Proliferation; survival; maturation                  |             | APP <sup>swe</sup>                                       | 112,120    |
|                                | Proliferation; differentiation; survival; maturation |             | APP <sup>swe</sup> /PS1 $\Delta$ E9                      | 121–123    |
|                                | Proliferation; differentiation; maturation           |             | 3xTg-AD  | 125,126    |
|                                | Proliferation; differentiation                       | Sporadic AD | Icv injection of A $\beta$ <sub>25-35</sub>              | 133        |
|                                | Survival; maturation                                 |             | Intrahippocampal injection of A $\beta$ <sub>25-35</sub> | 134        |
|                                | Proliferation; differentiation                       |             | Intrahippocampal injection of A $\beta$ <sub>1-42</sub>  | 135        |
| Proliferation; differentiation | Human AD   |             | 136  |            |
| Increase                       | Proliferation; differentiation                       | Familial AD | APP <sup>swe,ind</sup>                                   | 128,129    |
|                                | Proliferation; differentiation                       |             | APP <sup>swe</sup> /PS1 $\Delta$ E9                      | 130        |
|                                | Proliferation; differentiation                       | Human AD    |  | 137,138    |

Further perpetuating the controversy of results, alterations in adult hippocampal neurogenesis have been suggested to be stage-dependent, both referring to the stages of GC development and of disease progression. In the APPswe,ind mouse model, both morphological unfolding (dendrite extension, spine density) and function were enhanced early in GC maturation, yet became impaired at later stages, an effect that worsened with age <sup>139</sup>. In a PS1/PS2 double knock-out model, enhanced proliferation during early neurodegeneration stages was observed, fading at more advanced phases due to decreased new-neuron survival <sup>140</sup>. In line with these observations, significant changes in adult neurogenesis have been shown to occur before the onset of hallmark AD lesions. A recent study evaluated how the gradual pattern of A $\beta$  deposition into plaques in the hippocampus of two transgenic mouse models (APPswe and APPswe/PS1 $\Delta$ E9) correlated with the levels of adult neurogenesis. Elevated proliferation of neuroblasts exhibiting immature-neuron morphology was found specifically before plaque formation in both models, that overlapped with decreased survival and neuronal differentiation of new adult-born cells in the case of the APP-PS1 model <sup>141</sup>.

Studies using *post-mortem* samples from patients with AD are very limited and have produced variable results so far. One study reported that hippocampal neurogenesis was increased in patients with AD, as shown by an increase in expression of neuroblast, immature neuron and early differentiation markers, as PSA-NCAM and DCX, while expression of mature neuronal markers, like NeuN and calbindin, remained unchanged. A tendency for increased expression of some markers was found along disease severity, suggesting that the observed changes might be a compensatory mechanism in response to neurodegenerative processes <sup>137</sup>. Conversely, cell counts have demonstrated a decrease in DCX- and Sox2-positive cells in the DG of patients diagnosed with AD <sup>136</sup>. A different report revealed that while progenitor and neuroblast/immature neuron markers appear significantly increased along AD progression, this is not enough to compensate for the decrease in hippocampal stem cells <sup>138</sup>. Recently, hippocampal neurogenesis was also indicated to vary with disease aggravation. Whereas immature neurons seem to become gradually reduced, neuroblasts appear increased in moderate stages of AD <sup>142</sup>. Additionally, expression of proliferation and immature neuronal markers has been reported to be unchanged in the DG of presenile AD subjects <sup>143</sup>.

Current animal models only partially reflect AD pathology, and so do not fully correlate with human disease <sup>106</sup>. Notably, although it has been reported that transgenic mouse models of FAD display impaired learning and memory function, a clear link between these changes and compromised hippocampal neurogenesis is still lacking <sup>106,144</sup>.

A few recent examples can be listed when referring to the modulation of adult neurogenesis in sporadic rodent models of AD, which represent the most prevalent form of the disease. Intracerebroventricular injection of aggregated A $\beta$ <sub>25-35</sub> in mice was shown to decrease proliferation, differentiation, and the number of immature neurons in the DG <sup>133</sup>. Moreover, injection of this peptide into the CA1 region leads to decreased dendritic length and spine density, as well as total number

of mature neurons in the DG of rats, although proliferation and the number of immature neurons was unaffected<sup>134</sup>. In both models, these changes were suggested to correlate with impaired behaviour performance, including in the MWM and Y-Maze spontaneous alternation tasks<sup>133,134</sup>. Intrahippocampal CA1 injection of oligomeric A $\beta$ <sub>1-42</sub> leads to decreased proliferation and immature neuron differentiation in the DG of adult mice<sup>135</sup>. Interestingly, another study reported that infusion of A $\beta$ <sub>1-40</sub> and A $\beta$ <sub>1-42</sub> fibrils into the dorsal DG of rats originated a decrease in the number of mature neurons, while only A $\beta$ <sub>1-42</sub> caused a significant reduction in the number of immature neurons<sup>145</sup>.

### **1.2.6. Brain-derived neurotrophic factor and Alzheimer's disease – relevance for neurogenesis**

A $\beta$  has also been reported to impair the neuroprotective actions mediated by brain-derived neurotrophic factor (BDNF) signalling. This neurotrophin acts as an important modulator of neurogenesis, through activation of its high affinity full-length tyrosine kinase (TrkB-FL) receptors, which triggers a series of signalling pathways essential for the regulation of synaptic plasticity, cell proliferation, differentiation, survival and dendritic branching<sup>146-150</sup>. Cleavage of TrkB-FL receptors and subsequent loss of BDNF function has been identified in primary neuronal cultures incubated with A $\beta$ <sub>1-42</sub> and A $\beta$ <sub>25-35</sub>, resulting in increased levels of the corresponding truncated isoforms (TrkB-Tc) and intracellular domain fragment (TrkB-ICD). This cleavage is mediated by activation of extrasynaptic NMDARs and calpain activation, a calcium-dependent protease, and prevented in the presence of memantine (Fig. 6)<sup>151,152</sup>. Interestingly, these changes have been proposed to contribute to the cognitive decline observed in AD. *In vivo* studies suggest that BDNF in the DG has a relevant role in pattern discrimination, by a process that requires adult-born neurons<sup>87</sup>. Moreover, overexpression of TrkB-Tc was demonstrated to exacerbate spatial memory impairment, an effect attenuated by overexpression of TrkB-FL<sup>153</sup>. In fact, in agreement with what was observed *in vitro*, an imbalance in TrkB receptor isoforms was identified in post-mortem samples from AD patients<sup>152,154</sup>.

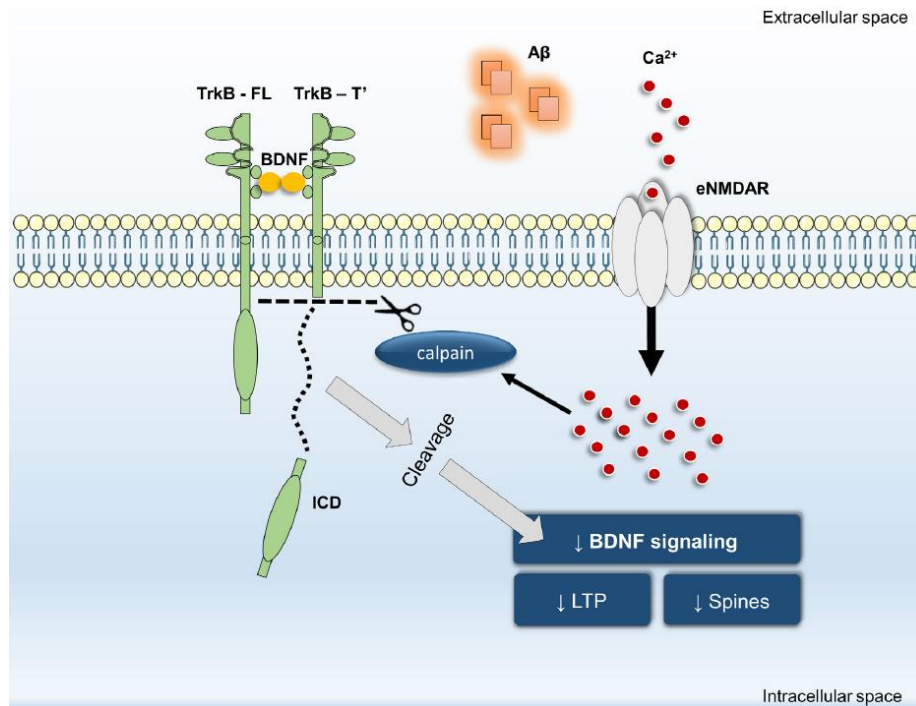


**Fig. 6 – Putative mechanism for the cleavage of TrkB-FL receptors in the presence of A $\beta$ .** Extracted from Tanqueiro et al, 2018 <sup>151</sup>.

Keeping the discrepancies in mind, together, this growing evidence from animal studies suggests the potential of modulating adult hippocampal neurogenesis as a therapeutic target for the development of disease-modifying treatments for AD. In this regard, studies have focused on compounds that enhance neurogenesis, yet not many have used models of AD <sup>23,110</sup>. For instance, an interesting work recently demonstrated improvement of neuronal differentiation and survival in the APP<sup>swe</sup>,ind mouse model, upon combined action of enhanced neurotrophic support and scyllo-inositol, a compound previously shown to ameliorate A $\beta$  pathology and cognitive function <sup>155</sup>. Protecting neurogenesis while improving cognitive deficits by pharmacologically diminishing microglial activation in APP/PS1 transgenic mice has also been suggested as a promising target <sup>123</sup>. Remarkably, drugs currently used in the management of AD, such as galantamine and memantine, have been shown to significantly potentiate neurogenesis *in vitro* and *in vivo* <sup>156</sup>. Nonetheless, strategies that directly and specifically modulate neurogenesis at the hippocampus are wanting <sup>23</sup>.

## 2. Aims

The neurotoxic mechanisms associated with AD have been extensively described, yet the pathogenesis of this disease remains unclear, as does the order of pathological events that characterize the various stages of progression, especially in preclinical and mild stages. Attending to the alarming increase in population aging and incidence of AD, understanding its pathophysiology and exploring novel efficient therapies represents a major issue worldwide.

Modulation of adult neurogenesis has been proposed as a potential disease-modifying target, although, to date, results from animal models have presented substantially variable results, and evidence from sporadic, more translatable models of human AD, is extremely limited. Therefore, the main objective of the present work was to evaluate adult hippocampal neurogenesis in a model of the initial stages of late-onset AD. To this end, three specific aims were considered: i) to obtain the model of disease by performing an intracerebroventricular injection of A $\beta$ <sub>1-42</sub> peptide in adult male Wistar rats, ii) to characterize the behaviour of these rats after the injection, and iii) to investigate how cell proliferation and neuronal differentiation in the DG of these animals is modulated after the injection.

### 3. Materials & Methods

#### 3.1. Ethical Concerns

All experimental procedures were conducted in conformity with the European Community legislation (86/609/EEC; Directive 2010/63/EU, 2012/707/EU). These procedures were approved by the Ethical Committee of the Faculty of Medicine, University of Lisbon and by the Animal Ethics Committee of *Instituto de Medicina Molecular* (iMM), as well as by the *Direção Geral de Alimentação e Veterinária* (DGAV), the Portuguese competent authority for animal protection. To minimize the number of animals used for *in vivo* procedures, optimal sample size was estimated to be 7 animals per group, by performing a power analysis with the G\*Power 3.1 software, based on previous experiments using the same model. Considering the variability associated with behaviour tests and disease manifestation, as well as possible complications arising from surgical procedures, it was decided to use 10 animals per group. Animal suffering was minimized to the greatest extent.

#### 3.2. Animals & Housing

For *in vivo* procedures, young-adult male Wistar rats were acquired from Charles River (Barcelona, Spain). Animals were housed together in groups of 5 per cage upon arrival, with unrestricted access to food and water, and under controlled temperature and light conditions (22°C; lights on between 7 am and 9 pm). A period of at least 5 days for acclimatization at the rodent facility of iMM before any experimental procedure was considered. Surgical procedures were performed during the light period of the 14/10h light/dark cycle, when the rats were 9-10 weeks-old, weighting 260-375g. After surgery, animals were kept in groups of 2-3 per cage to facilitate recovery. Rats were regularly monitored for general appearance, activity, feeding behaviour and body weight throughout the whole protocol, taking a closer attention during post-operative recovery.

For *in vitro* analysis, specifically primary neuronal cultures, 18/19-day pregnant Sprague-Dawley female rats were purchased from Charles River (Barcelona, Spain).

#### 3.3. Timeline for *in vivo* Experimental Procedures

Animals were divided in 2 groups: control (vehicle icv injection) and A $\beta$  (A $\beta$ <sub>1-42</sub> icv injection). Fig. 7 shows a representative timeline for studying the effects mediated by A $\beta$ <sub>1-42</sub> icv injection in adult hippocampal neurogenesis. BrdU was administrated intraperitoneally for 3 days at the beginning of the protocol, followed by A $\beta$ <sub>1-42</sub> injection 3 days later. To guarantee that neuronal differentiation occurred before sacrifice, a minimum of 28 days from the first BrdU injection was maintained, as well as a period of 2 weeks between A $\beta$ <sub>1-42</sub> peptide administration and the beginning of behavioural testing, as it has been reported that memory deficits become more evident from that point<sup>157</sup>. To

help minimize stress, handling of the animals was performed for at least 3 days before the first ip injections and again before behaviour tests. Rats were sacrificed at the end of behaviour assessment and brain tissue was processed for immunohistochemical analysis. Additionally, for histology, western blot and ELISA protocols, 3 rats from each group were sacrificed 3 and 14 days after icv injection, as these timepoints are reported to allow evaluation, respectively, of the presence and absence of A $\beta$ <sub>1-42</sub> in the hippocampus<sup>157</sup>.

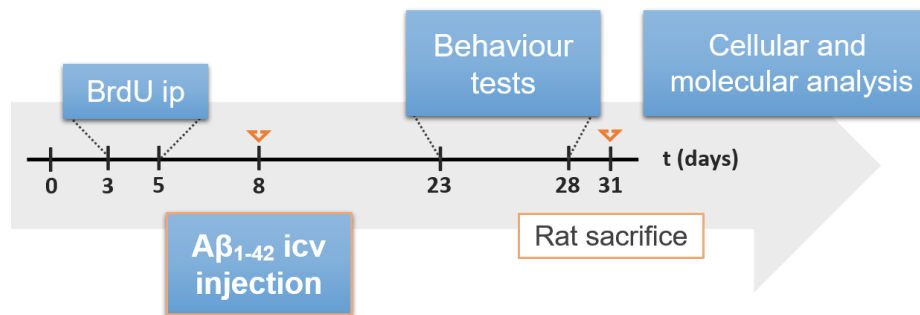


Fig. 7 – Timeline for *in vivo* experimental procedures.

### 3.4. BrdU Administration

To study neuronal differentiation and cell proliferation, a solution of 5-bromo-2'-deoxyuridine (BrdU) (Sigma-Aldrich, MO, USA) was prepared in a sterile solution of 0.9% NaCl. BrdU was injected intraperitoneally (ip) twice a day, with 8-9h interval, for 3 days at the beginning of the protocol (Fig. 7), at 100 mg per Kg of body weight. This compound is a synthetic nucleoside thymidine analogue widely used in the context of neurogenesis studies, since it is able to incorporate the DNA of cells in division, specifically during replication (S-phase of the cell cycle)<sup>62,158</sup>.

### 3.5. A $\beta$ <sub>1-42</sub> Peptide Injection

Aiming at obtaining an *in vivo* model of the sporadic form of AD, surgeries were performed to inject a solution of the 42-amino acid form of the amyloid  $\beta$  peptide intracerebroventricularly (icv), as previously described<sup>157,159</sup>. The solution was prepared at a concentration of 498  $\mu$ M by dissolving Amyloid  $\beta$ -Protein (1-42) (Bachem, CA, USA) in sterile Milli-Q<sup>®</sup> water (Merck, Darmstadt, Germany) previously set at pH 10.



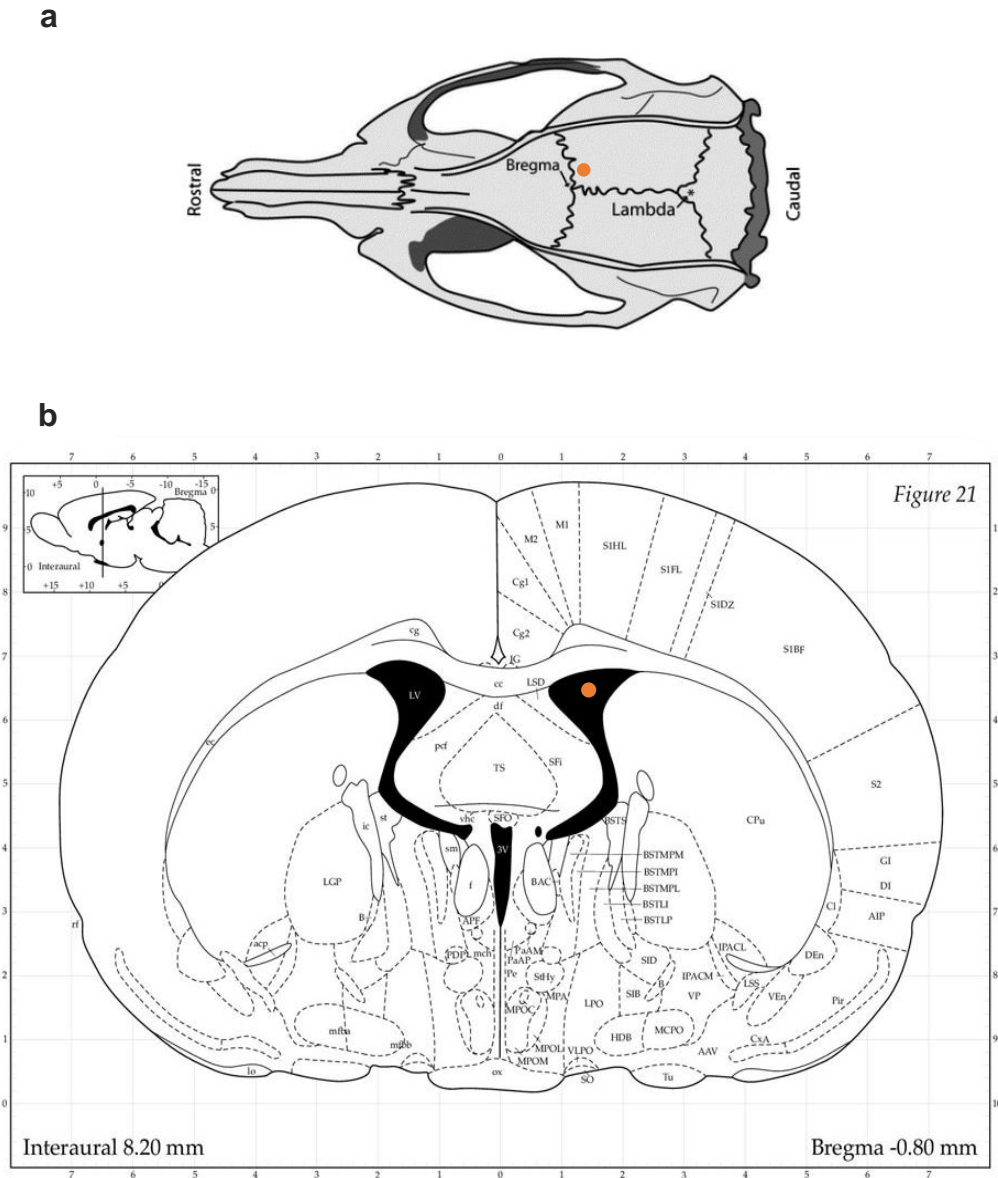


**Fig. 8 – Schematic representations of the stereotaxic coordinates used for the icv injection. (a)** Cranial sutures, anatomical location of bregma, and site of injection (orange dot), from a top view. Adapted from Assi et al, 2012 <sup>160</sup>. **(b)** Site of injection (orange dot), from a coronal view. Having bregma as a reference, the site of injection was defined as -0.8 mm anterior-posterior, +1.5 mm medial-lateral, +3.5 mm dorsal-ventral. Adapted from Paxinos and Watson, 1998 <sup>161</sup>.

For this, animals were anesthetized with isoflurane, containing 2-3% O<sub>2</sub>, first using a chamber with gas scavenging system, and then kept under deep anaesthesia via facial mask, throughout the whole surgical procedure. To prevent hypothermia, animals were kept on top of heating pads (37°C) at all times. After shaving the fur of the head, exposed skin was disinfected with Betadine® (Meda Pharmaceuticals, NJ, USA), and local anaesthetic emla® cream (AstraZeneca, London, UK) was applied inside the ear canal to minimize pain or discomfort once the animal was placed in the stereotaxic apparatus with ear bars to stabilize the position of the head. Lacryvisc® ophthalmic gel (Alcon, Hünenberg, Switzerland) was also applied to the eyes of the animal to prevent dehydration.

General analgesic buprenorphine (0.016 mg/ml, in NaCl) was administered subcutaneously (0.05 mg per kg of body weight). Next, animals were transferred to a stereotaxic apparatus (Stoelting, IL, USA). Using a scalpel, a longitudinal incision along the midline of the head was done to expose cranial sutures. Having bregma as a reference, the following coordinates were used for the site of injection: -0.8 mm anterior-posterior (AP), +1.5 mm medial-lateral (ML), +3.5 mm dorsal-ventral (DV) (Fig. 8a,b). A small hole was drilled in the skull, and the injection of 4  $\mu$ L of the A $\beta$ <sub>1-42</sub> solution was carried out directly inside the right lateral ventricle of the rats, with a 10  $\mu$ l, 33-gauge Microliter Syringe (Hamilton Company, NV, USA) and a Micro4™ MicroSyringe Pump Controller (World Precision Instruments, FL, USA), at a constant rate of 400 nl/min for 10 min. For control rats, the same volume of vehicle solution (Milli-Q® water, pH 10) was injected. After removing the syringe, the skin of the rat was sutured with Silkam® 4/0 silk sutures (Braun, Melsungen, Germany), and Bepanthen® Plus (Bayer, Leverkusen, Germany) was applied on top of the sutures. Animals were maintained individually on recovery cages until regaining ambulatory ability.

### 3.6. Behavioural Analysis

Patients suffering from AD usually present memory deficits at initial stages of the disease, that tend to aggravate along the disease progression, namely due to compromised hippocampal function<sup>12</sup>. Thus, evaluation of behavioural paradigms, specifically regarding memory performance, was a crucial step at attempting to characterize our model as an *in vivo* model of sporadic AD. For this, different test batteries were carried out using three distinct animal batches (Table 2). First, the open field (OF) and the novel object recognition (NOR) were performed during the dark period of the light/dark cycle, under red light, which is believed to be perceived by the rats as darkness<sup>162</sup>. Next, two new test batteries were implemented during daytime under dim light conditions, to see if changes in circadian rhythms could be influencing the paradigms tested. These included the OF and NOR, already performed in the first batch, but also the elevated plus maze (EPM), Y-Maze spontaneous alternation (SA), Y-maze forced alternation (FA) and Morris water maze (MWM) tests. The tests in Table 2 are listed in the same order in which they have been performed for each batch of animals.

In each day, rats were habituated to the test room for at least 30 min before starting any behaviour assessment. To erase any olfactory clues, for every test and between each trial, the arena and/or objects were carefully cleaned with a 30% ethanol solution. In every test, except for the Morris water maze test, the experimenter moved from the test room to an independent room immediately after placing the animal in the corresponding apparatus. Parameters assessed in the EPM, OF and MWM tests were recorded using the SMART V2.5 video-tracking software (Barcelona, Spain). In contrast, the NOR and Y-maze SA and FA tests were video recorded and posteriorly analysed by an observer blind to the experimental conditions, as is described ahead.

**Table 2 - Behaviour tests performed for each batch of rats and corresponding time of day.**

| <b>Batch number</b> | <b>Test battery</b>  | <b>Time of day</b>  |
|---------------------|--|---|
| <b>1</b>            | I. Open Field<br>II. Novel Object Recognition  | Dark period of the light/dark cycle;<br>Red light                         |
| <b>2</b>            | I. Elevated Plus Maze<br>II. Y-Maze Forced Alternation<br>III. Morris Water Maze                               | Light period of the light/dark cycle;<br>Dim light (approximately 15 lux) |
| <b>3</b>            | I. Elevated Plus Maze<br>II. Y-Maze Spontaneous Alternation<br>III. Open Field<br>IV. Novel Object Recognition | Light period of the light/dark cycle;<br>Dim light (approximately 15 lux) |

### **3.6.1. Open Field (OF)**

The OF test grants the opportunity to appraise rat locomotor activity <sup>163</sup>, which was tested since it can represent an important paradigm influencing learning and memory performance. The apparatus consists of an empty square box (60x60x40 cm), virtually divided in three concentric squares at a similar distance from each other (Fig. 9). Each animal was placed individually in the centre of the box and allowed to freely explore it for 5 min, without prior habituation. Results are presented as mean velocity (cm/s), total distance travelled (cm) and number of transitions between the peripheral, intermediate and central zones (PZ, IZ and CZ) (Fig. 9). In addition, this test was also used as part of the first day of the habituation phase for the NOR test.

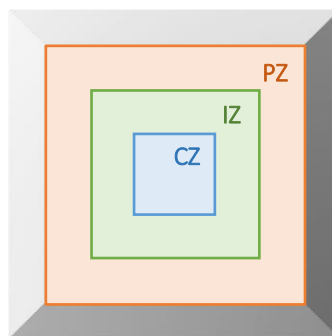


**Fig. 9 – Schematic representation the OF arena.** The arena was divided in three virtual concentric squares. PZ – Peripheral zone; IZ – Intermediate zone; CZ – Central zone.

### 3.6.2. Elevated Plus Maze (EPM)

Being one of the most commonly used tests for evaluation of anxiety-related behaviour in rodents <sup>164</sup>, the EPM test was performed to assess if changes in this paradigm could be influencing the cognitive performance of the animals. The maze consists of a plus-shaped structure elevated 50 cm above the ground, that is made up of four arms perpendicular to each other: two arms with no walls (open arms, 50x10 cm), alternated with two closed arms (50x10x30 cm) (Fig. 10). Without prior habituation, each animal was placed at the intersection of the maze, with the head facing one of the open arms, and allowed to move freely for 5 min. In this context, anxious-like behaviour can be studied due to the natural preference of rats for dark and enclosed spaces, and avoidance of open spaces where they feel unprotected <sup>164</sup>. Therefore, the time spent inside the open arms (%) and the number of entries in the open arms were measured, with more time spent in the open arms corresponding to a lower anxiety-related behaviour.

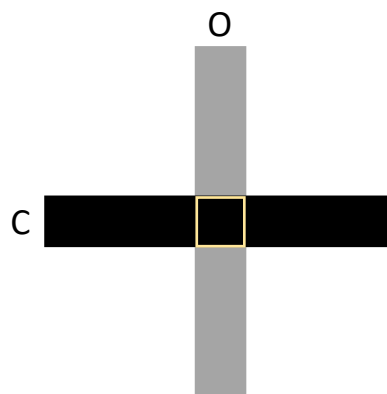


**Fig. 10 – Schematic representation of the EPM apparatus.** The structure is composed of two open arms (O), with no walls, alternated with two closed arms (C), at a 90-degree angle from each other.

### 3.6.3. Y-Maze Spontaneous Alternation (SA)

This test was implemented in order to evaluate spatial working memory performance, as it involves different parts of the brain, namely the hippocampus <sup>165–167</sup>. The Y-shaped maze is composed by three identical arms (50x10x30 cm), converging to an equal angle. Visual cues were placed on the walls at the end of each arm of the maze, to aid the animals in remembering which arms had already been visited (Fig. 11). Without prior habituation, each rat was positioned at the end of one arm, facing away from the centre, and allowed to move freely during 8 min. As healthy rodents tend to alternate between the arms, not visiting the same arm twice in a row, the sequence of arm entries was recorded, manually <sup>166,168</sup>. An arm entry was considered whenever the two forelimbs were completely inside that arm, and an alternation was denoted as consecutive entries in all three arms. Spontaneous alternations (%) for each animal was calculated as the number of actual

alternations, divided by the number of maximum alternations, where the maximum alternations possible is the total number of arm entries minus 2.

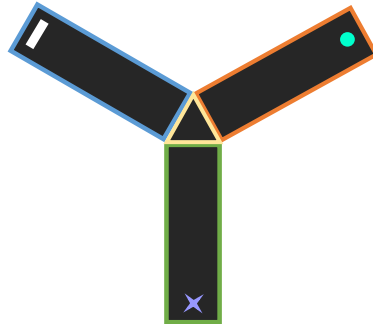


**Fig. 11 – Schematic representation of the apparatus used in the Y-Maze.** The structure consists of three identical arms that converge to an equal angle, with visual cues placed on the walls at the end of each arm.

#### **3.6.4. Y-Maze Forced Alternation (FA)**

Short-term memory performance and exploratory behaviour can be assessed by performing the Y-Maze FA test<sup>169,170</sup>. The same apparatus with the same visual cues as for the Y-Maze SA was used (Fig. 11), and the test was divided in two phases. On the learning phase, one of the three arms (novel arm) was blocked by a removable door, while the other two remained open (start arm and other arm). A rat was placed at the end of the start arm, facing away from the centre, and explored the maze for 10 min. On the test phase, the blocking door was removed after an inter-trial interval (ITI) of 3 h, and the animal was returned to the start arm, from which it was possible to explore the whole maze for 5 min, with the novel arm now available. The start arm, as well as the novel one, were changed between animals to avoid any preference for one of the arms. The time spent exploring each arm (s) and the total number of arm entries in both phases were recorded manually. The total number of arm entries was used to evaluate exploratory behaviour. Memory performance was expressed as presence time (%) inside each of the three arms during the test phase.

#### **3.6.5. Novel Object Recognition (NOR)**

The NOR test is divided in three phases, being particularly useful for evaluating memory performance, namely long-term memory<sup>171</sup>. In the habituation phase (3 consecutive days), each rat freely explored the empty OF arena for 15 min, followed by the familiarization phase (in the fourth day), where the animal was presented with the two to-be-familiarized objects (familiar objects) for 5 min. The animal then returned to its cage for 24 h. After this ITI, the rat returned to the arena for the test phase, where he was presented with one previously experienced object and a novel object, for

5 min. The objects consisted of two brown and two transparent glass bottles (base of 5 cm in diameter, 22 cm in height) filled with water, that were attached to the bottom of the box with velcro tape as represented in Fig. 12. These bottles were used interchangeably as familiar and novel objects. Data were obtained by manually recording the time (s) that a rat spent exploring the objects individually. Exploration was scored whenever the animal touched an object with its forepaws and/or bit, sniffed or reared towards the object. Running around the object, standing next to it with its head facing away or climbing it was excluded.

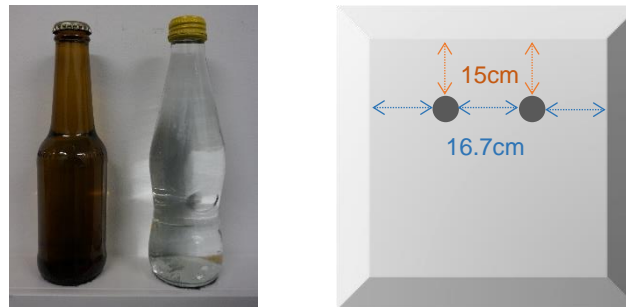


**Fig. 12 – Examples of the objects used in the NOR test as familiar and novel.** The bottles were attached to the bottom of the box, at 15 cm from the walls on one side, and approximately 16.7 cm from each other.

Total exploration time (s) of both objects in the familiarization or test phase was used as a measure of exploratory drive. Regarding long-term memory performance, results are presented as exploration time (%) for each object, and for each phase, being the time spent exploring that object divided by the total time spent exploring both objects. The novelty discrimination index, assessed in the test phase, was defined as the time spent exploring the novel object minus the time spent exploring the familiar object, divided by the total time spent exploring both objects.

### **3.6.6. Morris Water Maze (MWM)**

The MWM test is widely described as a way of evaluating hippocampal-dependent spatial learning and reference memory performance<sup>169,172</sup>. For this test, a circular pool with 180 cm in diameter and 60 cm in height was filled with water at a temperature of  $24 \pm 1$  °C, until it reached approximately 46 cm in height. The water was then made opaque by adding nontoxic water-based black paint. Visual reference cues were positioned on the walls of the room. The pool was virtually divided into 4 quadrants, and a black platform of 10 cm in diameter was placed at the centre of one of the quadrants, hidden 1 cm below water level (Fig. 13). The placing of the platform was changed between animals to avoid preference of the rats for any side of the room and/or pool. The test comprised two phases. First the learning, or acquisition phase, consisting of four days, with four trials per day for each animal. In every trial, a rat was placed inside the pool, near the wall and facing it.

The starting point was randomized between trials and was never on the same quadrant of the platform, neither on its intersections with neighbour quadrants. For instance, if the platform was placed on the first quadrant (Q1), the starting point was not 1, 1/2 or 4/1 (Fig. 13). A trial was finished if the animal found the platform within 60 s and remained on top of it for 10 s. If the animal could not find the platform and/or stand on it within 60 s, it was manually guided to the platform and allowed to remain there for 20 s. Trials were separated by an interval of at least 30 min. During this period, animals were towel-dried and remained on their home cages under heat lamps, to prevent hypothermia. The probe test was performed on the fifth day, consisting of a single trial in which the platform was removed, and the rat swam freely for 60 s.

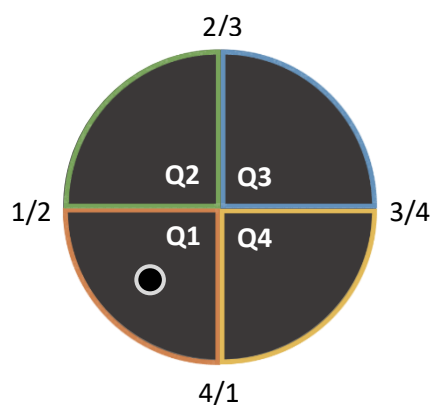


**Fig. 13 – Schematic representation of the MWM pool.** Virtual quadrants (Q1-4) and starting sites (1-4/1) are depicted. The platform (white circle) is illustrated in the centre of the first quadrant as an example.

Mean velocity (cm/s) was used as a measure of locomotor activity during acquisition phase. Results concerning learning and memory performance during this phase are presented as time to platform (s), being the mean time of the four trials in each day. For the probe test, these results are expressed as: time to platform, being the time that the rats took to reach the virtual area where the platform was previously located; time in Qp (%), defined as the percentage of time that the rats spent in the virtual platform area; rats that first visited the virtual platform area (%); and total number of platform crossings.

### 3.7. Animal Sacrifice and Tissue Processing

At the end of the protocol, animals were sacrificed for immunohistochemical examination by whole animal perfusion. After reaching the deep anaesthesia state with isoflurane, rats were perfused transcardially with phosphate-buffered saline (PBS) (NaCl 137mM, KCl 2.1mM, KH<sub>2</sub>PO<sub>4</sub> 1.8mM and Na<sub>2</sub>HPO<sub>4</sub>·2H<sub>2</sub>O 10mM, pH 7.4), followed by 4% paraformaldehyde (PFA) in PBS (pH 6.8-7.4) <sup>173</sup>. After decapitation, the brains were removed, post-fixed in 4% PFA (24 h, 4°C), and

subsequently submerged with 15% and 30% sucrose in PBS (4°C). Brains were then gelatine-embedded and coronally sectioned at a thickness of 40 µm using a cryostat Leica CM3050 S (Leica Biosystems, Wetzlar, Germany). Only coronal sections of the hippocampus from the left-brain hemisphere were collected, in ten series, each one comprising an anterior-posterior reconstruction of the hippocampus where sections are separated by 400 µm. Sections were collected to anti-freezing medium (30% glycerol, 30% ethylene glycol, phosphate buffer 0.1 M (8.9% Na<sub>2</sub>HPO<sub>4</sub>·2H<sub>2</sub>O, 7.8% NaH<sub>2</sub>PO<sub>4</sub>·2H<sub>2</sub>O, pH 7.3-7.4)), in 24-well plates and stored at -20°C.

The group of animals sacrificed on day 3 and 14 after icv injection were perfused transcardially only with PBS, so that the left hemisphere was used for histological analysis and the right hemisphere for molecular analysis. For histological analysis, left brain hemispheres were post-fixed in 4% PFA (72 h, 4°C), submerged in 15% and 30% sucrose (4°C), and then paraffin-embedded and sectioned at a thickness of 4 µm using a microtome Leica RM2245 (Leica Biosystems). One series of sixteen coronal sections of the hippocampus from left brain hemispheres were collected, beginning at -3.5 mm anterior-posterior from bregma. Sections were collected to microscope slides (Superfrost™ Plus, ThermoFisher Scientific, MA, USA) and stored at room temperature (RT). For western-blot and ELISA protocols, right brain hemispheres were sectioned at a thickness of 450 µm using a McIlwain™ Tissue Chopper (Campden Instruments, Loughborough, UK). DG, CA1-CA3 and SVZ regions were dissected individually and stored at -80°C.

### **3.8. Primary Neuronal Cultures**

Primary neuronal cultures were performed to appraise the effects of the same Aβ<sub>1-42</sub> peptide solution that was injected *in vivo* on TrkB receptor isoforms and cell death. First, foetuses from 18/19-day pregnant Sprague-Dawley rats were collected in Hank's balanced salt solution (HBSS), followed by brain dissection, cerebral cortex isolation and meninge removal. After being mechanically fragmented, the tissue was digested with a solution of 0.025% trypsin in HBSS (15 min, 37°C), and centrifuged at 1200 rpm to precipitate cells. Supernatant was discarded, and 20% Foetal Bovine Serum (FBS) in HBSS was added to the pellet. Cells were once more precipitated by centrifugation, the supernatant was removed and 2 ml of HBSS were added to the pellet. This was repeated four times to neutralize trypsin. To dissociate cells, resuspension by pipette aspiration was required between centrifugations. Next, cells were resuspended in Neurobasal medium supplemented with 0.5 mM L-glutamine, 25 mM glutamic acid, 2% B-27, and 25 U/mL penicillin/streptomycin, and then filtered using a BD Falcon™ Cell Strainer 70 µm (ThermoFisher Scientific) nylon filter, to obtain single cells and avoid cell clusters or tissue fragments. Cells were plated at 6 x 10<sup>4</sup> cells/cm<sup>2</sup> on coverslips, previously sterilized under UV light, coated with 10 µg/mL of poly-D-lysine (Sigma-Aldrich) overnight to improve cell adhesion, and washed with sterile Milli-Q® water. Cells were maintained at 37°C in a humidified atmosphere of 5% CO<sub>2</sub> for 14 days *in vitro* (DIV).



At 14 DIV, primary neuronal cultures were incubated with 20  $\mu\text{M}$  of  $\text{A}\beta_{1-42}$  prepared from the solution previously injected *in vivo* (24h, 37°C). These conditions were selected based on the literature and previous work done at our laboratory<sup>152,153</sup>.

Cell cultures were performed by João Gomes, Rita Belo and Sara Tanqueiro.

### 3.9. Cellular & Molecular Analysis

#### 3.9.1. Immunohistochemistry (IHC)

Free-floating IHC was performed to assess neuronal differentiation and cell proliferation in brain samples of rats injected with BrdU at the beginning of experiments (differentiation protocol). Details on primary antibodies used for this technique are listed in Table 3. A complete series of slices from each animal, using a specific antibody combination was considered  $n=1$ . Slices were degelatinized in PBS (3 x 10 min, 37°C), and treated with HCl 1M (10 min, 4°C), followed by HCl 2M (30 min, 37°C), to expose BrdU epitopes. Next, borate buffer 0.1M (pH 8.5) was applied (2 x 5 min, RT), and slices were washed with PBS (3 x 10 min). A blocking solution containing 3% bovine serum albumin (BSA) and 0.2% Triton™ X-100 in PBS was then added (1 h, RT). Slices were incubated with primary antibodies mouse anti-BrdU (1:500) and goat anti-DCX (1:500), prepared in the same blocking solution, for 22-24 h (4°C). After this period, slices were washed in PBS (3 x 10 min) and incubated with secondary antibodies anti-mouse Alexa Fluor 488 (1:500) and anti-goat Alexa Fluor 568 (1:500), and DAPI (4',6'-diamidino-2-phenylindole) (1:1000) (2 h, RT). After washing in PBS (3 x 10 min), slices were mounted on microscope slides (Superfrost™ Plus, ThermoFisher Scientific) with Mowiol, and glass coverslips on top. For NeuN staining, a similar protocol was followed, with a few exceptions. A blocking solution of 6% BSA and 0.2% Triton™ X-100 was used, and incubation with primary antibodies mouse anti-BrdU (1:500) and rabbit anti-NeuN (1:500) lasted two overnights (4°C). Secondary antibodies anti-mouse Alexa Fluor® 488 (1:500) and anti-rabbit Alexa Fluor® 568 (1:500) (Life Technologies) were used.

**Table 3 – Primary antibodies used to study neurogenesis by immunohistochemistry.**

| Antibody  | Host   | Supplier                            | Reference | Dilution |
|-----------|--------|-------------------------------------|-----------|----------|
| Anti-BrdU | Mouse  | Dako, CA, USA                       | M0744     | 1:500    |
| Anti-DCX  | Goat   | Santa Cruz Biotechnology, TX, USA   | sc-8066   | 1:500    |
| Anti-NeuN | Rabbit | Cell Signalling Technology, MA, USA | 12943S    | 1:500    |

### 3.9.1.1. Image Acquisition and Analysis

Because the dorsal hippocampus has been shown to be more related to cognition, namely spatial memory and pattern separation <sup>174,175</sup>, only the dorsal sections of the DG were analysed herein. Dorsal DG was defined as the totality of the coronal sections that went from the first section of the most anterior region, until approximately -4.16 mm from bregma (Fig. 14).

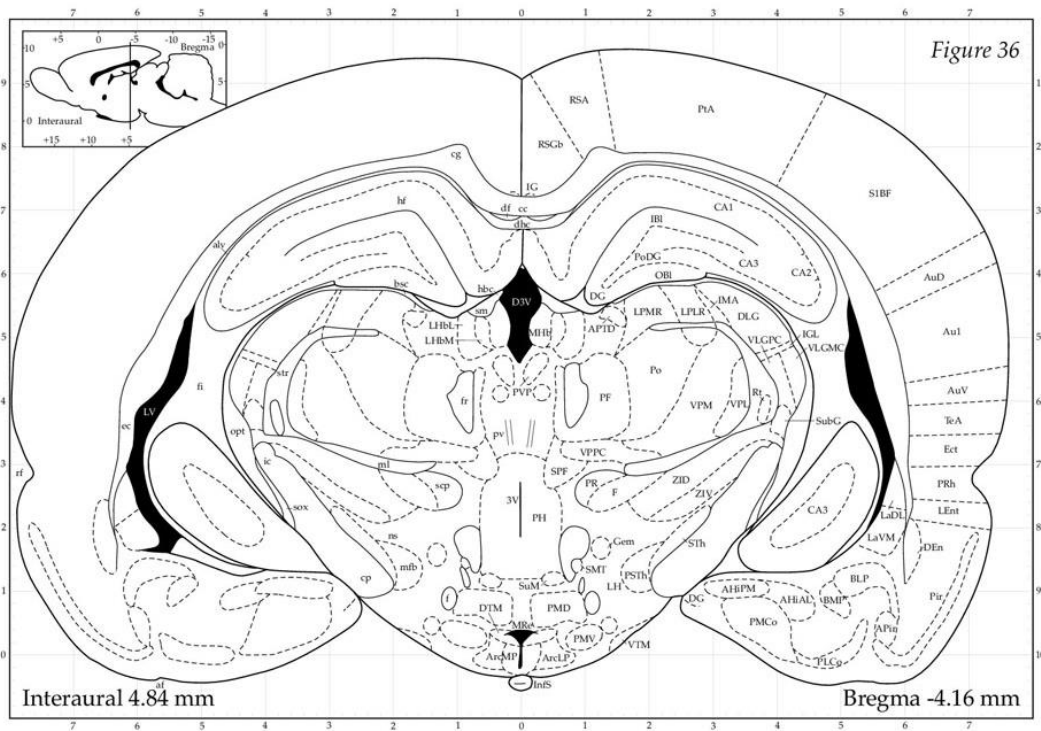


**Fig. 14 – Schematic representation of the dorsal-ventral DG interface (coronal view).** Adapted from Paxinos and Watson, 1998 <sup>161</sup>.

Images of the DG were captured using a Zeiss LSM 880 with Airyscan (Carl Zeiss, Oberkochen, Germany) confocal point-scanning microscope, with a 40x objective, throughout the entire thickness of each coronal section (40  $\mu\text{m}$ ). Quantification of BrdU-, DCX-, and NeuN-immunopositive cells was achieved by manually counting these cells within the DG layer, using the ZEN 2.3 software (Carl Zeiss). The area ( $\text{mm}^2$ ) of the DG of each section was measured by drawing a line around the whole DG cell layer, using the same software. The total volume ( $\text{mm}^3$ ) of dorsal DG for each animal was extrapolated by multiplying the sum of the areas by the distance between slices (400  $\mu\text{m}$ ). Results are presented as the number of immuno-positive cells per volume ( $\text{mm}^{-3}$ ) of DG of each section.

### **3.9.2. Histology**

To assess the presence of A $\beta$ , brain slices from rats sacrificed at 3 and 14 days post-surgery were stained with Congo red. Although this staining is able to bind several A $\beta$  species, from monomers to mature fibrils, a yellow-green birefringence is highlighted under crossed polarizers due to the spatial orientation of Congo red molecules along the axis of the fibrils, making it particularly useful for specific detection of amyloid deposition (protofibrils and fibrils)<sup>176</sup>. For this, the Bennhold's Congo red staining protocol was used, as previously described<sup>177</sup>. Briefly, sections were deparaffinized, hydrated in distilled water and stained with Congo red solution (1% Congo red (Sigma-Aldrich) in distilled water) for 30-60 min. After rinsing in distilled water, sections were rapidly differentiated (5-10 dips) in alkaline alcohol solution (0.01% sodium hydroxide, 50% ethanol), followed by rinsing in tap water (5 min) and counterstaining with Gill's haematoxylin (30 min). Sections were rinsed again in tap water (1 min), dipped in ammonia water until they turned blue, and rinsed once more in tap water (5 min). Finally, slices were dehydrated through 95% ethanol and 100% ethanol, cleared in xylene and mounted with resinous mount medium.

A sample from human kidney tissue with known amyloidosis content was used as a positive control. Slides were observed under polarized light using a Leica DM2500 microscope (Leica Microsystems). Representative pictures were taken with a 20x objective.

Congo red staining protocol was performed by the histology service of IMM.

### **3.9.3. Western Blot (WB)**

#### **3.9.3.1. Tissue Samples**

This technique was used to assess the levels of TrkB-FL receptors, and corresponding TrkB-ICD originated from its cleavage, in the DG, CA1-CA3 and SVZ regions of rats sacrificed at 3 and 14 days post-surgery. For this, tissue samples were homogenized under sonication with Radio Immuno Precipitation Assay (RIPA) lysis buffer (4% Nonidet<sup>®</sup> P40 Substitute (NP40), 1 mM ethylenediamine tetraacetic acid (EDTA), 150 mM NaCl, 50 mM Tris base), containing one cOmplete<sup>™</sup> Mini, protease inhibitor cocktail tablet (Roche, Penzberg, Germany) for each 10 ml. Absorbance was read at 750 nm (Infinite M200 multimode microplate reader, Tecan), and total protein quantification was performed using the Bradford assay and DC<sup>™</sup> Protein Assay kit (Bio-Rad Laboratories, CA, USA), with BSA as standard. After adding 6x sample buffer (36% glycerol, 12% SDS, 0.015% bromophenol blue, 720 mM dithiothreitol, 420 mM Tris, pH 6.8), samples were denatured (10 min, 95°C).

Proteins were separated by sodium dodecyl sulphate polyacrylamide gel electrophoresis (SDS-PAGE), in running buffer (0.1% SDS, 192 mM glycine, 25 mM Tris pH 8.3), at constant voltage (80-120 V), using 10% acrylamide/bis-acrylamide resolving gels (0.1% SDS, 0.1% ammonium

persulfate (APS), 0.04% N,N,N',N'-tetramethylethane-1,2-diamine (TEMED), 375 mM Tris pH 8.8), and 5% acrylamide/bis-acrylamide stacking gels (0.1% SDS, 0.1% APS, 0.1% TEMED, 125 mM Tris pH 6.8), with 1.5 mm thickness. NZYColour Protein Marker II (NZYTech, Lisbon, Portugal) was used as a protein molecular weight marker. Proteins were transferred to polyvinylidene difluoride (PVDF) membranes, previously soaked with methanol, in transfer buffer (10% methanol, 192 mM glycine, 25 mM Tris pH 8.3), at constant amperage (350 mA, 1h15), and blocked with 3% BSA in Tris buffered saline with Tween<sup>®</sup> 20 (TBS-T) (200 nM Tris, 1.5 M NaCl, 0.1% Tween<sup>®</sup> 20, pH 7.6) (1h, RT). All primary and secondary antibodies were prepared in the blocking solution. Glyceraldehyde-3-phosphate dehydrogenase (GAPDH) was used as loading control. Membranes were washed in TBS-T (3 x 5 min), followed by incubation with primary antibodies rabbit anti-Trk (C14) (1:1000) and mouse anti-GAPDH (1:5000), overnight (4°C). Information on primary antibodies is presented in Table 4. Next, membranes were again washed and incubated with secondary antibodies conjugated to horseradish peroxidase (HRP), IgG anti-rabbit (1:10 000) and IgG anti-mouse (1:10 000) (Santa Cruz Biotechnology), for 1h (RT). After washing, proteins were revealed with Clarity<sup>™</sup> Western ECL Substrate (Bio-Rad Laboratories), using ChemiDoc<sup>™</sup> XRS+ imaging system with Image Lab<sup>™</sup> software (Bio-Rad Laboratories). Resulting images were processed and analysed using Fiji 1.51s software (MD, USA) <sup>178</sup>. Results are expressed as protein levels (% CTL).

### **3.9.3.2. Samples from Primary Neuronal Cultures**

The levels of TrkB-FL/TrkB-ICD isoforms, as well as the levels of  $\alpha$ -II Spectrin and corresponding breakdown product (SBDP150), which reflect calpain activity, were assessed in the samples from primary neuronal cultures incubated with A $\beta$ <sub>1-42</sub> at 14 DIV. Samples were washed in ice-cold PBS and lysed with RIPA buffer with protease inhibitor. Adherent cells were scraped off the dish using a plastic cell scraper and the cell suspension was centrifugated for 10 min at 13 000 g and 4°C. The pellet was discarded, and the supernatant was kept for analysis. The following steps from total protein quantification to detection and analysis were performed as described for tissue samples, with the exception that proteins were separated by SDS-PAGE using 12% acrylamide/bis-acrylamide resolving gels. Primary antibodies used were rabbit anti-Trk (C14) (1:1000), mouse anti-spectrin  $\alpha$ -II (1:1000) and mouse anti-GAPDH (1:5000). Results are expressed as protein levels (% CTL).

Whenever the antibody host species was the same, membranes were stripped between incubations, by placing them in a stripping solution (200 mM glycine, 0.1% SDS, 1% Tween<sup>®</sup> 20, 50% acetic acid glacial, pH 2.2) for 30 min (RT), and washing them once in distilled water and twice for 15 min in TBS-T.

**Table 4 - Primary antibodies used to assess TrkB receptor and  $\alpha$ -II Spectrin levels by western blot.**

| Antibody                        | Host   | Supplier                 | Reference | Dilution |
|---------------------------------|--------|--------------------------|-----------|----------|
| Anti-Trk (C-14)                 | Rabbit | Santa Cruz Biotechnology | sc-11     | 1:1000   |
| Anti-Spectrin $\alpha$ II (C-3) | Mouse  | Santa Cruz Biotechnology | sc-48382  | 1:1000   |
| Anti-GAPDH                      | Mouse  | Ambion, CA, USA          | AM4300    | 1:5000   |

### 3.9.4. Enzyme-Linked Immunosorbent Assay (ELISA)

ELISA was used to determine the levels of soluble  $A\beta_{1-42}$  in samples of DG of rats sacrificed 3 and 14 days post-icv injection. Sample preparation and quantification of total protein was performed as described for western blot (see 3.3.3.). A commercial Human Amyloid  $\beta$ 42 Brain ELISA kit 96-Well Plate (Cat. #EZBRAIN42, Merck) was used. This kit provides a polystyrene microtiter plate pre-coated with a monoclonal capture antibody highly specific for the human  $A\beta_{1-42}$  peptide (antigen). Because low levels of  $A\beta$  were expected, a pre-incubation step was applied. For this, DG homogenate samples were added to the wells, incubated on a micro plate shaker for 5 min at RT, and then for 1h at 4°C, without shaking. After removing the samples, Antibody Conjugate Solution (detection antibody) was added to the wells, followed by standard solutions and samples. Since standard solutions from the kit were no longer available, standards were prepared, using an aliquot of the  $A\beta_{1-42}$  solution injected *in vivo* as stock (2.25 mg/ml), in the Standard/Sample Diluent of the kit, with the following concentrations: 0, 16, 62.5, 250 and 500 pg/ml. No duplicates of the standards or samples were analysed due to the limited number of wells available. The contents of the wells were thoroughly mixed on an orbital shaker (5 min, 500 rpm/min), and incubated overnight (18 h, 4°C). On the next day, solutions were removed from the wells and washed 5x with Washing Solution. Samples were incubated with Enzyme Conjugate Solution (streptavidin-peroxidase-conjugate) on an orbital plate shaker (30 min, 500 rpm/min), leading to the formation of an antibody-amyloid-antibody sandwich structure with the peroxidase linked over a streptavidin-biotin bridge. Solutions were removed from the wells and washed 5 more times before adding the Substrate Solution, resulting in the catalysis of an enzymatic reaction with a coloured product. This reaction was stopped approximately 25 min after by adding the Stop Solution. Absorbance was read at 450 nm and 590 nm using an Infinite M200 multimode microplate reader (Tecan, Männedorf, Switzerland). Because some of the samples had absorbance measurements above the values obtained for the standards, results are presented as the difference in absorbance units (% CTL) for all samples, and as protein levels (pg/ml) for the samples that were within the standard curve range (all except 1 control and 1  $A\beta$  injected rat, at 14 days post-injection). For this, protein levels were extrapolated from the difference in absorbance by performing a four parameter logistic (4PL) curve, using the MyAssays® online data analysis tool (Brighton, UK) <sup>179</sup>.

### **3.10. Statistical Analysis**

Gathered data is presented as the mean  $\pm$  standard error of the mean (SEM) for each animal group of animals. All statistical analyses were performed using the software Graphpad Prism 6 (CA, USA) for Windows. Unpaired two-tailed Student's *t*-test, Mann-Whitney test or one-way analyses of variance (ANOVA) followed by Bonferroni's multiple comparisons test were used to evaluate the significance of differences between means of two or more conditions. Evaluation of the significance of differences within the same group, was assessed by paired two-tailed Student's *t*-test or repeated-measures one-way ANOVA followed by Bonferroni's multiple comparisons test. Differences were considered statistically significant at  $p < 0.05$ . Significant outliers were calculated using the Grubbs' test ( $\alpha = 0.05$ )<sup>180</sup>.

## 4. Results

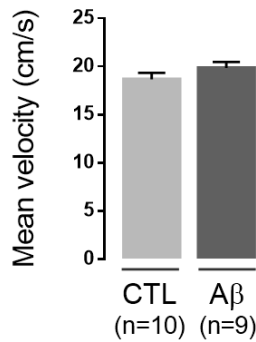
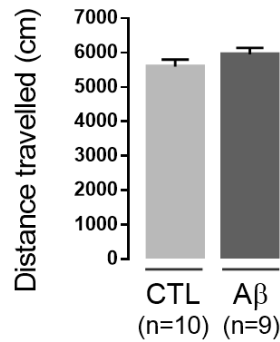
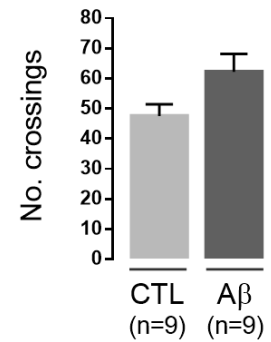
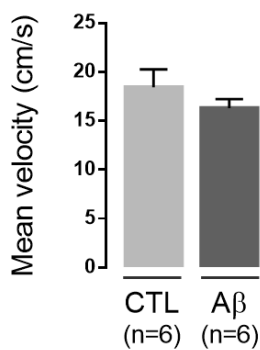
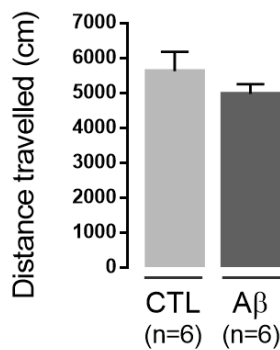
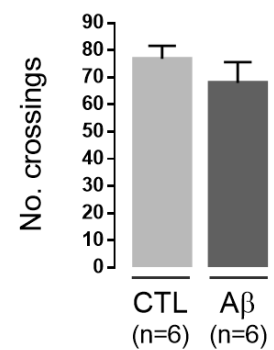
### 4.1. Behaviour characterization



Based on the literature as well as on previous work done at our group, the icv administration of A $\beta$ <sub>1-42</sub> peptide was expected to compromise learning and memory performance two weeks after icv injection, attempting to mimic some of the symptoms of the initial stages of sporadic AD<sup>157,181,182</sup>. Therefore, several behavioural paradigms were assessed, aiming at characterizing the cognitive performance of rats injected with A $\beta$ <sub>1-42</sub>, and thus validating it as a model of disease.

#### 4.1.1. A $\beta$ <sub>1-42</sub> peptide icv injection did not impact locomotor activity or anxiety-related behaviour

It has been reported that changes in locomotor activity, exploratory drive and anxiety-related behaviour can significantly influence rodent cognitive abilities<sup>168,183,184</sup>. These paradigms were therefore tested prior to evaluation of cognitive performance.

The OF test was used to assess locomotor and exploratory activity in two separate animal batches, one of them evaluated during the dark period of the light/dark rat cycle (night) (Fig. 15a), and the other one evaluated during the light period of the cycle (day) (Fig. 15b). In both cases, the test was performed during the first 5 min of the habituation phase of the NOR test. The mean velocity and distance travelled by the rats while they freely explored the OF arena were first quantified to assess locomotion. There were no significant differences in mean velocity between the control group (CTL) and the group of rats injected with A $\beta$ <sub>1-42</sub> peptide (A $\beta$ ), neither at night (CTL: 18.67 $\pm$ 0.6708 cm/s; A $\beta$ : 19.83 $\pm$ 0.6321 cm/s;  $p > 0.05$ ,  $n = 9-10$ ; Fig. 15a-I) nor during the day (CTL: 18.44 $\pm$ 1.822 cm/s; A $\beta$ : 16.30 $\pm$ 0.9189 cm/s;  $p > 0.05$ ,  $n = 6$ ; Fig. 15b-I). Likewise, no differences were observed between groups when looking at the distance travelled when the test was performed at night (CTL: 5600 $\pm$ 201.2 cm; A $\beta$ : 5949 $\pm$ 189.5 cm;  $p > 0.05$ ,  $n = 9-10$ ; Fig. 15a-II), or during the day (CTL: 18.44 $\pm$ 1.822 cm/s; A $\beta$ : 16.30 $\pm$ 0.9189 cm/s;  $p > 0.05$ ,  $n = 6$ ; Fig. 15b-II). Furthermore, the number of times that the rats entered the areas virtually delimiting a peripheral, an intermediate and a central zone was quantified as a way of appraising their exploratory drive. Similarly, there was no change for this parameter at night (CTL: 47.56 $\pm$ 3.898; A $\beta$ : 62.22 $\pm$ 5.916;  $p > 0.05$ ,  $n = 9-10$ ; Fig. 15a-III), or during the day (CTL: 76.83 $\pm$ 4.757; A $\beta$ : 68.00 $\pm$ 7.607;  $p > 0.05$ ,  $n = 6$ ; Fig. 15b-III).


**a-I****a-II****a-III****b-I****b-II****b-III**

**Fig. 15 – Locomotor and exploratory activity remained unchanged two weeks after A $\beta$ <sub>1-42</sub> peptide injection, as assessed by the OF test.** The OF test was performed during the first 5 minutes of the first day of the NOR habituation phase, both at night, under red light (**a**) and during the day, under dim light (**b**). Mean velocity (**I**), distance travelled (**II**) and number of crossings (**III**) between three virtual concentric squares, delimiting the periphery, the centre and an intermediate zone, were quantified. No significant differences were observed for any of the parameters when the test was performed at night or during the day ( $p > 0.05$  for all comparisons, unpaired Student's t-test). Data are expressed as mean  $\pm$  SEM (n=6-10).  : the test was performed during the dark period of the light/dark rat cycle;  : the test was carried out during the light period of the light/dark rat cycle.

Locomotor activity of the rats was also evaluated during the four days of the acquisition phase of the MWM test (Fig. 16). For this, mean velocity was calculated as the average of four trials for each day, measured during the time in which the rats were trying to reach a hidden platform inside a pool previously filled with water. This parameter did not differ between the groups in any of the timepoints (CTL, day 1:  $24.59 \pm 1.025$ , day 2:  $21.08 \pm 1.131$ , day 3:  $19.51 \pm 1.660$ , day 4:  $18.34 \pm 1.244$  cm/s; A $\beta$ , day 1:  $24.86 \pm 1.161$ , day 2:  $25.16 \pm 1.302$ , day 3:  $21.11 \pm 1.762$ , day 4:  $20.58 \pm 2.076$  cm/s;  $p > 0.05$ , n=7; Fig. 16), showing no changes in locomotor activity after A $\beta$ <sub>1-42</sub> peptide injection.



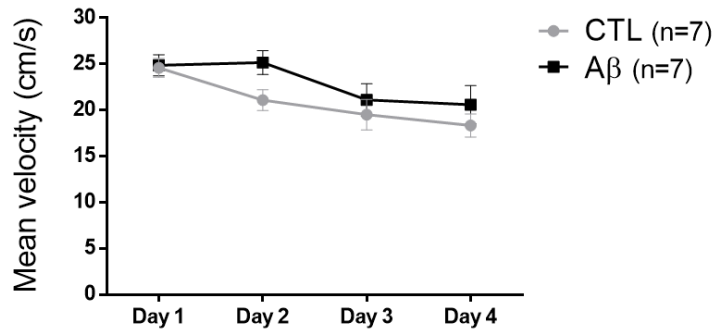



**Fig. 16 – The A $\beta_{1-42}$  peptide injection did not affect locomotor activity during the acquisition phase of the MWM test.** The acquisition phase of the MWM test comprises the first four days of the test. Mean velocity at each day was calculated as the mean of four trials. No significant differences were observed when comparing the A $\beta$  with the controls at the different timepoints ( $p > 0.05$ , ordinary one-way ANOVA followed by a Bonferroni's multiple comparison test). Data are expressed as mean  $\pm$  SEM ( $n=7$ ).  : the test was carried out during the light period of the light/dark rat cycle.

The EPM test was used for evaluation of anxiety-related behaviour (Fig. 17). This test relies on the notion that rodents tend to prefer dark enclosed spaces, avoiding heights and/or open spaces<sup>164,185</sup>. Thus, the time spent in the open arms of the maze during the 5 min of the test, as well as the number of times that the animals entered these arms were quantified as an inverse measure of anxious-related behaviour. There were no differences in the time in the open arms (CTL:  $29.17 \pm 3.34$  %; A $\beta$ :  $32.53 \pm 3.513$  %;  $p > 0.05$ ,  $n=13-14$ ; Fig. 17a), or in the number of open arm entries (CTL:  $43.99 \pm 3.736$  %; A $\beta$ :  $47.03 \pm 3.562$  %;  $p > 0.05$ ,  $n=13-14$ ; Fig. 17b). The absence of changes in these parameters indicate that the A $\beta_{1-42}$  peptide injection did not cause any noticeable signs of anxiety, when compared with control animals.

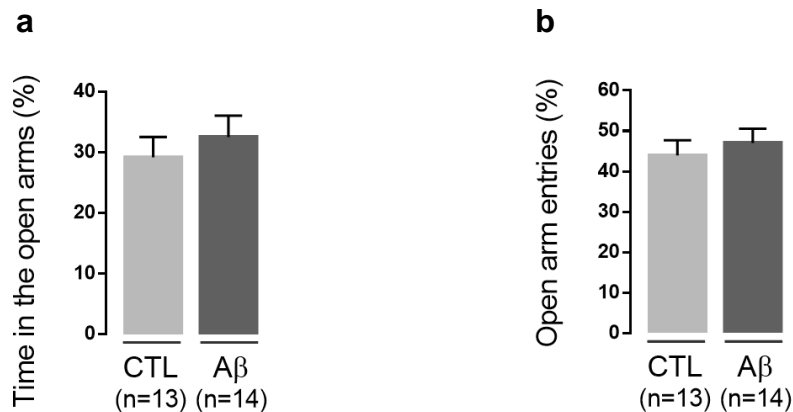



**Fig. 17 – Anxiety-related behaviour was not influenced by the A $\beta_{1-42}$  peptide injection.** Anxious-related behaviour was evaluated by the EPM test two weeks after surgeries, on the day prior to evaluation of cognitive performance. The % of time that the rats spent in the open arms of the structure (a) and the % of entries in these arms (b) were quantified. No significant differences were observed for any of these measures ( $p > 0.05$ , unpaired Student's  $t$ -test). Data are expressed as mean  $\pm$  SEM ( $n=13-14$ ).  : the test was carried out during the light period of the light/dark rat cycle.

No differences were observed regarding general locomotor and exploratory activity or anxiety-related behaviour two weeks after the animals were icv injected with A $\beta$ <sub>1-42</sub> peptide. Taken together, these results suggest that differences in cognitive performance should not be attributed to impaired locomotion or to changes in exploratory drive or anxious-like behaviour.

#### 4.1.2. A $\beta$ <sub>1-42</sub> peptide icv injection did not impair spatial working and short-term memory performance

Many behavioural tests used to examine cognitive function, including memory performance, rely on the proclivity of rodents to actively explore novel objects and environments, without the need to introduce exogenous reinforcements that might lead, for instance, to increased stress levels<sup>183,186</sup>. Taking advantage of this feature, the Y-Maze SA and FA tests were performed in order to evaluate spatial working memory (Fig. 18) and short-term reference memory (Fig. 19) performance, respectively. In the Y-Maze SA test, the number of spontaneous alternations between the 3 arms of the maze was quantified while the animals freely explored the structure for 8 min. Here, a difference in spontaneous alternations was not observed (CTL: 71 $\pm$ 2.0 %; A $\beta$ : 76 $\pm$ 3.8 %;  $p > 0.05$ ,  $n = 6$ ; Fig. 18), indicating that the rats injected with A $\beta$  present no working memory impairment.

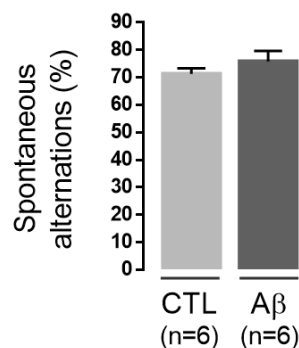


**Fig. 18 – Spatial working memory performance did not change after the A $\beta$ <sub>1-42</sub> peptide injection.** Working memory performance was evaluated by the Y-Maze SA test by measuring the % of spontaneous alternations between the 3 arms of the structure. No significant differences were observed for this parameter ( $p > 0.05$ , unpaired Student's  $t$ -test). Data are expressed as mean  $\pm$  SEM ( $n = 6$ ).  : the test was carried out during the light period of the light/dark rat cycle.

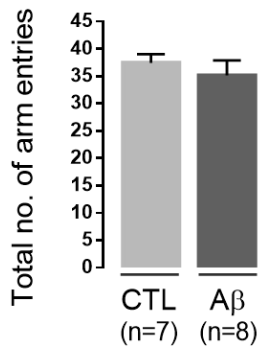
The Y-Maze FA test was divided in two tasks. During training, only two of the arms were available for exploration by the rats: the arm where the animals begun testing, designated as start arm (S), and a second one, designated as other arm (O). The test phase begun after an ITI of 3 h, when the third arm, designated as novel arm (N), became accessible for exploration. The total number of times that the animals entered the available arms was used as a measure of exploratory drive in both tasks. No significant differences were observed for this parameter during training (CTL:  $37 \pm 1.6$  %; A $\beta$ :  $35 \pm 2.8$  %;  $p > 0.05$ ,  $n = 7-8$ ; Fig. 19a-I) or during the test phase (CTL:  $22 \pm 2.6$  %; A $\beta$ :  $25 \pm 1.4$  %;  $p > 0.05$ ,  $n = 7-8$ ; Fig. 19b-I). Likewise, no differences were seen when comparing the time that the rats spent exploring either the start or the other arm during training, within the control group (S:  $41 \pm 2.9$  %; O:  $41 \pm 2.6$  %;  $p > 0.05$ ,  $n = 7-8$ ; Fig. 19a-II), nor within the A $\beta$  group (S:  $43 \pm 2.0$  %; O:  $38 \pm 1.7$  %;  $p > 0.05$ ,  $n = 7-8$ ; Fig. 19a-II), showing that the rats had no preference for any of the arms.

When looking at the test phase, it is expected that control animals spend more time exploring the novel arm, as they should be able to distinguish it from the other two, while rats that present short-term memory deficits should not be able to distinguish this novel arm<sup>170</sup>. When comparing the time spent exploring the novel arm with the time spent in the other two arms, no significant differences were observed within the control group (S:  $33 \pm 4.2$  %; O:  $25 \pm 2.8$  %; N:  $42 \pm 4.4$  %;  $p > 0.05$ ,  $n = 7-8$ ; Fig. 19b-II), although a tendency for an increase in the time spent in the novel arm when compared to the other arm ( $p = 0.0787$ ) is observed. On the other hand, when looking at this parameter within the A $\beta$  group, it was seen that these rats spent a significant greater amount of time exploring the novel arm when compared to the other two (S:  $31 \pm 1.4$  %; O:  $25 \pm 2.0$  %; N:  $44 \pm 1.6$  %;  $**p < 0.01$ ,  $n = 7-8$ ; Fig. 19b-II). Despite these differences, the number of rats that visited the novel arm when they were first placed in the maze for the test phase did not differ significantly between the two groups (CTL:  $85.7 \pm 14.3$  %; A $\beta$ :  $87.5 \pm 12.5$  %;  $p > 0.05$ ,  $n = 7-8$ ; Fig. 19b-III). Hence, the A $\beta$  injection did not cause short-term memory deficits, when evaluated two weeks after the procedure, as these rats were able to recognize the novelty item.

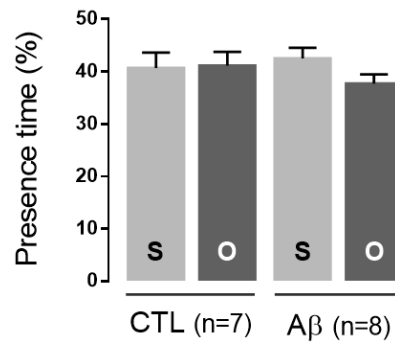


## a Training

### a-I

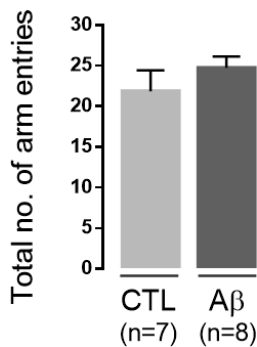


### a-II

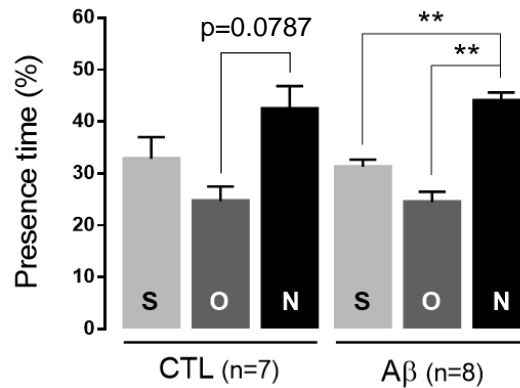


## b Test

### b-I




### b-II



### b-III

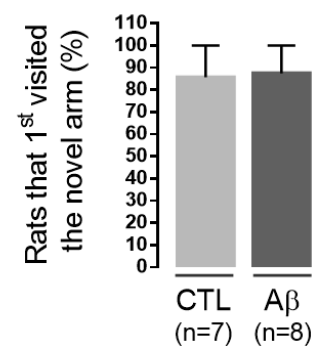


**Fig. 19 – Rats injected with A $\beta$ <sub>1-42</sub> peptide showed no impairment in short-term reference memory performance, as assessed by the Y-Maze FA test.** The Y-Maze FA test was divided in two phases: a training phase (a) and a test phase (b). The total number of arm entries (I) was quantified during both phases as a measure of exploratory behaviour. No significant differences were observed for this parameter ( $p > 0.05$ , unpaired Student's  $t$ -test). During training, there were no differences in the % of presence time (a-II) within the arm where the rats were first placed (start arm, S) and a second arm (other arm, O), showing that the rats had no preference for any of the two arms available ( $p > 0.05$ , paired Student's  $t$ -test). During the test phase, the ability of the rats to distinguish the novel arm (N) was assessed by quantifying the % of presence time in this arm when compared to the other two (b-II). While there were no differences in this measure for control rats, animals injected with A $\beta$  spent a significant greater amount of time exploring the novel arm (CTL:  $p > 0.05$ ; A $\beta$ :  $**p < 0.01$ , repeated-measures one-way ANOVA followed by a Bonferroni's multiple comparison test), showing that short-term memory performance was not impaired in these rats. Notwithstanding, the % of rats that first visited the novel arm (b-III) after being placed in the maze on the test phase showed no differences ( $p > 0.05$ , Mann-Whitney test). Data are expressed as mean  $\pm$  SEM ( $n = 7-8$ ).  : the test was carried out during the light period of the light/dark rat cycle.

#### **4.1.3. A $\beta$ <sub>1-42</sub> peptide injected rats showed distinct episodic long-term memory performance when evaluated during the dark and the light phases of the light/dark cycle**

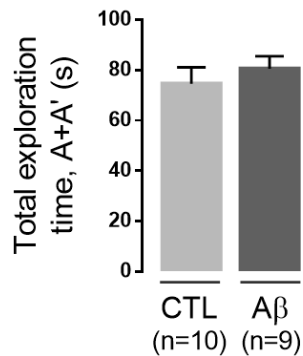
As for the Y-Maze tests, appraisal of episodic long-term memory performance by the NOR test, stands on the principal of rodent predisposition to explore novelty, in this case using objects with specific characteristics that can be discriminated by the animals. For this test, which was performed at night as well as during daytime, the rats were first habituated to the OF arena, and then familiarized with two identical objects during a training phase designated as A and A'. Next, for the test phase, after an ITI of 24 h, one of these objects was replaced with a novel one, designated as B.

The total exploration time of the two objects served as a measure of exploratory drive in both phases of the test. No significant differences were observed for this parameter when the test was performed at night, neither during training (CTL: 75 $\pm$ 6.5 s; A $\beta$ : 81 $\pm$ 5.0 s;  $p > 0.05$ ,  $n = 9-10$ ; Fig. 20a-I), nor during the test phase (CTL: 71 $\pm$ 8.1 s; A $\beta$ : 62 $\pm$ 4.6 s;  $p > 0.05$ ,  $n = 9-10$ ; Fig. 20b-I). During training, the animals showed no preference for either of the identical objects that they were being familiarized with, as seen by the absence of differences in the time that the animals spent exploring these objects within the control group (A: 45 $\pm$ 2.8 %; A': 55 $\pm$ 2.7 %;  $p > 0.05$ ,  $n = 9-10$ ; Fig. 20a-II), and within the A $\beta$  group (A: 53 $\pm$ 2.8 %; A': 47 $\pm$ 2.8 %;  $p > 0.05$ ,  $n = 9-10$ ; Fig. 20a-II). It is anticipated that animals with impaired long-term memory performance should not be able to recognize the novel object as such, spending a similar amount of time exploring the novel object and the familiar one<sup>187</sup>. When referring to the control group during the test phase, there were no significant differences in the time exploring these objects (A: 46 $\pm$ 3.7 %; B: 54 $\pm$ 3.7 %;  $p > 0.05$ ,  $n = 9-10$ ; Fig. 20b-II). However, the rats injected with A $\beta$  spent a significantly greater amount of time exploring the novel object compared to the familiar one (A: 44 $\pm$ 1.9 %; B: 56 $\pm$ 1.9 %;  $*p < 0.05$ ,  $n = 9-10$ ; Fig. 20b-II). Nonetheless, quantification of the novelty discrimination index demonstrates no differences between the groups (CTL: 0.074 $\pm$ 0.073; A $\beta$ : 0.12 $\pm$ 0.037;  $p > 0.05$ ,  $n = 9-10$ ; Fig. 20b-III). Therefore, the results obtained during the night suggest that the control group had compromised memory performance. Moreover, the A $\beta$ <sub>1-42</sub> peptide injection did not lead to a long-term memory impairment when assessed by the NOR test during the night.

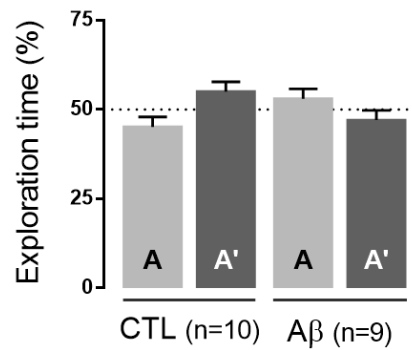


## a Training

### a-I

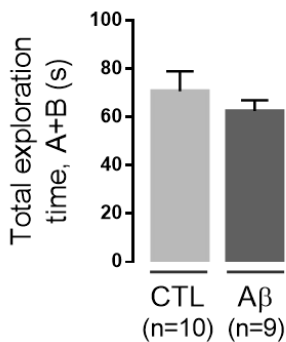


### a-II

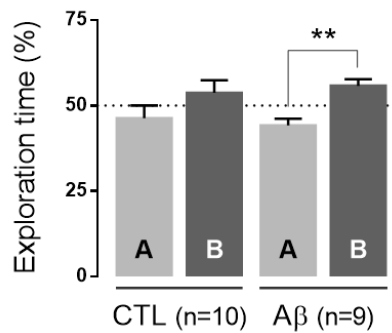


## b Test

### b-I




### b-II



### b-III

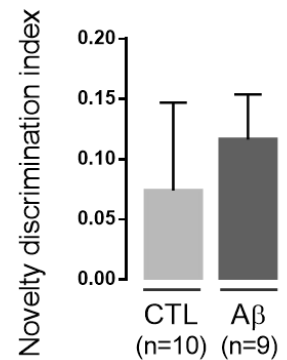


**Fig. 20 – A $\beta$ <sub>1-42</sub> peptide injected rats showed no impairment in episodic long-term memory performance at night.**

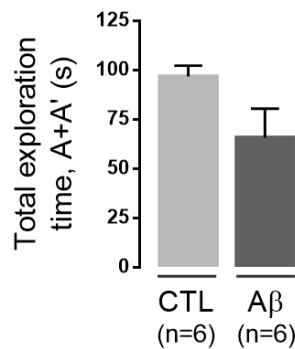
The NOR test was first used to assess long-term memory performance during the dark period of the light/dark cycle, under red light. Total exploration time (I) of the two objects (A+A') and (A+B) was quantified during the training phase (a) and the test phase (b), respectively, where A and A' correspond to the time spent exploring the familiar objects and B to the time spent exploring the novel object. No differences in this parameter were observed between groups in either of the phases ( $p > 0.05$  for all comparisons, unpaired Student's *t*-test). No differences in the % of exploration time of the familiar objects were observed during the training phase (a-II) ( $p > 0.05$ , paired Student's *t*-test), showing that the rats had no preference for any of the two identical objects. When comparing the % of exploration time of the familiar and the novel objects during the test phase (b-II), no differences were observed for control rats ( $p > 0.05$ , paired Student's *t*-test), however the rats injected with A $\beta$  spent a significant greater amount of time exploring the novel object than the familiar one (\*\* $p < 0.01$ , paired Student's *t*-test), exhibiting no impairment in long-term memory performance. The novelty discrimination index (b-III) in the test phase was calculated as  $(B-A)/(B+A)$ . There were no significant differences between groups for this parameter ( $p > 0.05$ , unpaired Student's *t*-test). Data are expressed as mean  $\pm$  SEM ( $n=9-10$ ).  : the test was performed during the dark period of the light/dark rat cycle.

When the NOR was performed during the day, no significant changes in exploratory activity were observed between the groups during the training phase (CTL:  $97 \pm 5.6$  s; A $\beta$ :  $66 \pm 15$  s;  $p > 0.05$ ,  $n = 6$ ; Fig. 21a-I), yet during the test phase, the animals injected with A $\beta$  spent a significantly lower amount of time exploring the objects (CTL:  $89 \pm 7.2$  s; A $\beta$ :  $56 \pm 10$  s;  $*p < 0.05$ ,  $n = 6$ ; Fig. 21b-I), indicative of less exploratory drive. Regarding the time spent exploring the objects during training, results were comparable to the ones obtained at night, as the rats showed no preference for any of the identical objects within the controls (A:  $56 \pm 5.5$  %; A':  $45 \pm 5.5$  %;  $p > 0.05$ ,  $n = 6$ ; Fig. 21a-II), or within the A $\beta$  group (A:  $54 \pm 6.9$  %; A':  $47 \pm 6.9$  %;  $p > 0.05$ ,  $n = 6$ ; Fig. 21a-II). In the test phase, the time that the rats spent exploring the novel object comparing with the familiar one was similar, both for the control group (A:  $48 \pm 2.3$  %; B:  $52 \pm 2.3$  %;  $p > 0.05$ ,  $n = 6$ ; Fig. 21b-II), and for the A $\beta$  group (A:  $50 \pm 5.7$  %; B:  $50 \pm 5.8$  %;  $p > 0.05$ ,  $n = 6$ ; Fig. 21b-II). Consistently, there were no differences between the groups when examining the novelty discrimination index (CTL:  $0.040 \pm 0.045$ ; A $\beta$ :  $0.0017 \pm 0.11$ ;  $p > 0.05$ ,  $n = 6$ ; Fig. 21b-III). Taken together, these results appear to indicate that during the day, long-term memory performance was compromised in both experimental groups (control and A $\beta$ ).

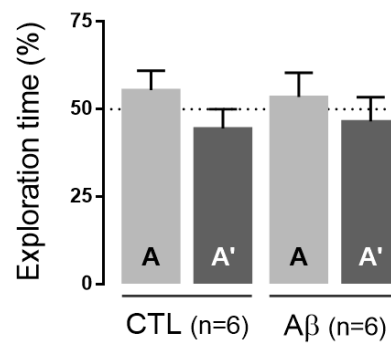


### a Training

#### a-I

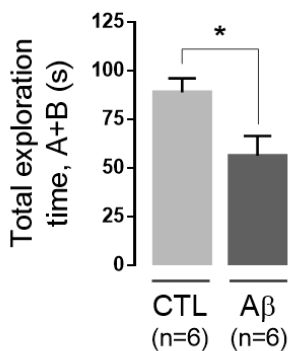


#### a-II

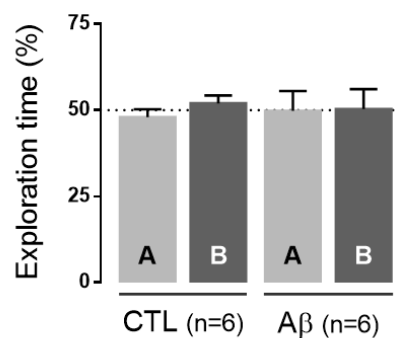


### b Test

#### b-I




#### b-II



#### b-III

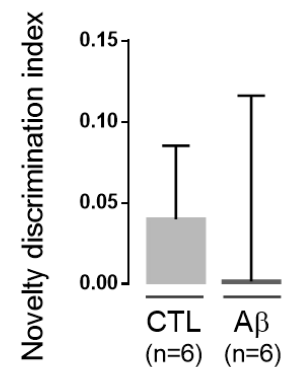


**Fig. 21 – A $\beta$ <sub>1-42</sub> peptide injected rats showed impaired episodic long-term memory performance when evaluated during the day.** The NOR test was used to assess long-term memory performance during the light period of the rats' cycle, under dim light. Total exploration time (I) of the two objects (A+A') and (A+B) was quantified during the training phase (a) and test phase (b), respectively. No differences in this parameter were observed between groups during training ( $p>0.05$ , unpaired Student's  $t$ -test), yet the A $\beta$  rats spent a significant lower amount of time exploring the objects during the test phase when compared to controls ( $*p<0.05$ , unpaired Student's  $t$ -test). No differences in the % of exploration time of the familiar objects were observed during the training phase (a-II) ( $p>0.05$ , paired Student's  $t$ -test), showing that the rats had no preference for any of the two identical objects. During the test phase, neither the control rats nor the ones injected with A $\beta$  were able to recognize the novel object (b-II), as they spent a similar amount of time exploring both objects ( $p>0.05$ , paired Student's  $t$ -test). There were no significant differences between the groups for the novelty discrimination index (b-III),  $(B-A)/(B+A)$ , in the test phase ( $p>0.05$ , unpaired Student's  $t$ -test). Data are expressed as mean  $\pm$  SEM ( $n=6$ ). A, A': familiar objects; B: novel object.  : the test was carried out during the light period of the light/dark rat cycle.

#### **4.1.4. No changes in spatial learning and memory performance were observed after A $\beta$ <sub>1-42</sub> peptide injection**


The MWM test provides a way of examining hippocampal-dependent spatial learning and reference memory in rats, taking advantage of their noteworthy swimming skills<sup>183,188</sup>. This test comprises a four-day acquisition phase, where the ability of the animals to learn the location of a hidden platform is evaluated, followed by a probe test on the fifth day, where the platform is removed and the ability of the animals to recall its previous location is appraised.

For each day of acquisition, the time that the rats spent to reach the platform was calculated as the mean of four trials. No significant differences were observed for any of the timepoints when comparing the control group with the A $\beta$ <sub>1-42</sub> (CTL, day 1: 45 $\pm$ 4.1, day 2: 24 $\pm$ 5.3, day 3: 14 $\pm$ 2.3, day 4: 15 $\pm$ 3.0 s; A $\beta$ , day 1: 35 $\pm$ 3.4, day 2: 15 $\pm$ 4.6, day 3: 11 $\pm$ 2.2, day 4: 12 $\pm$ 3.2 s;  $p>0.05$ ,  $n=7$ ; Fig. 22a). During the probe test, there was also no change in the time that the rats spent to reach the area where the platform had been removed from (CTL: 5.7 $\pm$ 0.68 s; A $\beta$ : 6.7 $\pm$ 0.78 s;  $p>0.05$ ,  $n=7$ ; Fig. 22b-I), or in the number of times that the animals crossed this area (CTL: 4.7 $\pm$ 0.78; A $\beta$ : 4.3 $\pm$ 0.61;  $p>0.05$ ,  $n=7$ ; Fig. 22b-II). Additionally, no significant differences were observed between the groups when looking at the time that the rats spent in the quadrant where the platform had been previously located (Qp) (CTL: 54.33 $\pm$ 4.740 %; A $\beta$ : 47.75 $\pm$ 3.738 %;  $p>0.05$ ,  $n=7$ ; Fig. 22b-III), or in the number of animals that first visited the platform area when they were placed in the pool (CTL: 71.4 $\pm$ 18.4 %; A $\beta$ : 71.4 $\pm$ 18.4 %;  $p>0.05$ ,  $n=7$ ; Fig. 22b-IV). These results point out that hippocampal-dependent spatial learning and memory performance was not compromised two weeks after the rats were injected with A $\beta$ <sub>1-42</sub> peptide.



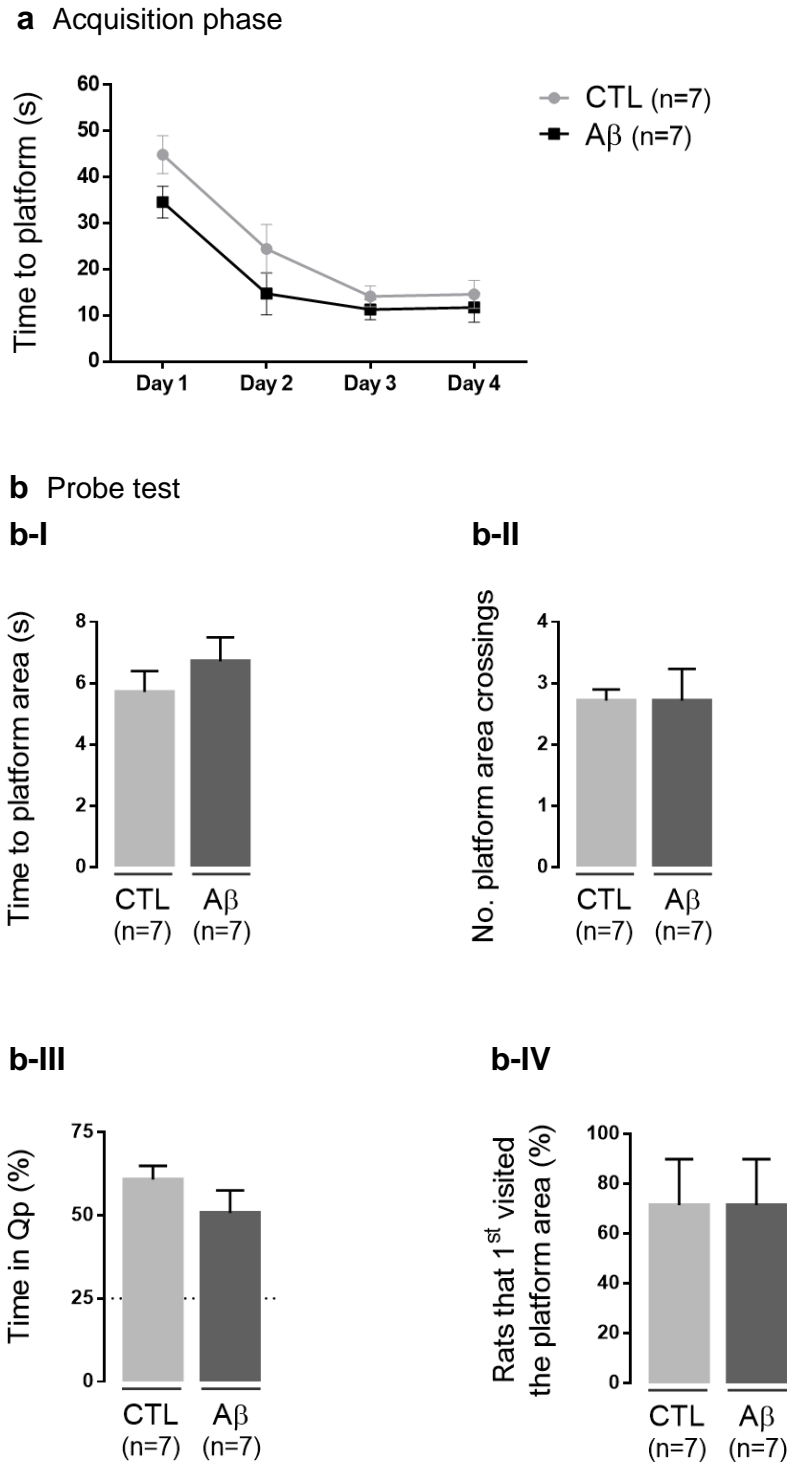


**Fig. 22 – Spatial learning and memory performance was not changed after Aβ<sub>1-42</sub> peptide injection, as evaluated by the MWM test.** The MWM test was performed in two phases: a four-day acquisition phase (a) and a probe test (b) on the fifth day. During acquisition, the time that the rats spent to reach the hidden platform was quantified for each day as the mean of four trials, allowing the representation of a learning curve for the location of the platform along the four days. No significant differences were observed when comparing the Aβ with the controls at the different timepoints ( $p > 0.05$ , ordinary one-way ANOVA followed by a Bonferroni's multiple comparison test). During the probe test, the time spent to reach the area where the platform had previously been located (b-I), the number of times that the rats crossed this area (b-II) and the time spent in the quadrant where the platform had been located (Qp) (b-III) were quantified. No significant

differences were observed for any of these parameters ( $p > 0.05$  for all comparisons, unpaired Student's t-test), indicating that the animals from both groups were able to memorize the previous platform location, showing no impairment in spatial learning and memory performance. Accordingly, there were no changes in the % of rats that first visited the platform area (**b-III**) after being placed in the maze ( $p > 0.05$ , Mann-Whitney test). Data are expressed as mean  $\pm$  SEM ( $n=7$ ).  : the test was carried out during the light period of the light/dark rat cycle.

## 4.2. Cellular and molecular analysis

Although no major differences were found regarding the phenotype of the rats following  $A\beta_{1-42}$  peptide injection, cellular and molecular analyses, mainly of the DG, were performed in order to search for a putative  $A\beta$ -mediated effect on neurogenesis.

### 4.2.1. Changes in soluble $A\beta_{1-42}$ or $A\beta_{1-42}$ deposits were not observed 3 or 14 days after icv injection

The levels of soluble  $A\beta_{1-42}$ , which include monomeric and oligomeric forms, were examined by ELISA in DG samples of rats sacrificed 3 and 14 days after icv injection with  $A\beta_{1-42}$  peptide at 2.25 mg/ml. Absorbance measured in these samples did not change between the groups, when quantified 3 days after the injection (CTL: 100.0 %;  $A\beta$ : 80.33 %;  $n=2$ ; Fig. 23a), or 14 days after (CTL: 99.99 %;  $A\beta$ : 107.8 %;  $n=2$ ; Fig. 23a). Moreover, protein levels were also similar between groups, at 3 days (CTL: 554 pg/ml;  $A\beta$ : 400 pg/ml;  $n=2$ ; Fig. 23b) and 14 days (CTL: 386 pg/ml;  $A\beta$ : 345 pg/ml;  $n=1$ ; Fig. 23b) post icv injection.

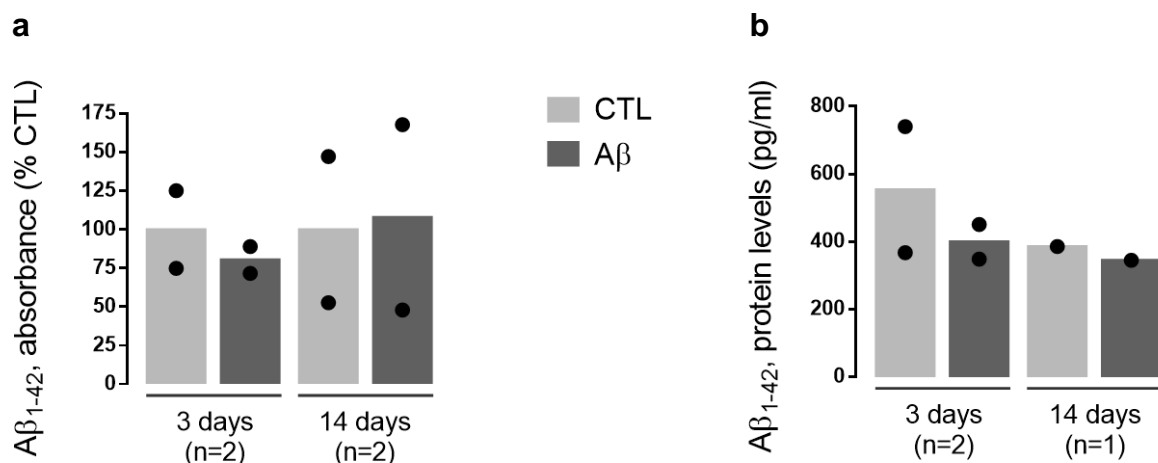
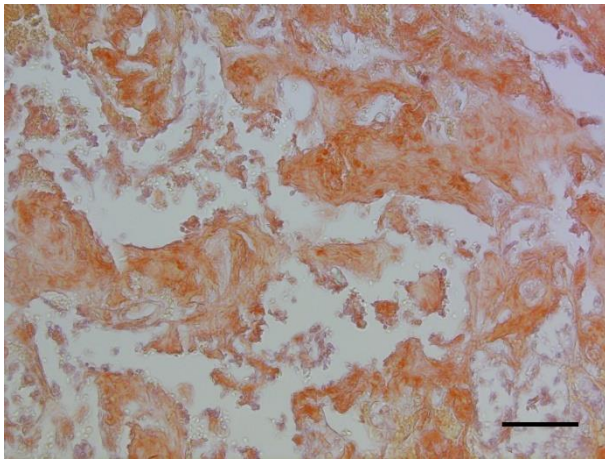


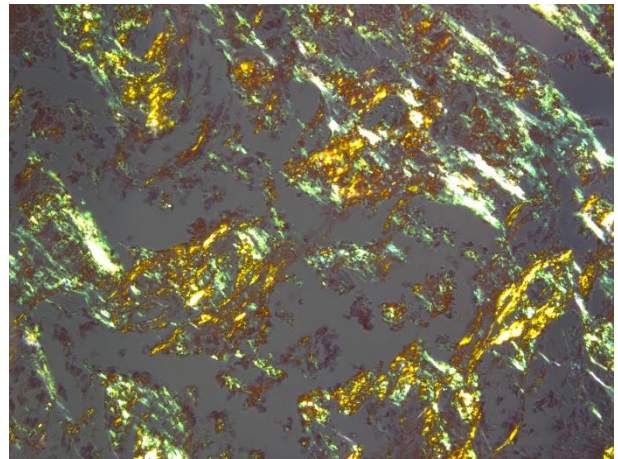
**Fig. 23 – Soluble  $A\beta_{1-42}$  levels in the DG did not change at 3 or 14 days post  $A\beta_{1-42}$  injection.** Absorbance levels were read at 450 and 590 nm, and the difference in absorbance units was quantified and normalized (100%) for control (**a**). Protein levels were calculated from this difference in absorbance by a 4PL analysis (**b**). Preliminary data are expressed as the mean ( $n=2$ ) or presented as individual values ( $n=1$ ).

The formation of A $\beta$  deposits was also assessed in three samples from animals of each group sacrificed 3 and 14 days after the injection, using a Congo red staining. Human kidney samples were used as positive controls for amyloidosis, when observed under bright-field microscopy (Fig. 24a-I) and under polarized light (Fig. 24a-II). The latter denotes a clear formation of A $\beta$  aggregates, highlighted by the presence of intense yellow-green birefringence. On the other hand, A $\beta_{1-42}$  injected rats did not exhibit any birefringence, showing that A $\beta$  aggregates were absent in these animals (Fig. 24b-II). Therefore, no differences were noticeable in any of the samples tested, in any of the timepoints or between the groups (representative images from the DG of one A $\beta_{1-42}$  injected rat, sacrificed at 3 days post-injection, Fig. 24b). Moreover, the presence of A $\beta$  deposits was also not observed in other brain regions, such as the SVZ (close to the injection site).

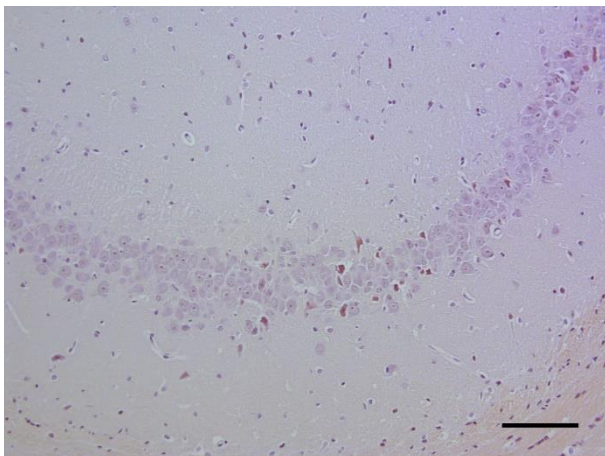
**a-I**



**a-II**



**b-I**



**b-II**



**Fig. 24 – A $\beta$  aggregates were absent at 3 or 14 days post A $\beta_{1-42}$  injection.** Representative pictures were obtained from human kidney tissue samples (a), serving as positive controls, and from DG samples (b) of an animal sacrificed 3 days after A $\beta$  injection. These samples were observed under bright field (I) and polarized light (II), illustrating the absence of A $\beta$  deposition in the samples of the rats injected with A $\beta_{1-42}$  peptide (absent yellow-green birefringence in b-II), opposed to the substantial amounts of deposits observed for the positive controls (intense yellow-green birefringence in a-II). Scale bar = 100  $\mu$ m.

#### 4.2.2. Levels of TrkB receptor isoforms in the DG and SVZ did not seem to change 3 or 14 days after A $\beta$ <sub>1-42</sub> icv injection

Signalling mediated by BDNF has been shown to be compromised in the presence of A $\beta$ , due to the cleavage of its TrkB-FL receptors, in a process that is dependent on calpain activation<sup>151,152</sup>. Therefore, the levels of these receptors, as well as the corresponding TrkB-ICD originated from its cleavage, were used as an indirect measure of the presence of A $\beta$  in the DG (Fig. 25) and in the SVZ (Fig. 26). For this, samples from rats sacrificed 3 and 14 days after the A $\beta$ <sub>1-42</sub> peptide or vehicle (VEH CTL) injection were analysed by WB, as well as samples from age-matched rats in which no injection had been performed, to serve as negative controls (Neg CTL).

No significant differences between the three groups were observed in the levels of TrkB-FL receptors in DG samples of rats sacrificed 3 days (Neg CTL: 99.98 $\pm$ 14.44 %; VEH CTL: 93.75 $\pm$ 6.753 %; A $\beta$ : 94.90 $\pm$ 17.92 %;  $p > 0.05$ ,  $n = 3$ ; Fig. 25b-I) and 14 days (Neg CTL: 100.0 $\pm$ 22.36 %; VEH CTL: 110.1 $\pm$ 23.17 %; A $\beta$ : 101.2 $\pm$ 6.992 %;  $p > 0.05$ ,  $n = 3$ ; Fig. 25b-I) after the icv injection. Accordingly, no significant changes were seen when comparing the levels of TrkB-ICD in the same samples, neither at 3 days (Neg CTL: 99.99 $\pm$ 31.15 %; VEH CTL: 72.10 $\pm$ 12.60 %; A $\beta$ : 65.10 $\pm$ 20.24 %;  $p > 0.05$ ,  $n = 3$ ; Fig. 25b-II), nor at 14 days (Neg CTL: 99.98 $\pm$ 35.50 %; VEH CTL: 102.3 $\pm$ 35.09 %; A $\beta$ : 117.0 $\pm$ 45.71 %;  $p > 0.05$ ,  $n = 3$ ; Fig. 25b-II) post A $\beta$ <sub>1-42</sub> injection.

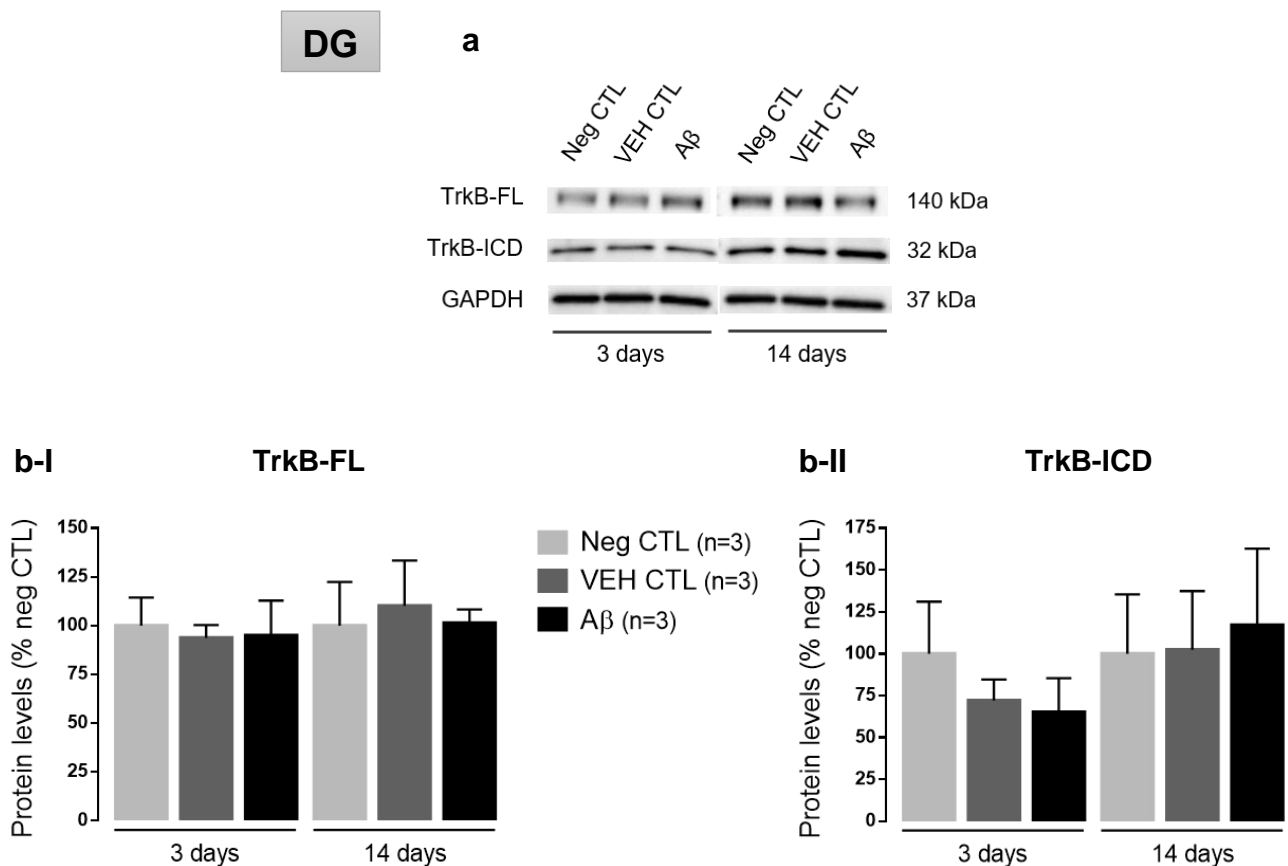


**Fig. 25 – Levels of TrkB receptor isoforms in the DG were not changed at 3 and 14 days after A $\beta$ <sub>1-42</sub> peptide injection.** Representative western-blot in (a) depict immunoreactive bands for TrkB-FL (~140 kDa), TrkB-ICD (~32 kDa) and GAPDH (loading control; ~37 kDa) obtained from DG samples at the timepoints corresponding to 3 and 14 days after the A $\beta$ <sub>1-42</sub> peptide injection. Protein levels were quantified and normalized (100%) for the corresponding negative controls at 3 and 14 days. TrkB-FL (**b-I**) and TrkB-ICD (**b-II**) levels show no change at any of the timepoints, when comparing between the groups ( $p > 0.05$  for all comparisons, ordinary one-way ANOVA followed by a Bonferroni's multiple comparison test). Data are expressed as mean  $\pm$  SEM ( $n = 3$ ). Neg CTL: age-matched control rats to which no icv injection was performed; VEH CTL: control rats injected with vehicle solution.

When looking at the samples from the SVZ, preliminary results show an identical pattern to the one observed for the DG regarding the levels of TrkB receptor isoforms. Although the number of samples is too small to take any clear conclusions, no differences seem to be present between the three groups in the levels of TrkB-FL receptors in SVZ samples from rats sacrificed at 3 days (Neg CTL: 99.99 %; VEH CTL: 110.3 %; A $\beta$ : 102.4 %;  $n = 2$ ; Fig. 26b-I) and 14 days (Neg CTL: 99.99 %; VEH CTL: 105.9 %; A $\beta$ : 118.5 %;  $n = 2$ ; Fig. 26b-I) after the icv injection. Similarly, no changes seem to be observed when comparing the levels of TrkB-ICD in the same samples at the 3 days timepoint (Neg CTL: 99.97 %; VEH CTL: 125.1 %; A $\beta$ : 108.3 %;  $n = 2$ ; Fig. 26b-II), or at the 14 days timepoint (Neg CTL: 100.0 %; VEH CTL: 127.1 %; A $\beta$ : 110.4 %;  $n = 2$ ; Fig. 26b-II).

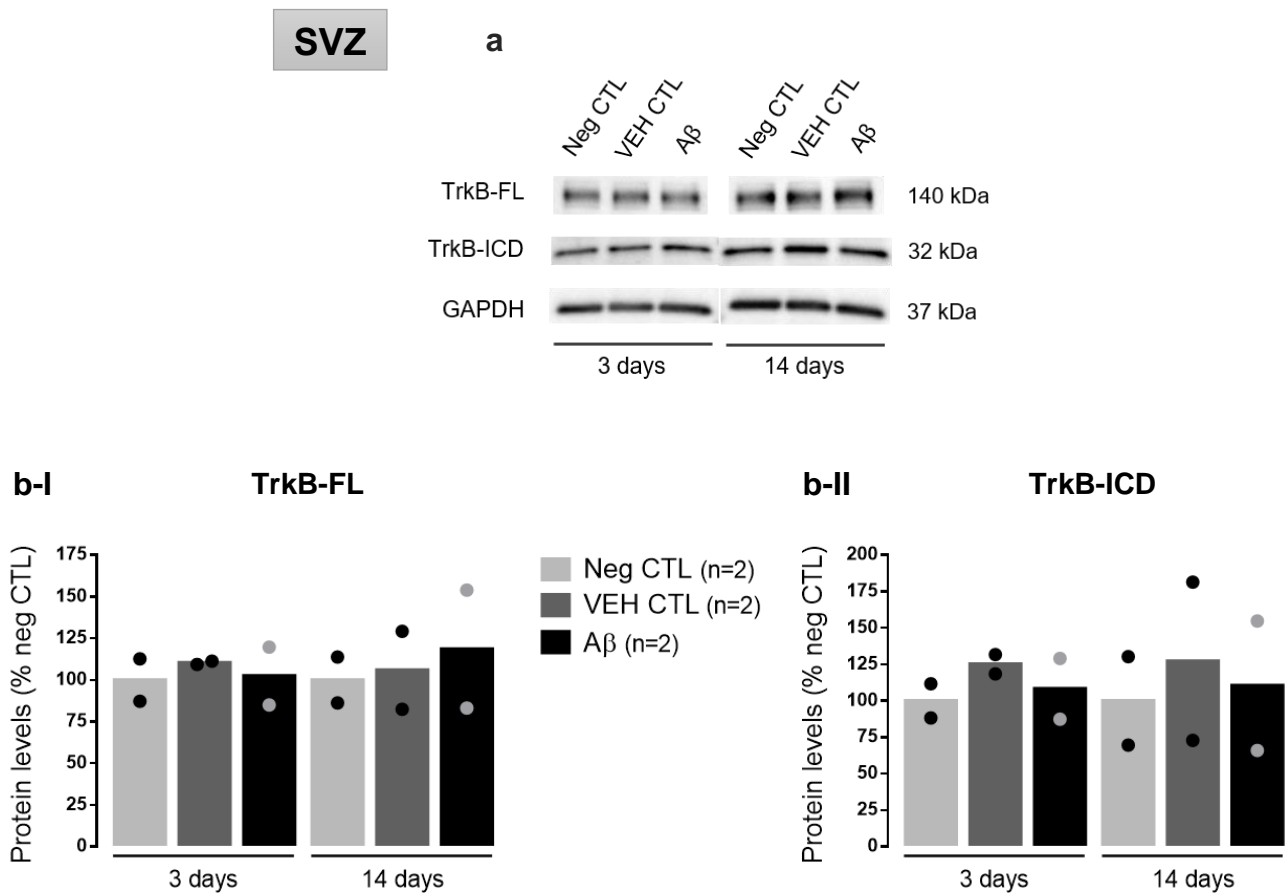


**Fig. 26 – Levels of TrkB receptor isoforms in the SVZ did not change at 3 and 14 days after A $\beta$ <sub>1-42</sub> peptide injection.** Representative western-blot in (a) depict immunoreactive bands for TrkB-FL (~140 kDa), TrkB-ICD (~32 kDa) and GAPDH (loading control; ~37 kDa) obtained from SVZ samples at the timepoints corresponding to 3 and 14 days after the A $\beta$ <sub>1-42</sub> peptide injection. Protein levels were quantified and normalized (100%) for the corresponding negative controls at 3 and 14 days. TrkB-FL (b-I) and TrkB-ICD (b-II) levels do not tend to differ at any of the timepoints, when comparing between the groups. Preliminary data are expressed as mean (n=2). Neg CTL: age-matched control rats to which no icv injection was performed; VEH CTL: control rats injected with vehicle solution.

#### 4.2.3. Primary cortical neuronal cultures incubated with A $\beta$ <sub>1-42</sub> show a tendency for an increase in TrkB receptor cleavage and calpain activity

Given the unexpected results that were obtained in the *in vivo* experiments, we decided to examine the viability of the A $\beta$ <sub>1-42</sub> peptide *in vitro*, using a well-established protocol in our institute. To do this, TrkB receptor cleavage as well as calpain activity were assessed in primary cortical neuronal culture samples incubated for 24 h with an A $\beta$ <sub>1-42</sub> peptide solution (20  $\mu$ M) prepared from the solution used for icv injection. Preliminary data revealed an approximately 30% decrease in the levels of TrkB-FL receptor (CTL: 100.0 %; A $\beta$ : 69.88 %; n=1; Fig. 27b-I), when comparing the sample incubated with vehicle with the one incubated with A $\beta$ , accompanied by an approximately 19% increase in the levels of TrkB-ICD (CTL: 100.0 %; A $\beta$ : 118.9 %; n=1; Fig. 21b-II). These results are emphasised by the tendency for an increase of about 70% in the ratio between the levels of TrkB-ICD and TrkB-FL in the sample incubated with A $\beta$  (CTL: 100.0 %; A $\beta$ : 170.1 %; n=1; Fig. 27b-III).

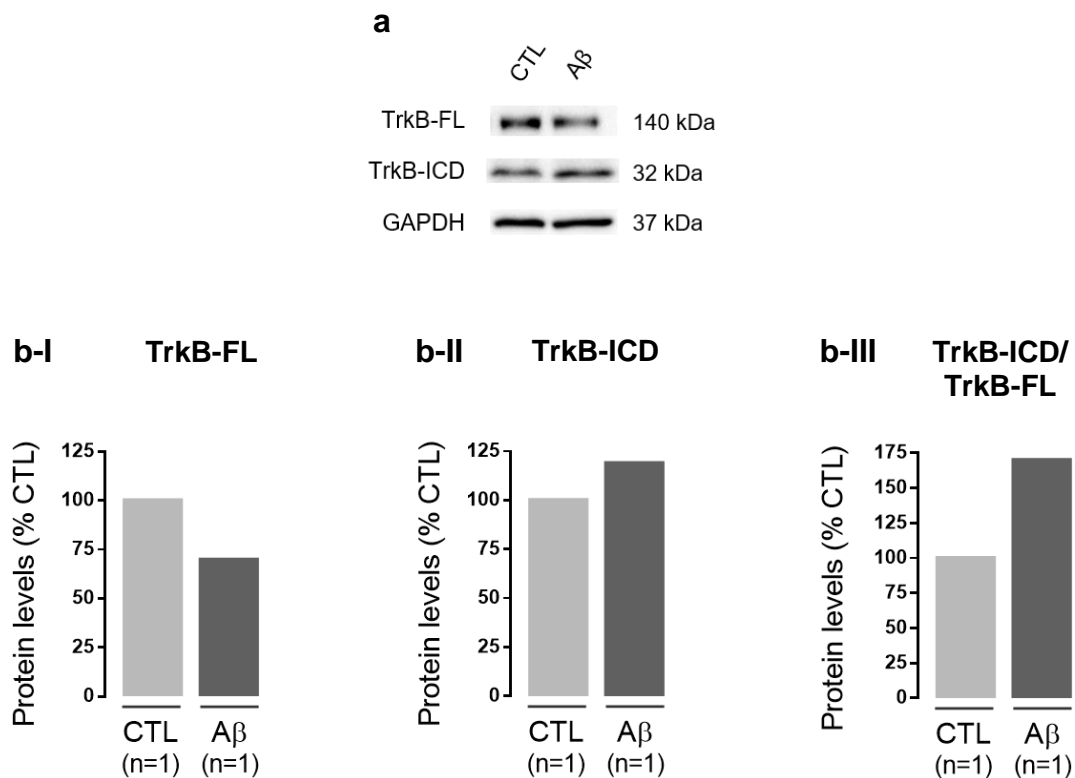


**Fig. 27 – TrkB receptor cleavage tends to be increased in primary neuronal cultures after incubation with A $\beta$ <sub>1-42</sub> peptide.** Representative western-blots in (a) depict immunoreactive bands for TrkB-FL (~140 kDa), TrkB-ICD (~32 kDa) and GAPDH (loading control; ~37 kDa) obtained from primary cortical neuronal culture samples incubated with an A $\beta$ <sub>1-42</sub> peptide solution (20  $\mu$ M, 24 h) at 14 DIV. Protein levels were quantified and normalized (100%) for control. Levels of TrkB-FL (b-I) tend to decrease, while levels of TrkB-ICD (b-II) tend to increase, in the sample incubated with A $\beta$  when comparing with the sample incubated with vehicle (CTL). This is emphasised by the tendency for an increase in the ratio TrkB-ICD/TrkB-FL (b-III) in the sample incubated with A $\beta$ . Preliminary data are presented as individual values (n=1).

Besides TrkB receptors, another protein that has been shown to be cleaved by calpains is  $\alpha$ -II Spectrin, giving rise to two spectrin breakdown products (SBDP) with 145 and 150 kDa. Detection of these fragments by WB can therefore be used as a measure of calpain activity<sup>152,189</sup>. The term SBDP150 was used herein when referring to both fragments, since sometimes it is not possible to obtain them in separate bands. Corroborating the tendency observed for increased TrkB-FL receptor cleavage, preliminary results showed an approximately 39% decrease in the levels of  $\alpha$ -II Spectrin in the A $\beta$ <sub>1-42</sub> treated culture (CTL: 100.0 %; A $\beta$ : 60.78 %; n=1; Fig. 28b-I), accompanied by an approximately 92% increase in the levels of SBDP150 (CTL: 100.0 %; A $\beta$ : 191.8 %; n=1; Fig. 28b-II). As for TrkB, these evidences were emphasised by the tendency for an increase of about 216% in the ratio between the levels of SBDP150 and  $\alpha$ -II Spectrin in the sample incubated with A $\beta$  (CTL: 100.0 %; A $\beta$ : 315.6 %; n=1; Fig. 28b-III).

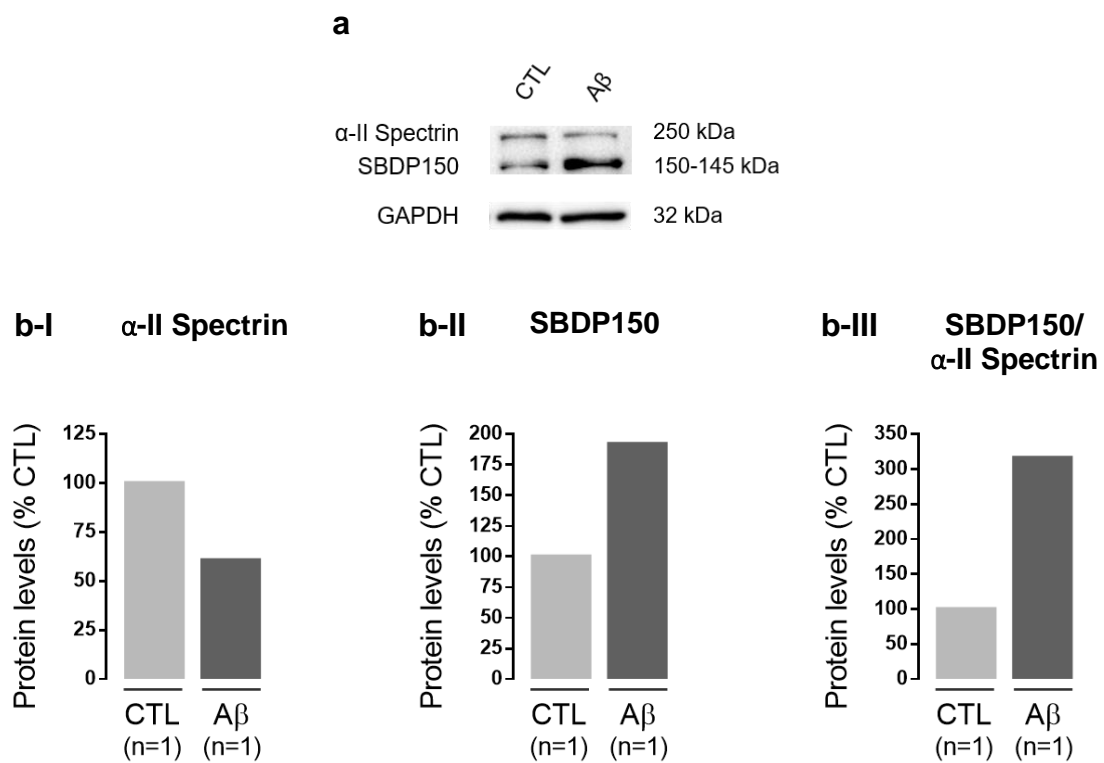


**Fig. 28 –  $\alpha$ -II Spectrin cleavage tends to be increased in primary neuronal cultures incubated with  $A\beta_{1-42}$  peptide, indicating increased calpain activity.** Representative western-blot images in (a) depict immunoreactive bands for  $\alpha$ -II Spectrin (~250 kDa), SBDP150 (~150-145 kDa) and GAPDH (loading control; ~37 kDa) obtained from primary cortical neuronal culture samples incubated with an  $A\beta_{1-42}$  peptide solution (20  $\mu$ M, 24 h) at 14 DIV. Protein levels were quantified and normalized (100%) for control. Levels of  $\alpha$ -II Spectrin (**b-I**) tend to decrease, while levels of SBDP150 (**b-II**) tend to increase, in the  $A\beta$  treated sample when comparing with the sample incubated with vehicle (CTL). As for TrkB, this is emphasised by the tendency for an increase in the ratio between the levels of SBDP150 and  $\alpha$ -II Spectrin (**b-III**) in the sample incubated with  $A\beta$ . Preliminary data are presented as individual values (n=1). SBDP150: Spectrin breakdown products at 150-145 kDa.

#### **4.2.4. Cell proliferation and neuronal differentiation in the DG after $A\beta_{1-42}$ icv injection**

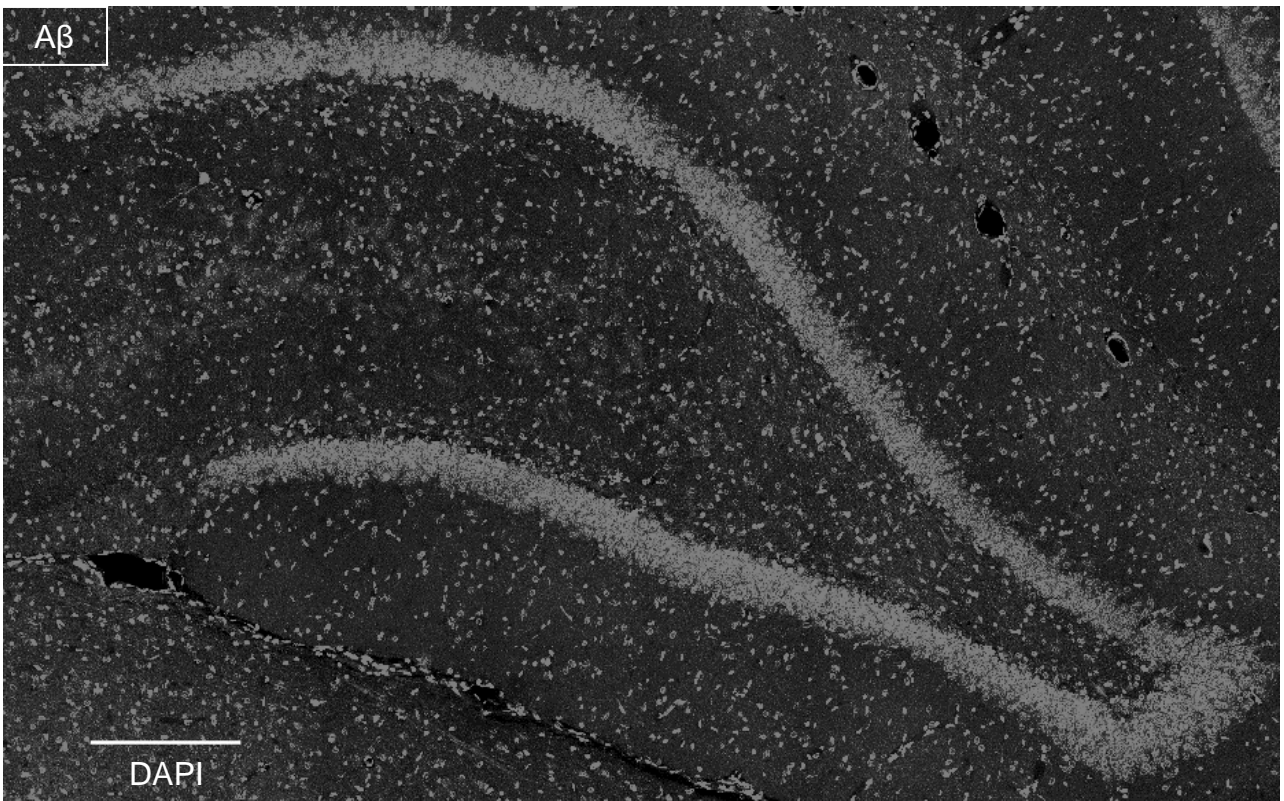
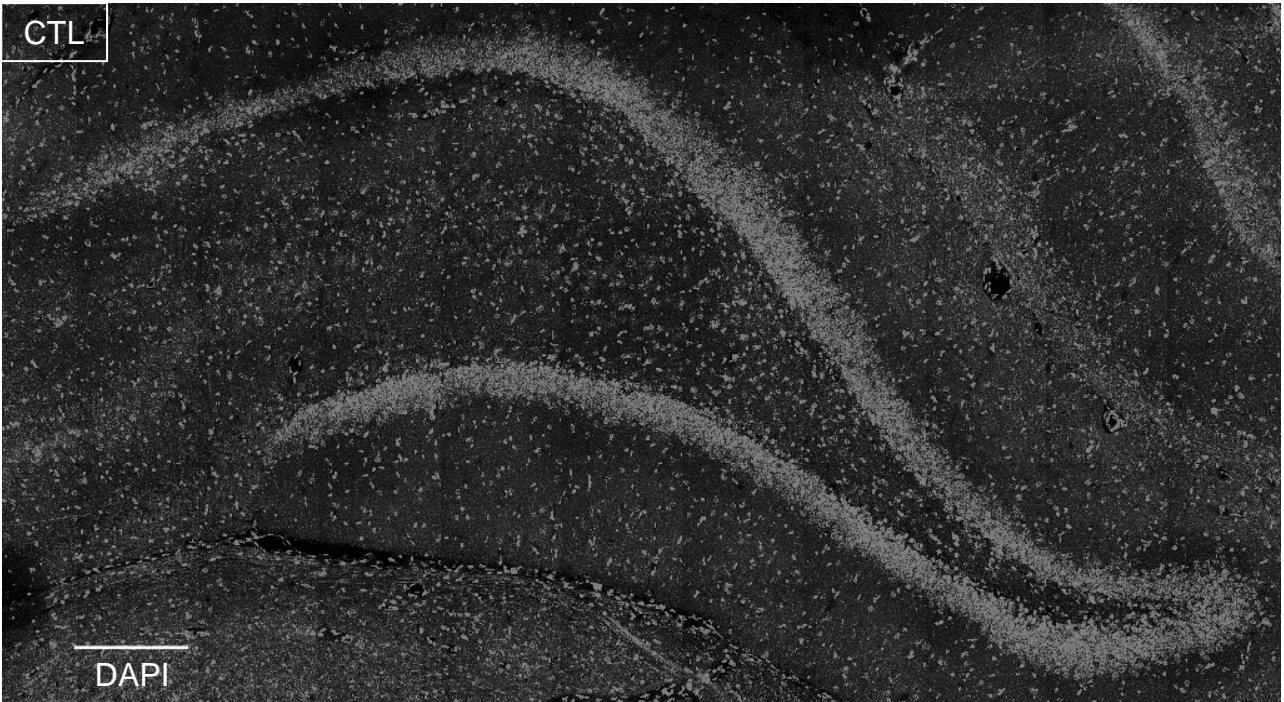
Regarding the effect mediated by  $A\beta$  in DG neurogenesis, two animal samples were analysed with discrepant results. Thus, in this section, results for each  $A\beta$  rat were individually described. To facilitate the interpretation of results, one animal was identified as  $A\beta$ I (black dot on the graphs), and the other as  $A\beta$ II (white dot on the graphs).

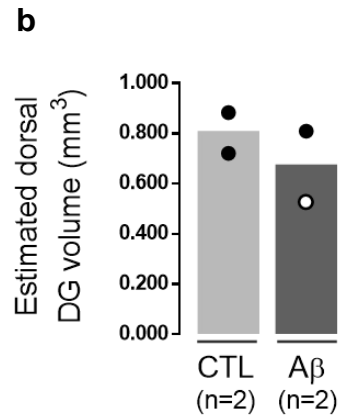
##### **4.2.4.1. Dorsal DG volume**

To determine if eventual changes in cell proliferation might be due to changes in the volume of the DG caused by the  $A\beta$  injection, the total dorsal DG volume was estimated from representative coronal sections (Fig. 29). While the volume estimated for  $A\beta$ I was similar to what was observed for controls,  $A\beta$ II showed a lower volume (CTL: 0.8023 mm<sup>3</sup>;  $A\beta$ I: 0.8094 mm<sup>3</sup>,  $A\beta$ II: 0.5266 mm<sup>3</sup>;  $A\beta$  (mean): 0.6680 mm<sup>3</sup>; n=2; Fig. 29b).



**a**

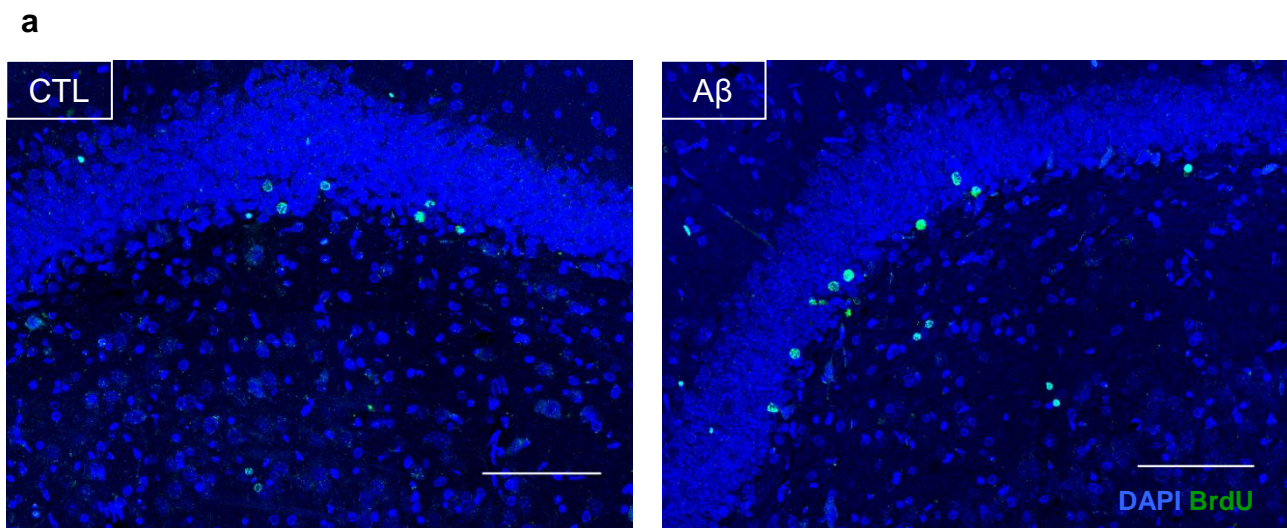




**Fig. 29 – Dorsal DG volume estimated from representative coronal sections.** Representative confocal images (a) show whole sections of the DG of control and A $\beta$  injected rats, where nuclei were immunostained with DAPI (light grey). Dorsal DG volume was estimated (b) by multiplying the sum of the areas by the distance between slices (400  $\mu$ m). Preliminary data are expressed as mean (n=2). Scale bar = 200  $\mu$ m. A $\beta$ I: black dot; A $\beta$ II: white dot.

#### 4.2.4.2. Cell proliferation

Since BrdU incorporates the DNA of dividing cells, quantification of BrdU-immuno-positive (BrdU<sup>+</sup>) cells within the layers of the dorsal DG was used as a measure of cell proliferation for the rats sacrificed at the end of the protocol, around 30 days after they were intraperitoneally injected with BrdU. The number of BrdU<sup>+</sup> cells appears to be identical when comparing the rats injected with vehicle with the ones injected with A $\beta$  (CTL: 101.3; A $\beta$ I: 107.5, A $\beta$ II: 104.0; A $\beta$  (mean): 105.8; n=2; Fig. 30b-I). Yet when we look at the cell density, that is, the number of BrdU<sup>+</sup> cells per volume, A $\beta$ I and A $\beta$ II show distinct results. Once again, cell density for A $\beta$ I and controls appears coincident, but when accounting for the lower volume of A $\beta$ II, cell density seems to be greater than for controls and A $\beta$ I (CTL: 1269 mm<sup>-3</sup>; A $\beta$ I: 1328 mm<sup>-3</sup>, A $\beta$ II: 1975 mm<sup>-3</sup>; A $\beta$  (mean): 1652 mm<sup>-3</sup>; n=2; Fig. 30b-II).



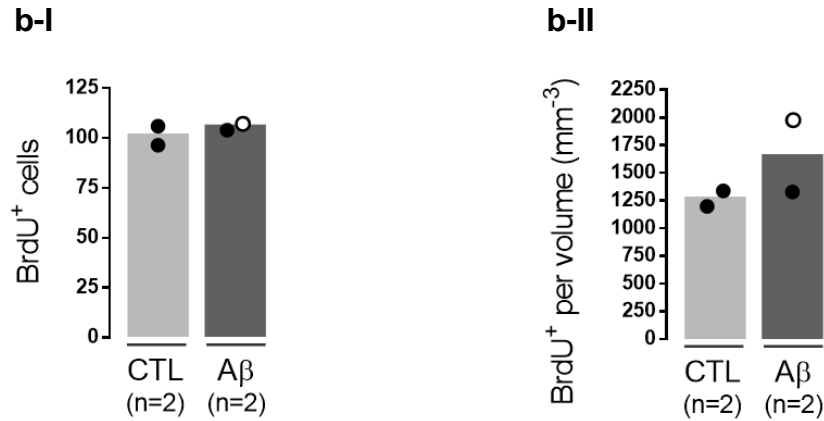


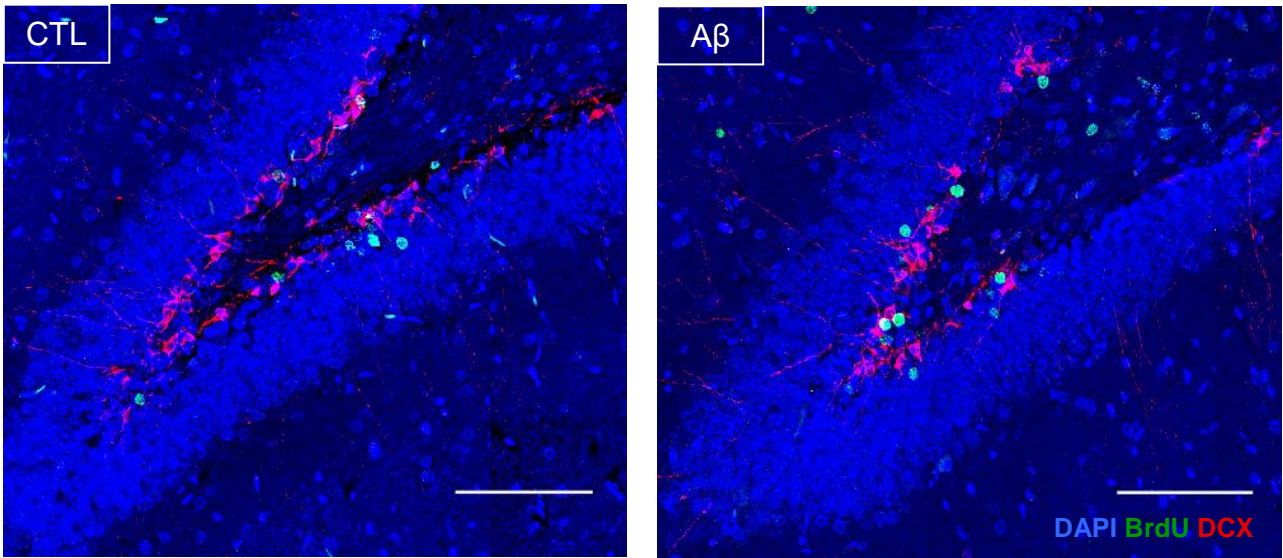
**Fig. 30 – Cell proliferation in the dorsal DG following Aβ icv injection.** Representative confocal images (a) of the DG for control and Aβ injected rats show nuclei immunostained with DAPI (blue), and BrdU (green). BrdU-immuno-positive cells (b-I) and BrdU-immuno-positive cells per volume of DG (b-II) were quantified. Preliminary data are expressed as mean (n=2). Scale bar = 100 μm. AβI: black dot; AβII: white dot.

#### 4.2.4.3. Neuronal differentiation

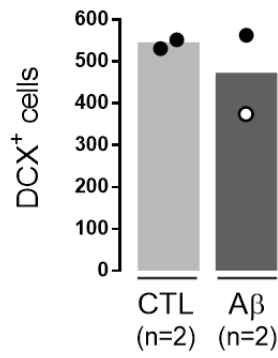
DCX is a microtubule-associated protein specifically expressed in the cytoplasm of neuroblasts and immature neurons during adult hippocampal neurogenesis<sup>190</sup>. Hence, quantification of DCX<sup>+</sup> cells in the dorsal DG was used to examine the presence of these types of cells at the end of the protocol, when the animals were sacrificed. Controls and AβI show comparable results regarding the total number of DCX<sup>+</sup> cells, whereas AβII seems to have a decrease in this parameter (CTL: 542.0; AβI: 563.0, AβII: 374.0; Aβ (mean): 469.0; n=2; Fig. 31b-I). When comparing cell density, that is, the number of DCX<sup>+</sup> cells per volume, we can see that it does not tend to change between the control animals and the Aβ (CTL: 6949 mm<sup>-3</sup>; AβI: 7103, AβII: 7122; Aβ (mean): 7113 mm<sup>-3</sup>; n=2; Fig. 31b-II), since contrary to BrdU density, the number of DCX<sup>+</sup> cells and volume decrease in AβII.

Cells that incorporated BrdU in the beginning of the protocol can be followed to evaluate immature neuron differentiation in rats that were injected with Aβ<sub>1-42</sub> when compared to controls. In fact, cells that differentiated into immature neurons can be denoted by looking at cells that are double-positive for BrdU and DCX (BrdU<sup>+</sup>DCX<sup>+</sup>). Preliminary data shows that the number of BrdU<sup>+</sup>DCX<sup>+</sup> cells for AβI tends to be greater than what was observed for controls, while AβII appears to be similar when comparing with controls (CTL: 7.00; AβI: 27.0, AβII: 10.0; Aβ (mean): 18.5; n=2; Fig. 31c-I). Considering the number of BrdU<sup>+</sup>DCX<sup>+</sup> cells per volume, a tendency for an increase in AβI and AβII can be noticed, although for AβI this increase is greater (CTL: 93.3 mm<sup>-3</sup>; AβI: 341 mm<sup>-3</sup>, AβII: 190 mm<sup>-3</sup>; Aβ (mean): 266 mm<sup>-3</sup>; n=2; Fig. 31c-II). The same trend as for the number of BrdU<sup>+</sup>DCX<sup>+</sup> cells is observed when we express it as the percentage from the total number of BrdU<sup>+</sup> cells (CTL: 7.08 %; AβI: 25.5 %, AβII: 9.09 %; Aβ (mean): 17.3 %; n=2; Fig. 31c-III).

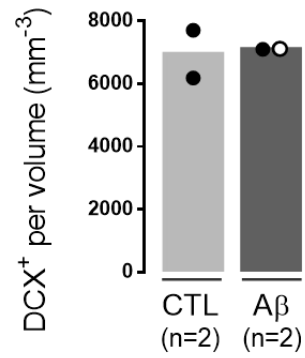
a



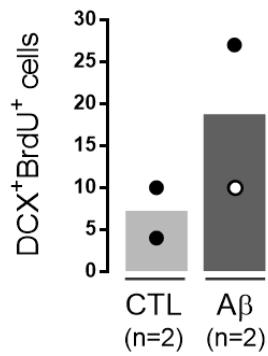
b-I



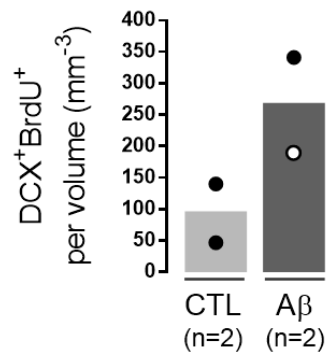
b-II



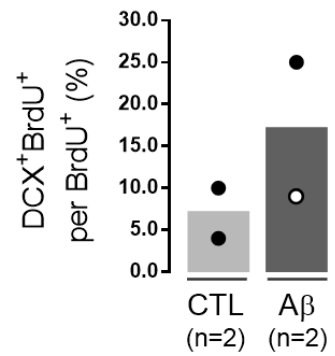
c-I



c-II

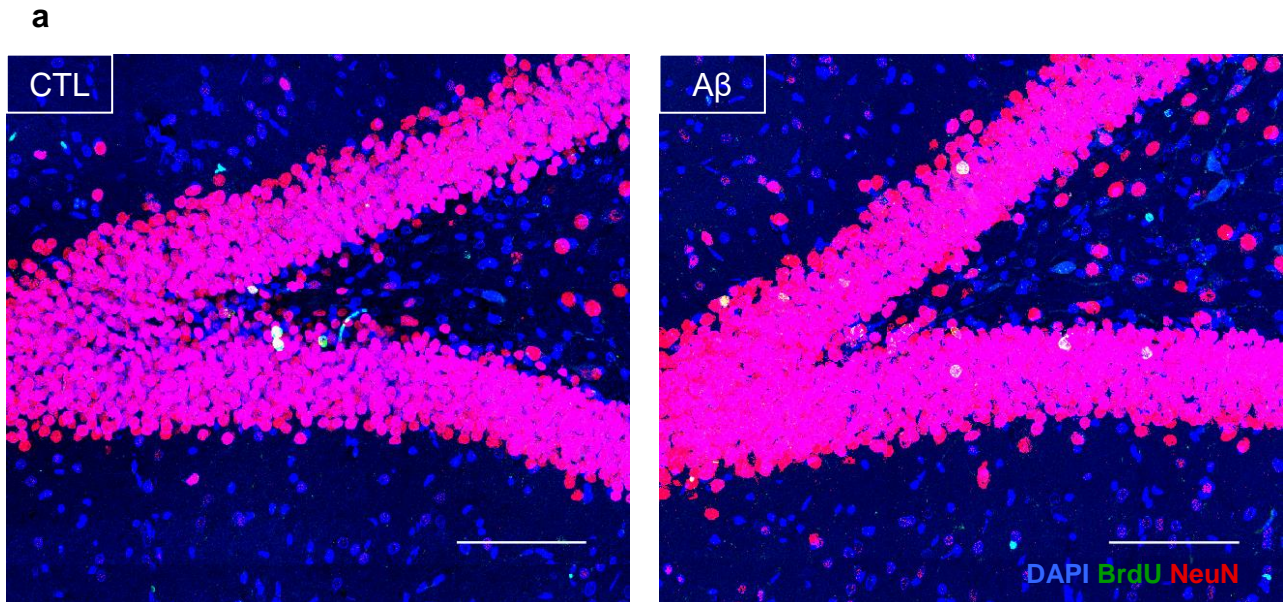


c-III



**Fig. 31 – Immature neuron differentiation after A $\beta$  injection.** Representative confocal images (a) of the dorsal DG for control and A $\beta$  injected rats show nuclei immunostained with DAPI (blue), nuclei stained with BrdU (green), and immature neurons immunostained for DCX (red). Quantitative analysis of DCX-immuno-positive cells (b-I), DCX-immuno-positive cells per volume (b-II), DCX/BrdU double-positive cells (c-I), DCX/BrdU double-positive cells per volume (c-II) and the percentage of DCX/BrdU double-positive cells from the total BrdU positive cells (c-III) were evaluated. Preliminary data are expressed as mean (n=2). Scale bar = 100  $\mu$ m. A $\beta$ I: black dot; A $\beta$ II: white dot; DCX: doublecortin.

To further analyse neuronal differentiation, cells were stained for NeuN, a neuronal nuclei protein marker expressed in mature neurons in the later stages of differentiation during adult hippocampal neurogenesis, alongside the fading of DCX expression<sup>191,192</sup>. Consequently, quantification of NeuN<sup>+</sup>BrdU<sup>+</sup> cells in the dorsal DG was used to assess mature neuron differentiation after A $\beta_{1-42}$  peptide injection, showing similar results when comparing with the controls (CTL: 89.00; A $\beta$ I: 102, A $\beta$ II: 88; A $\beta$  (mean): 95.00; n=2; Fig. 32b-I). On the other hand, the number of NeuN<sup>+</sup>BrdU<sup>+</sup> cells per volume seems to be greater for A $\beta$ II than for controls, while for A $\beta$ I appears to be unchanged (CTL: 1092 mm<sup>-3</sup>; A $\beta$ I: 1235, A $\beta$ II: 1666; A $\beta$  (mean): 1451 mm<sup>-3</sup>; n=2; Fig. 32b-II). Moreover, the percentage of NeuN<sup>+</sup>BrdU<sup>+</sup> cells per total BrdU<sup>+</sup> cells revealed no tendency to change for any of the rats injected with A $\beta$ , as compared with control rats (CTL: 86.4 %; A $\beta$ I: 93.6, A $\beta$ II: 89.8; A $\beta$  (mean): 91.7 %; n=2; Fig. 32b-III).



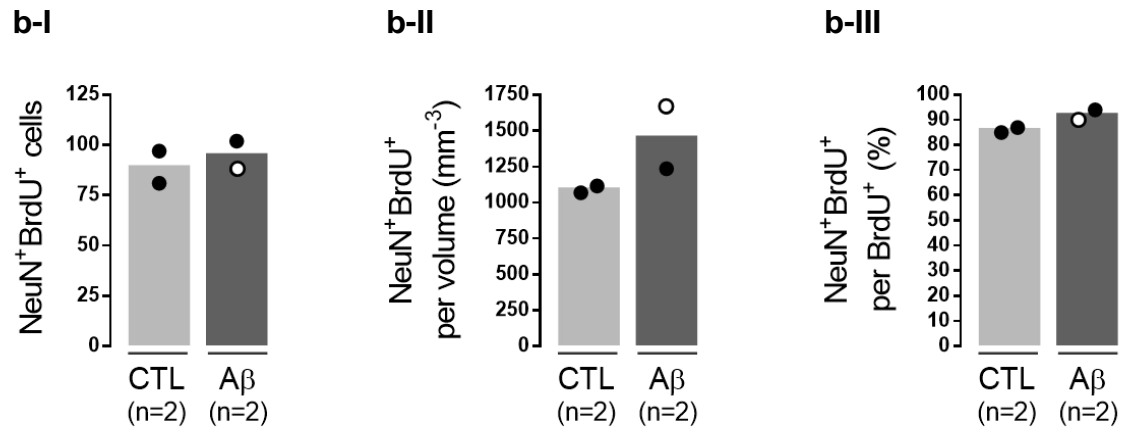


**Fig. 32 – Mature neuron differentiation in the dorsal DG after Aβ icv injection.** Representative confocal images (a) of the DG for control and Aβ injected rats show nuclei immunostained with DAPI (blue), with BrdU (green), and mature neurons immunostained for NeuN (red). Quantitative analysis of NeuN/BrdU double-positive cells (**b-I**), NeuN/BrdU double-positive cells per volume (**b-II**) and the percentage of NeuN/BrdU double-positive cells from the total BrdU positive cells (**b-III**) was assessed. Preliminary data are expressed as mean (n=2). Scale bar = 100 μm. AβI: black dot; AβII: white dot; NeuN: neuronal nuclei.

## 5. Discussion

The SGZ represents one of the main neurogenic niches in the adult brain, that has been increasingly revealed as a major player in learning and memory function. Yet how this process is modulated in association with neurodegenerative diseases like AD remains largely unclear, as do its consequences on cognitive function, especially in the sporadic form of the pathology. In the present work, potential alterations in neurogenesis in the DG of male Wistar rats were examined in a model of the sporadic form of AD.

According to previous studies, as well as previous work done at our institute using the same animal model, no significant differences were observed regarding locomotor and exploratory activity of the rats two weeks after they were injected with A $\beta$ <sup>157,181,182</sup>. Additionally, no changes in mean swimming velocity were observed during the acquisition phase of the MWM test. In fact, several studies using both rats and mice, report that impaired performance in cognitive tasks, including the MWM, was not associated with changes in locomotion or exploratory drive<sup>159,193</sup>. Importantly, the absence of alterations in motor function parallels the early stages of human sporadic AD, since these usually manifest only in more advanced stages of the disease<sup>10</sup>.

No changes in anxiety-related behaviour were expected, based on former experiments performed at our institute. However, this type of behaviour was assessed in the OF test, by measuring the time that the rats spent at the centre of the arena, where the lighting is more intense, and so tends to be avoided when the animals show increased anxiety<sup>182,194</sup>. Here, a more specific test for this kind of behaviour, the EPM, was used. We found no differences in the time spent in the open arms of the maze or in the number of entries in these arms, thus corroborating the previous results obtained with a distinct task. In line with this evidence, Colaianna and colleagues (2010), showed that soluble A $\beta$ <sub>1-42</sub> icv administration 7 days prior to testing, did not lead to significant changes in the EPM<sup>195</sup>. Notwithstanding, some studies report impaired performance in this test, namely in Wistar rats tested 20 days after the injection of soluble A $\beta$ <sub>1-42</sub>, and in Swiss albino mice tested 7 days after they were injected with aggregated forms of the peptide<sup>196,197</sup>. Nevertheless, differences in animal species used, in the timepoint for behaviour testing or in the preparation of the peptide solution might help explain the dissonant results.

Regarding the cognitive function tasks, the Y-Maze SA and FA tests were performed, aiming at evaluating short-term memory performance, since this type of memory is compromised in human AD, typically manifesting from early stages<sup>10</sup>. Contrary to what was expected, there were no changes in spontaneous alternation behaviour, indicating that the A $\beta$  injection did not affect spatial working memory performance. These results contradict what has been reported in previous studies following the same protocol as ours, in which impaired performance in the Y-Maze SA was observed<sup>157,181,182</sup>. Furthermore, comparable impairments have been demonstrated in albino mice injected with soluble A $\beta$ , and F344 rats injected with aggregated A $\beta$ , when tested after 4 and 16 days, respectively<sup>198,199</sup>.

Concerning the Y-Maze FA task, no differences were detected in the total number of arm entries in the training and test phases, or in the time spent inside the two identical arms available during training, suggesting that changes in cognitive performance could not be attributed to altered exploratory behaviour or preference for one of the identical arms. Curiously, A $\beta$ -injected rats were able to distinguish the novel arm in the test phase after an ITI of 3h, demonstrating no short-term reference memory impairment. Surprisingly, control rats were unable to distinguish the novel arm, despite showing a tendency, possibly suggesting a deleterious effect of the vehicle solution. Nonetheless, the high percentage of animals that first visited the novel arm, which was identical in the two experimental groups, might support the absence of cognitive impairment. To my knowledge, short-term memory performance using this test has not yet been evaluated in a model of sporadic AD induced by icv infusion of A $\beta_{1-42}$  peptide. However, the results obtained were unexpected, since this type of memory is impaired when assessed by different tasks in other models of AD. The injection of soluble or aggregated forms of A $\beta$  to either Wistar rats or albino mice, was shown to compromise short-term memory performance in the NOR test, even though with ITIs distinct from ours (30 and 90 min, respectively) <sup>157,197</sup>. In transgenic mice overexpressing APP, short-term memory impairment was observed using the Y-Maze FA task with an ITI of 5 or 30 min, yet this was not tested in early stages of the pathology, before plaque deposition <sup>169,200</sup>.

One of the most prominent features of human AD at early and mild stages is episodic memory impairment, with the inability to retain memory of recent events in a long-term fashion <sup>12</sup>. Hence, to further characterize our model, this type of memory was assessed in the NOR test with an ITI of 24h. The task was performed in two separate batches, one during the dark phase (night) of the light/dark cycle, under red light, and another during the light phase (day) under low intensity illumination. Similar to what was observed for the Y-Maze FA, when the NOR was performed at night, the rats injected with A $\beta$  were able to distinguish the novelty item, whereas the control ones were not, implying once again that the vehicle may have negatively influenced cognitive performance. Importantly, the novelty discrimination index did not significantly differ between the groups at night, thus supporting a comparable long-term memory impairment. On the other hand, long-term memory performance in both groups appears to be impaired, since neither the A $\beta$ -injected animals nor the control ones were able to recognize the novel object. Despite this, the novelty discrimination index was unchanged during daytime. In both phases of the light/dark cycle, the animals did not show alterations in exploratory drive or preference for any of the two identical objects during the training phase. Nonetheless, the fact that exploratory drive was compromised during the test phase, when it was performed during the day but not at night, might explain, at least in part, the differences in behaviour observed between the phases of the cycle. Another aspect that may have contributed to these differences is the fact that rodents are naturally more active at night, and so the differences between the groups may have become less evident during the day <sup>186,201</sup>. Previous reports using this model were mainly performed during the light phase of the cycle. In this regard, former work from



our group has demonstrated compromised long-term memory performance in the NOR, without any changes in exploratory activity <sup>182</sup>. Also using Wistar rats, other authors have reported memory impairment in the NOR (24 h ITI), when evaluated 2 h or 7 days after the infusion of soluble A $\beta$ , although the concentration used was lower (0.02 nmol), than the one used in the present work (2 nmol) <sup>202,203</sup>. Of note, a previous study showed a decrease in exploratory drive associated with no differences in cognitive performance, when assessing working memory in the NOR (3 min ITI) 7 days after icv injection <sup>195</sup>.

Due to the absence of cognitive impairments in the previously analysed tasks, it was hypothesized that diffusion of the peptide could specifically induce hippocampal-dependent spatial learning/memory impairment. Therefore, this type of memory was examined using the MWM test, since adequate performance in this task has been shown to be highly dependent, although not exclusively, on the integrity of the hippocampus <sup>183,204</sup>. Contrary to the literature, our results show no change in any of the parameters tested, revealing preserved spatial learning during the 4-day acquisition phase, as well as absent memory impairment in the probe test. Several studies focusing on analogous models of sporadic AD have addressed changes in performance in the MWM. Cheng and colleagues (2017), have recently described impaired learning throughout a 4-day acquisition phase, starting two weeks after the icv administration of soluble A $\beta$  in Wistar rats, but also decreased time and distance travelled in Qp during the probe test <sup>205</sup>. Likewise, F344 and Sprague-Dawley rats injected with aggregated forms of the peptide (2.2 nmol), that were evaluated 12 and 5 days afterwards, respectively, presented impaired learning during acquisition and compromised memory performance in the probe test, including increased time to reach the platform area, decreased number of crossings in this area, and decreased time in Qp <sup>159,199</sup>.

Different effects on cognition caused by distinct aggregation states of the peptide have been suggested, yet most studies do not assess the exact composition of the injected solutions, nor the amyloid burden in brain samples caused by this injection. As an example, a study using C57BL/6J mice has demonstrated that icv administration of A $\beta$ <sub>1-42</sub> in its monomeric, oligomeric or fibrillary form, leads to an impairment in long-term memory performance in the NOR, specifically triggered by oligomers, and not by other forms, supporting the notion that oligomeric A $\beta$ <sub>1-42</sub> constitutes the most neurotoxic form of the peptide <sup>26,206</sup>. In addition, although the amount of peptide injected was low (7.5 pmol/injection, one 2 h before training and another 2 h before the test phase), the impairment was observed sole in the day after the first injection, yet it was lost after 10 days, suggesting an acute effect of the peptide in this case <sup>206</sup>. Considering that no changes in cognitive function were observed two weeks after the A $\beta$ <sub>1-42</sub> icv injection using various tasks to assess different behavioural paradigms, we decided to investigate the presence of the peptide in different aggregation states.

In the case of our work, the peptide was prepared in an alkaline solution providing conditions for it to remain in its soluble, mostly monomeric, state <sup>207,208</sup>. After the injection, the peptide is expected to spontaneously form oligomers, as this is reported to occur at physiological pH <sup>209,210</sup>.

Moreover, previous studies have shown the presence of the peptide in the hippocampus of mice and rats after being icv-infused <sup>157,210,211</sup>. Canas and colleagues (2009) demonstrated the presence of A $\beta$ <sub>1-42</sub> monomers and oligomers by WB, as well as increased levels, by ELISA, in the hippocampus of Wistar rats 2 days after the injection (2 nmol) <sup>157</sup>. Although our results are still preliminary due to the reduced sample size and methodological limitations, contrary to what was anticipated, the levels of soluble A $\beta$ <sub>1-42</sub> in the DG do not tend to be changed at 3 or 14 days after the injection, as revealed by ELISA.

Furthermore, no deposition of insoluble amyloid was anticipated to occur in our samples, since A $\beta$  aggregates were absent in brain sections stained with Congo red and Thioflavin S, when using an identical of AD <sup>157</sup>. Indeed, no deposits were denoted in brain sections from rats sacrificed at 3 or 14 days after the injection, as assessed by Congo red staining. Despite these results, increased A $\beta$  deposits have been demonstrated in the hippocampus by IHC, namely in Sprague-Dawley rats, 12 days after the injection of oligomeric A $\beta$ <sub>1-42</sub>, even though the concentration used was considerably higher (1  $\mu$ mol) <sup>210</sup>.

Considering the hypothesis that the properties of the peptide, or peptide solution, could be altered, possibly due to unexpected degradation, we decided to examine one of the canonical mechanisms of A $\beta$ -induced toxicity associated with loss of BDNF neuroprotective actions, that has been well described in our group, both *in vivo* and *in vitro* <sup>151,152,212</sup>. Thus, the levels of TrkB-FL and TrkB-ICD receptors were measured, aiming at identifying whether the A $\beta$  was indeed functionally active. The levels of TrkB receptor isoforms remained unaltered in rats sacrificed at 3 and 14 days post- administration of A $\beta$ <sub>1-42</sub>, indicating that the cleavage of TrkB-FL receptors did not occur, contrary to what was expected if the A $\beta$  was functional. This was evidenced in the DG, but also in the SVZ, which is closer to the site of injection. In contrast, and in line with previous results, a likely increase in the cleavage of TrkB-FL receptors was revealed in the presence of A $\beta$ <sub>1-42</sub>, when incubating primary cortical neurons with the peptide solution prepared for injection <sup>151,152</sup>. Moreover, a probable increase in the cleavage of  $\alpha$ -II Spectrin and, consequently, calpain activation was observed, further corroborating what was obtained for TrkB receptors, as it was previously published <sup>151,152</sup>. Albeit the sample size for these measures needs to be increased, together, these results suggest that the function of the A $\beta$  peptide used in the icv injection seems to be intact, yet absent in brain samples.

Adult hippocampal neurogenesis is proposed to play a significant role in supporting hippocampal plasticity mechanisms and, subsequently, cognitive function dependent on this structure <sup>52,70,106</sup>. To evaluate if the A $\beta$  injection could have induced changes in neurogenesis, proliferation and differentiation in the DG were evaluated at the end of the protocol. Our findings regarding the dorsal DG volume of the two samples differ, being that A $\beta$ I seems to have no change in volume, while A $\beta$ II appears to show decreased volume. Although to my current knowledge, changes in the volume of the DG have not yet been assessed in this model, a decrease may be

expected, since hippocampal atrophy is present in preclinical stages of human AD, despite being more prominent in later stages<sup>213,214</sup>. Similar alterations can be observed in transgenic AD mouse models<sup>215</sup>. In fact, a causal link between A $\beta$  in the CSF and hippocampal atrophy leading to memory loss has been identified in patients with mild cognitive impairment<sup>216</sup>. Nonetheless, the possible contribution of experimenter's error to our results when obtaining the brain slices cannot be excluded at this point.

Regarding cell proliferation, although there seems to be a trend for an increase in A $\beta$ II when looking at cell density, the actual number of BrdU<sup>+</sup> cells is unaltered. Therefore, the tendency in both samples appears coincidental, showing no change in this parameter. On one hand, these findings go in line with the absence of molecular and behavioural changes, yet most published reports in animal models of AD and also in human samples indicate a reduction in proliferation<sup>106,107,117</sup>. Specifically using sporadic rodent models, it was shown that cell proliferation was decreased at the end of the protocol, approximately 20 days after bilateral intrahippocampal (CA region) infusion of soluble A $\beta$ <sub>1-42</sub> (0.9 or 1.8 nmol) in mice<sup>135,217</sup>. In these studies, proliferation was quantified either as cell density, using the minichromosome maintenance protein 2 (MCM2) proliferation marker, or as the number of BrdU<sup>+</sup> cells, yet neither referred to possible DG volume changes. Even though increased or unaltered proliferation has not yet been demonstrated in sporadic AD models, several transgenic models using a variety of protocols to assess neurogenesis have shown decreased, increased and even unchanged proliferation<sup>119,130-132</sup>. Notably, absent changes in cell proliferation in mice models harbouring APP, PS1 or both mutations, have been reported either before or after amyloid deposition occurred, when accounting for the number of cells or cell density (BrdU and Ki67 labelling)<sup>131,132</sup>. Again, eventual changes in volume were not considered in these works.

Distinct results were also observed between the two samples when referring to cell differentiation. While a tendency for an increase in neuroblast proliferation and immature neuron differentiation (BrdU<sup>+</sup>DCX<sup>+</sup>) can be denoted for A $\beta$ I, this was not associated with changes in the total number of neuroblasts and immature neurons (DCX<sup>+</sup>). Furthermore, the number of cells that differentiated into mature GCs (BrdU<sup>+</sup>NeuN<sup>+</sup>) from the beginning of the protocol appears unaltered in A $\beta$ I. These results may indicate that the new immature neurons did not survive on a long-term basis. Conversely, whereas there does not seem to be a change in neuroblast proliferation and immature neuron differentiation (BrdU<sup>+</sup>DCX<sup>+</sup>) for A $\beta$ II, a trend for a decrease in the total number of neuroblasts and immature neurons (DCX<sup>+</sup>), proportional to the decrease in volume was observed. Interestingly, as for A $\beta$ I, A $\beta$ II showed no tendency for a change in the number of cells that differentiated into mature GCs (BrdU<sup>+</sup>NeuN<sup>+</sup>). Although the total number of mature GCs alone was not quantified, a decrease in new neuron survival might be present. Similar to what is observed for proliferation, most authors point to a reduction in neuronal differentiation using various models of AD<sup>106,107,117</sup>. Contrary to our observations, reports using sporadic AD models show a decrease in neuroblasts/immature neurons, expressed as DCX<sup>+</sup> cell density, as well as a decrease in neuroblast

proliferation/immature neuron differentiation, expressed as BrdU<sup>+</sup>DCX<sup>+</sup> cell number, observed after soluble A $\beta$ <sub>1-42</sub> intrahippocampal injection<sup>135,217</sup>. In accordance with A $\beta$ I, but not A $\beta$ II, Jin et al (2004) showed an increase in BrdU<sup>+</sup>DCX<sup>+</sup> cells, although this was shown qualitatively and not by stereological analysis<sup>128</sup>. Curiously, co-expression of BrdU and NeuN has not only been shown to be increased and decreased, namely in APP/PS1 and APP/PS1/tau mice, respectively, but also unaltered in PS1 transgenic mice<sup>126,130,218</sup>.

Significantly, unaltered proliferation accompanied by impaired long-term survival of new neurons has been suggested in APP/PS1 mice with A $\beta$  deposition, even though no specific markers for neuronal death were used in this study<sup>132</sup>. Notwithstanding, it is important to mention that our results are only preliminary, and the number of samples analysed needs to be increased to determine whether some or all the observed tendencies would be further perpetuated or, on the contrary, dissipated. In addition, as published studies show a high variability of results and also methods, it is suggested that clearer conclusions on how neurogenesis is modulated in AD could be achieved by thoroughly comparing distinct rodent models using the same age, gender, genetic background, and identical methods of evaluating neurogenesis. Moreover, considering that changes in neurogenesis may be stage-dependent, characterization according to neuropathology stage is still necessary<sup>102,106</sup>.

Some methodological limitations must be taken into account when hypothesizing about the lack of behavioural and molecular/cellular changes. The possibility that precipitation of at least some amount of the A $\beta$  peptide may have occurred in the syringe before the injection cannot be ruled out. In fact, a white precipitate was present, on occasion, on the tip of the syringe, despite the use of two needles with different gauge size. If this is the case, a much lower and most likely variable amount of peptide would actually be administered to the ventricle of the rats, and reach target locations like the hippocampus, possibly in different aggregation states. Of note, low levels of soluble A $\beta$ <sub>1-42</sub> adding to the physiological concentrations, may be undetectable by ELISA. Besides these aspects, some degree of imprecision regarding the injection site can be associated with the method employed, and therefore may also contribute to a high variability in the presently described model.

Importantly, if the vehicle has a negative impact on cognition, then, uncompromised performance in A $\beta$  animals may have resulted from a balanced effect of the infusion of low amyloid amounts. Indeed, neuroprotective effects of A $\beta$ , especially in its nonfibrillar form, and in low concentrations, ranging mainly from pM to nM values that resemble basal levels of the peptide, have been described *in vitro* and *in vivo*, including noteworthy beneficial effects upon short- and long-term memory<sup>22,219</sup>. Furthermore, these A $\beta$ -related improvements can potentially be paralleled with increased neurogenesis denoted in studies using low concentrations of A $\beta$ <sup>115,116</sup>.

## 6. Conclusions and Future Perspectives

In the present work, the A $\beta$ <sub>1-42</sub> peptide icv injection did not impair spatial learning, nor short-term and long-term memory performance, evaluated two weeks after the injection. Additionally, we failed to identify the presence of soluble or deposited A $\beta$ <sub>1-42</sub> peptide in the brain samples from rats sacrificed at 3 and 14 days after the injection, either directly or indirectly. Despite this, preliminary results revealed the presence of an active peptide in the solution prepared for injection. Examination of cell proliferation and neuronal differentiation at the end of the protocol revealed a discrepancy between the two samples analysed.

Overall, albeit the injection of A $\beta$  described herein has been previously referred to as a feasible way of obtaining a model of sporadic AD, in the conditions of the present work, we were not able to observe the expected behavioural phenotype, or any associated cellular and molecular changes. Further experimental optimization is therefore required in the future, to obtain a model that thoroughly represents the initial stages of AD pathology.

The solubility of the A $\beta$  peptide in the vehicle solution should be assessed, as well as the structural composition of the amyloid species in solution, in terms of aggregation state. Moreover, preparation of a more uniform solution, made up mostly of oligomeric A $\beta$ <sub>1-42</sub>, may be considered for future studies, as previously described<sup>206</sup>. Characterization of the amyloid deposition pattern along several timepoints and on different brain structures could also be helpful for a better interpretation of eventual cognitive outcomes. Accordingly, behaviour tests may be performed at distinct timepoints after the injection, since transient changes in cognition could be occurring more acutely or later in the protocol.

To reduce the potential variability conferred by imprecision of the injection site, only the animals in which the desired coordinates of injection are verified upon brain dissection, should be included in upcoming studies. Importantly, to test the hypothesis of a deleterious effect of the vehicle solution, the behaviour tests should be repeated using vehicle controls plus negative controls, in which no solution would be injected.

Regarding both the molecular and cellular analyses, increasing the sample size will be essential to extract clearer conclusions pertaining to the validity of our model. Following methodological optimization, a correlation between eventual changes in neurogenesis and cognitive function, induced by the A $\beta$  injection, will hopefully be achievable. Of interest, cell proliferation should be further investigated using a more specific protocol of BrdU administration, only at the end of the protocol, and/or by resorting to other proliferation markers. In addition, although the consequences of icv administration of soluble or aggregated A $\beta$ <sub>1-42</sub> peptide on neurogenesis have not yet been characterized, previous reports have depicted alterations on hippocampal synaptic plasticity, namely associated with compromised function of dentate GCs, possibly due to A $\beta$ -induced morphological changes<sup>220,221</sup>. As these types of changes have been described in other models of AD like the

APPswe,ind and triple transgenic, examining possible changes in morphology in the presently described model, would be invaluable to fully characterize putative shifts in the process of neurogenesis<sup>126,139</sup>.

## 7. References

1. Hippus, H. & Neundörfer, G. The discovery of Alzheimer's disease. *Dialogues Clin. Neurosci.* **5**, 101–8 (2003).
2. WHO | Dementia. *WHO* (2017).
3. 2018 Alzheimer's disease facts and figures. *Alzheimer's Dement.* **14**, 367–429 (2018).
4. Prince, M. *et al.* World Alzheimer Report 2015: The Global Impact of Dementia - An analysis of prevalence, incidence, cost and trends. *Alzheimer's Dis. Int.* **84** (2015).
5. WHO | The top 10 causes of death. *WHO* (2017).
6. Beard, J. R., Officer, A. M. & Cassels, A. K. The world report on ageing and health. *Gerontologist* **56**, S163–S166 (2016).
7. Anderson, H. S. Alzheimer's Disease☆. in *Reference Module in Biomedical Sciences* (Elsevier, 2015).
8. Ballard, C. *et al.* Alzheimer's disease. *Lancet* **377**, 1019–31 (2011).
9. Castellani, R. J., Moreira, P. I., Zhu, X. & Perry, G. Alzheimer's Disease: Pathology and Pathogenesis. *Ref. Modul. Biomed. Sci.* 160–163 (2014).
10. Zabar, Y. Dementia: Mild Cognitive Impairment, Alzheimer's Disease, Lewy Body Dementia, Frontotemporal Lobar Dementia, Vascular Dementia. in *Netter's Neurology* (eds. Jones, H. R. *et al.*) 219–243 (Elsevier Saunders, 2012).
11. Förstl, H. & Kurz, A. Clinical features of Alzheimer's disease. *Eur. Arch. Psychiatry Clin. Neurosci.* **249**, 288–90 (1999).
12. Gold, C. A. & Budson, A. E. Memory loss in Alzheimer's disease: implications for development of therapeutics. *Expert Rev. Neurother.* **8**, 1879–91 (2008).
13. Huntley, J. D. & Howard, R. J. Working memory in early Alzheimer's disease: a neuropsychological review. *Int. J. Geriatr. Psychiatry* **25**, 121–132 (2010).
14. Mufson, E. J. *et al.* Molecular and cellular pathophysiology of preclinical Alzheimer's disease. *Behav. Brain Res. Mufson al. Behav. Brain Res.* **311**, 54–69 (2016).
15. Thal, D. R., Rüb, U., Orantes, M. & Braak, H. Phases of A beta-deposition in the human brain and its relevance for the development of AD. *Neurology* **58**, 1791–800 (2002).
16. Grothe, M. J. *et al.* In vivo staging of regional amyloid deposition. *Neurology* **89**, 2031–2038 (2017).
17. Braak, H. & Braak, E. Neuropathological staging of Alzheimer-related changes. *Acta Neuropathol.* **82**, 239–259 (1991).
18. Braak, H., Alafuzoff, I., Arzberger, T., Kretschmar, H. & Del Tredici, K. Staging of Alzheimer disease-associated neurofibrillary pathology using paraffin sections and immunocytochemistry. *Acta Neuropathol.* **112**, 389–404 (2006).
19. Ghiso, J., Tomidokoro, Y., Revesz, T., Frangione, B. & Rostagno, A. Cerebral amyloid

- angiopathy and Alzheimer's disease. *Hirosaki Igaku* **61**, S111–S124 (2010).
20. Hirano, A. Hirano bodies and related neuronal inclusions. *Neuropathol. Appl. Neurobiol.* **20**, 3–11 (1994).
  21. Funk, K. E., Mrak, R. E. & Kuret, J. Granulovacuolar degeneration (GVD) bodies of Alzheimer's disease (AD) resemble late-stage autophagic organelles. *Neuropathol. Appl. Neurobiol.* **37**, 295–306 (2011).
  22. Carrillo-Mora, P., Luna, R. & Colín-Barenque, L. Amyloid beta: multiple mechanisms of toxicity and only some protective effects? *Oxid. Med. Cell. Longev.* **2014**, 795375 (2014).
  23. Kumar, A., Singh, A. & Ekavali. A review on Alzheimer's disease pathophysiology and its management: an update. *Pharmacol. Reports* **67**, 195–203 (2015).
  24. Hardy, J. & Allsop, D. Amyloid deposition as the central event in the aetiology of Alzheimer's disease. *Trends Pharmacol. Sci.* **12**, 383–388 (1991).
  25. Cummings, J. L. Alzheimer's Disease. *N. Engl. J. Med.* **351**, 56–67 (2004).
  26. Mohamed, T., Shakeri, A. & Rao, P. P. N. Amyloid cascade in Alzheimer's disease: Recent advances in medicinal chemistry. *Eur. J. Med. Chem.* **113**, 258–272 (2016).
  27. Chow, V. W., Mattson, M. P., Wong, P. C. & Gleichmann, M. An overview of APP processing enzymes and products. *Neuromolecular Med.* **12**, 1–12 (2010).
  28. Murphy, M. P. & Levine, H. Alzheimer's disease and the amyloid- $\beta$  peptide. *J. Alzheimer's Dis.* **19**, 311–323 (2010).
  29. Barage, S. H. & Sonawane, K. D. Amyloid cascade hypothesis: Pathogenesis and therapeutic strategies in Alzheimer's disease. *Neuropeptides* **52**, 1–18 (2015).
  30. Kumar, K., Kumar, A., Keegan, R. M. & Deshmukh, R. Recent advances in the neurobiology and neuropharmacology of Alzheimer's disease. *Biomed. Pharmacother.* **98**, 297–307 (2018).
  31. Reitz, C. Alzheimer's disease and the amyloid cascade hypothesis: a critical review. *Int. J. Alzheimers. Dis.* **2012**, 369808 (2012).
  32. Bilousova, T. *et al.* Synaptic Amyloid- $\beta$  Oligomers Precede p-Tau and Differentiate High Pathology Control Cases. *Am. J. Pathol.* **186**, 185–98 (2016).
  33. Castellani, R. J. *et al.* Active glycation in neurofibrillary pathology of Alzheimer disease: N $\epsilon$ -(Carboxymethyl) lysine and hexitol-lysine. *Free Radic. Biol. Med.* **31**, 175–180 (2001).
  34. Lewczuk, P., Mroczko, B., Fagan, A. & Kornhuber, J. Biomarkers of Alzheimer's disease and mild cognitive impairment: A current perspective. *Adv. Med. Sci.* **60**, 76–82 (2015).
  35. Sheikh-Bahaei, N., Sajjadi, S. A. & Pierce, A. L. Current Role for Biomarkers in Clinical Diagnosis of Alzheimer Disease and Frontotemporal Dementia. *Curr. Treat. Options Neurol.* **19**, 46 (2017).
  36. Wurtman, R. Biomarkers in the diagnosis and management of Alzheimer's disease. *Metabolism* **64**, S47–S50 (2015).
  37. El Kadmiri, N., Said, N., Slassi, I., El Moutawakil, B. & Nadifi, S. Biomarkers for Alzheimer



- Disease: Classical and Novel Candidates' Review. *Neuroscience* **370**, 181–190 (2018).
38. Blennow, K. & Zetterberg, H. The Past and the Future of Alzheimer's Disease Fluid Biomarkers. *J. Alzheimer's Dis.* **62**, 1125–1140 (2018).
  39. Nakamura, A. *et al.* High performance plasma amyloid- $\beta$  biomarkers for Alzheimer's disease. *Nature* **554**, 249–254 (2018).
  40. Cummings, J., Lee, G., Mortsdorf, T., Ritter, A. & Zhong, K. Alzheimer's disease drug development pipeline: 2017. *Alzheimer's Dement. Transl. Res. Clin. Interv.* **3**, 367–384 (2017).
  41. Puzzo, D., Gulisano, W., Palmeri, A. & Arancio, O. Rodent models for Alzheimer's disease drug discovery. *Expert Opin. Drug Discov.* **10**, 703–711 (2015).
  42. Gallagher, M. & Rapp, P. R. The use of animal models to study the effects of aging on cognition. *Annu. Rev. Psychol.* **48**, 339–370 (1997).
  43. Newman, M. *et al.* Animal Models of Alzheimer's Disease. in *Animal Models for the Study of Human Disease* 1031–1085 (Elsevier, 2017).
  44. Prüßing, K., Voigt, A. & Schulz, J. B. *Drosophila melanogaster* as a model organism for Alzheimer's disease. *Mol. Neurodegener.* **8**, 35 (2013).
  45. Do Carmo, S. & Cuello, A. C. Modeling Alzheimer's disease in transgenic rats. *Mol. Neurodegener.* **8**, 37 (2013).
  46. Benedikz, E., Kloskowska, E. & Winblad, B. The rat as an animal model of Alzheimer's disease. *J. Cell. Mol. Med.* **13**, 1034–1042 (2009).
  47. Gibbs, R. A. *et al.* Genome sequence of the Brown Norway rat yields insights into mammalian evolution. *Nature* **428**, 493–521 (2004).
  48. Zhao, S. *et al.* Human, mouse, and rat genome large-scale rearrangements: stability versus speciation. *Genome Res.* **14**, 1851–60 (2004).
  49. Ellenbroek, B. & Youn, J. Rodent models in neuroscience research: is it a rat race? *Dis. Model. Mech.* **9**, 1079–1087 (2016).
  50. Winner, B., Kohl, Z. & Gage, F. H. Neurodegenerative disease and adult neurogenesis. *Eur. J. Neurosci.* **33**, 1139–1151 (2011).
  51. Lawlor, P. A. & Young, D. A $\beta$  Infusion and Related Models of Alzheimer Dementia. in *Animal Models of Dementia* 347–370 (Humana Press, 2011).
  52. Ming, G. li & Song, H. Adult Neurogenesis in the Mammalian Brain: Significant Answers and Significant Questions. *Neuron* **70**, 687–702 (2011).
  53. Hsieh, J. & Song, H. Adult Neurogenesis. in *Epigenetic Regulation in the Nervous System* 301–321 (Elsevier, 2013).
  54. Semple, B. D., Blomgren, K., Gimlin, K., Ferriero, D. M. & Noble-Haeusslein, L. J. Brain development in rodents and humans: Identifying benchmarks of maturation and vulnerability to injury across species. *Prog. Neurobiol.* **106–107**, 1–16 (2013).

55. Chapouton, P. & Godinho, L. Neurogenesis. in *The Zebrafish: Cellular and Developmental Biology, Part A* **100**, 72–126 (Academic Press, 2010).
56. Gibb, R. & Kovalchuk, A. Brain Development. in *The Neurobiology of Brain and Behavioral Development* 3–27 (Elsevier, 2018).
57. Andersen, S. L. Trajectories of brain development: point of vulnerability or window of opportunity? *Neurosci. Biobehav. Rev.* **27**, 3–18
58. Beattie, R., Mukhtar, T., Taylor, V. & Taylor, V. Fundamentals of Neurogenesis and Neural Stem Cell Development. in *Neural Surface Antigens* 1–13 (Elsevier, 2015).
59. Budday, S., Steinmann, P. & Kuhl, E. Physical biology of human brain development. *Front. Cell. Neurosci.* **9**, 257 (2015).
60. Jiang, X. & Nardelli, J. Cellular and molecular introduction to brain development. *Neurobiol. Dis.* **92**, 3–17 (2016).
61. Altman, J. & Das, G. D. Autoradiographic and histological evidence of postnatal hippocampal neurogenesis in rats. *J. Comp. Neurol.* **124**, 319–335 (1965).
62. Eriksson, P. S. *et al.* Neurogenesis in the adult human hippocampus. *Nat. Med.* **4**, 1313–1317 (1998).
63. Ngwenya, L. B., Heyworth, N. C., Shwe, Y., Moore, T. L. & Rosene, D. L. Age-related changes in dentate gyrus cell numbers, neurogenesis, and associations with cognitive impairments in the rhesus monkey. *Front. Syst. Neurosci.* **9**, 102 (2015).
64. Molina-Navarro, M. M. & García-Verdugo, J. M. Neurobiology. in *Adult Neurogenesis in the Hippocampus* 1–17 (Elsevier, 2016).
65. Sorrells, S. F. *et al.* Human hippocampal neurogenesis drops sharply in children to undetectable levels in adults. *Nature* **555**, 377–381 (2018).
66. Boldrini, M. *et al.* Human Hippocampal Neurogenesis Persists throughout Aging. *Cell Stem Cell* **22**, 589–599.e5 (2018).
67. Mathews, K. J. *et al.* Evidence for reduced neurogenesis in the aging human hippocampus despite stable stem cell markers. *Aging Cell* **16**, 1195–1199 (2017).
68. Lazarov, O. & Marr, R. A. Neurogenesis and Alzheimer’s disease: At the crossroads. *Exp. Neurol.* **223**, 267–281 (2010).
69. Urbán, N. & Guillemot, F. Neurogenesis in the embryonic and adult brain: same regulators, different roles. *Front. Cell. Neurosci.* **8**, 396 (2014).
70. Kempermann, G., Song, H. & Gage, F. H. Neurogenesis in the Adult Hippocampus. *Cold Spring Harb. Perspect. Biol.* **7**, a018812 (2015).
71. Braun, S. M. G. & Jessberger, S. Adult neurogenesis: mechanisms and functional significance. *Development* **141**, 1983–6 (2014).
72. Bergmann, O., Spalding, K. L. & Frisén, J. Adult Neurogenesis in Humans. *Cold Spring Harb. Perspect. Biol.* **7**, a018994 (2015).

73. Borsini, A., Zunszain, P. A., Thuret, S. & Pariante, C. M. The role of inflammatory cytokines as key modulators of neurogenesis. *Trends Neurosci.* **38**, 145–57 (2015).
74. Feliciano, D. M., Bordey, A. & Bonfanti, L. Noncanonical Sites of Adult Neurogenesis in the Mammalian Brain. *Cold Spring Harb. Perspect. Biol.* **7**, a018846 (2015).
75. Nualart, F. Unconventional Neurogenic Niches and Neurogenesis Modulation by Vitamins. *J. Stem Cell Res. Ther.* **4**, 2157–7633 (2014).
76. Fröhlich, F. Microcircuits of the Hippocampus. in *Network Neuroscience* 97–109 (Elsevier, 2016).
77. Toni, N. & Schinder, A. F. Maturation and Functional Integration of New Granule Cells into the Adult Hippocampus. *Cold Spring Harb. Perspect. Biol.* **8**, a018903 (2015).
78. Bartsch, T. & Butler, C. Transient amnesic syndromes. *Nat. Rev. Neurol.* **9**, 86–97 (2013).
79. Amaral, D. G., Scharfman, H. E. & Lavenex, P. The dentate gyrus: fundamental neuroanatomical organization (dentate gyrus for dummies). *Prog. Brain Res.* **163**, 3–22 (2007).
80. Spalding, K. L. *et al.* Dynamics of Hippocampal Neurogenesis in Adult Humans. *Cell* **153**, 1219–1227 (2013).
81. Jessberger, S., Aimone, J. B. & Gage, F. H. Neurogenesis. in *Learning and Memory: A Comprehensive Reference* 839–858 (Elsevier, 2008).
82. Bonaguidi, M. A. *et al.* Diversity of Neural Precursors in the Adult Mammalian Brain. *Cold Spring Harb. Perspect. Biol.* **8**, a018838 (2016).
83. Ehninger, D. & Kempermann, G. Neurogenesis in the adult hippocampus. *Cell Tissue Res.* **331**, 243–250 (2008).
84. Lie, D. C. & Jessberger, S. Cellular and Molecular Regulation. in *Adult Neurogenesis in the Hippocampus* 41–55 (Elsevier, 2016).
85. Overall, R. W., Walker, T. L., Fischer, T. J., Brandt, M. D. & Kempermann, G. Different Mechanisms Must Be Considered to Explain the Increase in Hippocampal Neural Precursor Cell Proliferation by Physical Activity. *Front. Neurosci.* **10**, 362 (2016).
86. Zhao, C., Deng, W. & Gage, F. H. Mechanisms and Functional Implications of Adult Neurogenesis. *Cell* **132**, 645–660 (2008).
87. Yau, S., Li, A. & So, K.-F. Involvement of Adult Hippocampal Neurogenesis in Learning and Forgetting. *Neural Plast.* **2015**, 1–13 (2015).
88. Bartsch, T. & Wulff, P. The hippocampus in aging and disease: From plasticity to vulnerability. *Neuroscience* **309**, 1–16 (2015).
89. Lazarov, O. & Hollands, C. Hippocampal neurogenesis: Learning to remember. *Prog. Neurobiol.* **138–140**, 1–18 (2016).
90. Spiers, H. J., Maguire, E. A. & Burgess, N. Hippocampal Amnesia. *Neurocase* **7**, 357–382 (2001).

91. Kesner, R. P. An analysis of dentate gyrus function (an update). *Behav. Brain Res.* (2017).
92. Kempermann, G. Adult Neurogenesis: An Evolutionary Perspective. *Cold Spring Harb. Perspect. Biol.* **8**, a018986 (2016).
93. Wu, M. V., Sahay, A., Duman, R. S. & Hen, R. Functional Differentiation of Adult-Born Neurons along the Septotemporal Axis of the Dentate Gyrus. *Cold Spring Harb. Perspect. Biol.* **7**, a018978 (2015).
94. Alves, N. D. *et al.* Chronic stress targets adult neurogenesis preferentially in the suprapyramidal blade of the rat dorsal dentate gyrus. *Brain Struct. Funct.* **223**, 415–428 (2018).
95. Scharfman, H. E., Sollas, A. L., Smith, K. L., Jackson, M. B. & Goodman, J. H. Structural and functional asymmetry in the normal and epileptic rat dentate gyrus. *J. Comp. Neurol.* **454**, 424–39 (2002).
96. Rangel, L. M. *et al.* Temporally selective contextual encoding in the dentate gyrus of the hippocampus. *Nat. Commun.* **5**, 3181 (2014).
97. Kheirbek, M. A., Tannenholz, L. & Hen, R. NR2B-Dependent Plasticity of Adult-Born Granule Cells is Necessary for Context Discrimination. *J. Neurosci.* **32**, 8696–8702 (2012).
98. Dupret, D. *et al.* Spatial Relational Memory Requires Hippocampal Adult Neurogenesis. *PLoS One* **3**, e1959 (2008).
99. Canales, J. J. *Adult neurogenesis in the hippocampus: health, psychopathology, and brain disease.* (Elsevier Inc., 2016).
100. Seib, D. R. M. & Martin-Villalba, A. Neurogenesis in the Normal Ageing Hippocampus: A Mini-Review. *Gerontology* **61**, 327–335 (2014).
101. Ernst, A. & Frisén, J. Adult Neurogenesis in Humans- Common and Unique Traits in Mammals. *PLOS Biol.* **13**, e1002045 (2015).
102. Winner, B. & Winkler, J. Adult neurogenesis in neurodegenerative diseases. *Cold Spring Harb. Perspect. Biol.* **7**, a021287 (2015).
103. Peng, L. & Bonaguidi, M. A. Function and Dysfunction of Adult Hippocampal Neurogenesis in Regeneration and Disease. *Am. J. Pathol.* **188**, 23–28 (2018).
104. Barulli, D. & Stern, Y. Efficiency, capacity, compensation, maintenance, plasticity: emerging concepts in cognitive reserve. *Trends Cogn. Sci.* **17**, 502–9 (2013).
105. Kempermann, G. The neurogenic reserve hypothesis: what is adult hippocampal neurogenesis good for? *Trends Neurosci.* **31**, 163–169 (2008).
106. Mu, Y. & Gage, F. H. Adult hippocampal neurogenesis and its role in Alzheimer's disease. *Mol. Neurodegener.* **6**, 85 (2011).
107. Martinez-Canabal, A. Reconsidering hippocampal neurogenesis in Alzheimer's disease. *Front. Neurosci.* **8**, 147 (2014).
108. Suh, J. *et al.* ADAM10 missense mutations potentiate  $\beta$ -amyloid accumulation by impairing

- prodomain chaperone function. *Neuron* **80**, 385–401 (2013).
109. Lazarov, O. & Demars, M. P. All in the Family: How the APPs Regulate Neurogenesis. *Front. Neurosci.* **6**, 81 (2012).
  110. Hollands, C., Bartolotti, N. & Lazarov, O. Alzheimer's Disease and Hippocampal Adult Neurogenesis; Exploring Shared Mechanisms. *Front. Neurosci.* **10**, 178 (2016).
  111. Ghosal, K., Stathopoulos, A. & Pimplikar, S. W. APP intracellular domain impairs adult neurogenesis in transgenic mice by inducing neuroinflammation. *PLoS One* **5**, e11866 (2010).
  112. Haughey, N. J. *et al.* Disruption of neurogenesis by amyloid b-peptide , and perturbed neural progenitor cell homeostasis , in models of Alzheimer's disease. *J. Neurochem.* **83**, 1509–1524 (2002).
  113. Gargantini, E. *et al.* Obestatin promotes proliferation and survival of adult hippocampal progenitors and reduces amyloid- $\beta$ -induced toxicity. *Mol. Cell. Endocrinol.* **422**, 18–30 (2016).
  114. He, N. *et al.* Amyloid- $\beta$ (1-42) oligomer accelerates senescence in adult hippocampal neural stem/progenitor cells via formylpeptide receptor 2. *Cell Death Dis.* **4**, e924 (2013).
  115. López-Toledano, M. A. & Shelanski, M. L. Neurogenic Effect of  $\beta$ -Amyloid Peptide in the Development of Neural Stem Cells. *J. Neurosci.* **24**, 5439–5444 (2004).
  116. Heo, C. *et al.* Effects of the monomeric, oligomeric, and fibrillar A $\beta$ 42 peptides on the proliferation and differentiation of adult neural stem cells from subventricular zone. *J. Neurochem.* **102**, 493–500 (2007).
  117. Chuang, T. T. Neurogenesis in mouse models of Alzheimer's disease. *Biochim. Biophys. Acta - Mol. Basis Dis.* **1802**, 872–880 (2010).
  118. Wen, P. H. *et al.* The presenilin-1 familial Alzheimer disease mutant P117L impairs neurogenesis in the hippocampus of adult mice. *Exp. Neurol.* **188**, 224–237 (2004).
  119. Choi, S. H. *et al.* Non-Cell-Autonomous Effects of Presenilin 1 Variants on Enrichment-Mediated Hippocampal Progenitor Cell Proliferation and Differentiation. *Neuron* **59**, 568–580 (2008).
  120. Krezymon, A. *et al.* Modifications of Hippocampal Circuits and Early Disruption of Adult Neurogenesis in the Tg2576 Mouse Model of Alzheimer's Disease. *PLoS One* **8**, e76497 (2013).
  121. Zeng, Q., Zheng, M., Zhang, T. & He, G. Hippocampal neurogenesis in the APP/PS1/nestin-GFP triple transgenic mouse model of Alzheimer's disease. *Neuroscience* **314**, 64–74 (2016).
  122. Hamilton, A. & Holscher, C. The effect of ageing on neurogenesis and oxidative stress in the APP<sup>swE</sup>/PS1<sup>deltaE9</sup> mouse model of Alzheimer's disease. *Brain Res.* **1449**, 83–93 (2012).
  123. Biscaro, B., Lindvall, O., Tesco, G., Ekdahl, C. T. & Nitsch, R. M. Inhibition of microglial activation protects hippocampal neurogenesis and improves cognitive deficits in a transgenic mouse model for Alzheimer's disease. *Neurodegener. Dis.* **9**, 187–98 (2012).
  124. Hollands, C. *et al.* Depletion of adult neurogenesis exacerbates cognitive deficits in

- Alzheimer's disease by compromising hippocampal inhibition. *Mol. Neurodegener.* **12**, 64 (2017).
125. Rodríguez, J. J. *et al.* Impaired Adult Neurogenesis in the Dentate Gyrus of a Triple Transgenic Mouse Model of Alzheimer's Disease. *PLoS One* **3**, e2935 (2008).
  126. Valero, J., Mastrella, G., Neiva, I., Sánchez, S. & Malva, J. O. Long-term effects of an acute and systemic administration of LPS on adult neurogenesis and spatial memory. *Front. Neurosci.* **8**, 83 (2014).
  127. Moon, M., Cha, M.-Y. & Mook-Jung, I. Impaired hippocampal neurogenesis and its enhancement with ghrelin in 5XFAD mice. *J. Alzheimers. Dis.* **41**, 233–41 (2014).
  128. Jin, K. *et al.* Enhanced neurogenesis in Alzheimer's disease transgenic (PDGF-APP<sup>Sw,Ind</sup>) mice. *Proc. Natl. Acad. Sci.* **101**, 13363–13367 (2004).
  129. López-Toledano, M. A. & Shelanski, M. L. Increased neurogenesis in young transgenic mice overexpressing human APP(Sw, Ind). *J. Alzheimers. Dis.* **12**, 229–40 (2007).
  130. Yu, Y. *et al.* Increased hippocampal neurogenesis in the progressive stage of Alzheimer's disease phenotype in an APP/PS1 double transgenic mouse model. *Hippocampus* **19**, 1247–1253 (2009).
  131. Yetman, M. J. & Jankowsky, J. L. Wild-type neural progenitors divide and differentiate normally in an amyloid-rich environment. *J. Neurosci.* **33**, 17335–41 (2013).
  132. Verret, L., Jankowsky, J. L., Xu, G. M., Borchelt, D. R. & Rampon, C. Alzheimer's-Type Amyloidosis in Transgenic Mice Impairs Survival of Newborn Neurons Derived from Adult Hippocampal Neurogenesis. *J. Neurosci.* **27**, 6771–6780 (2007).
  133. Wang, C. *et al.* Simvastatin prevents  $\beta$ -amyloid<sub>25–35</sub>-impaired neurogenesis in hippocampal dentate gyrus through  $\alpha$ 7nAChR-dependent cascading PI3K-Akt and increasing BDNF via reduction of farnesyl pyrophosphate. *Neuropharmacology* **97**, 122–132 (2015).
  134. Ramírez, E., Mendieta, L., Flores, G. & Limón, I. D. Neurogenesis and morphological-neural alterations closely related to amyloid  $\beta$ -peptide (25–35)-induced memory impairment in male rats. *Neuropeptides* **67**, 9–19 (2018).
  135. Zheng, M. *et al.* Intrahippocampal injection of A $\beta$ <sub>1–42</sub> inhibits neurogenesis and down-regulates IFN- $\gamma$  and NF- $\kappa$ B expression in hippocampus of adult mouse brain. *Amyloid* **20**, 13–20 (2013).
  136. Crews, L. *et al.* Increased BMP6 Levels in the Brains of Alzheimer's Disease Patients and APP Transgenic Mice Are Accompanied by Impaired Neurogenesis. *J. Neurosci.* **30**, 12252–12262 (2010).
  137. Jin, K. *et al.* Increased hippocampal neurogenesis in Alzheimer's disease. *Proc. Natl. Acad. Sci.* **101**, 343–347 (2004).
  138. Perry, E. K. *et al.* Neurogenic abnormalities in Alzheimer's disease differ between stages of neurogenesis and are partly related to cholinergic pathology. *Neurobiol. Dis.* **47**, 155 (2012).

139. Sun, B. *et al.* Imbalance between GABAergic and Glutamatergic Transmission Impairs Adult Neurogenesis in an Animal Model of Alzheimer's Disease. *Cell Stem Cell* **5**, 624–633 (2009).
140. Chen, Q. *et al.* Adult neurogenesis is functionally associated with AD-like neurodegeneration. *Neurobiol. Dis.* **29**, 316–326 (2008).
141. Unger, M. S. *et al.* Early Changes in Hippocampal Neurogenesis in Transgenic Mouse Models for Alzheimer's Disease. *Mol. Neurobiol.* **53**, 5796–5806 (2016).
142. Ekonomou, A. *et al.* Stage-specific changes in neurogenic and glial markers in Alzheimer's disease. *Biol. Psychiatry* **77**, 711–9 (2015).
143. Boekhoorn, K., Joels, M. & Lucassen, P. J. Increased proliferation reflects glial and vascular-associated changes, but not neurogenesis in the presenile Alzheimer hippocampus. *Neurobiol. Dis.* **24**, 1–14 (2006).
144. Ashe, K. H. Learning and Memory in Transgenic Mice Modeling Alzheimer's Disease. *Learn. Mem.* **8**, 301–308 (2001).
145. Verdurand, M. *et al.* Differential effects of amyloid-beta 1–40 and 1–42 fibrils on 5-HT<sub>1A</sub> serotonin receptors in rat brain. *Neurobiol. Aging* **40**, 11–21 (2016).
146. Ribeiro, F. F. *et al.* Axonal elongation and dendritic branching is enhanced by adenosine A<sub>2A</sub> receptors activation in cerebral cortical neurons. *Brain Struct. Funct.* **221**, 2777–2799 (2016).
147. Thiele, C. J., Li, Z. & McKee, A. E. On Trk - the TrkB signal transduction pathway is an increasingly important target in cancer biology. *Clin. Cancer Res.* **15**, 5962–5967 (2009).
148. Diógenes, M. J. *et al.* Enhancement of LTP in Aged Rats is Dependent on Endogenous BDNF. *Neuropsychopharmacology* **36**, 1823–1836 (2011).
149. Ribeiro, A. F. F. da C. Unveiling the trophic actions of adenosine A<sub>2A</sub> receptors in neurite outgrowth and postnatal neurogenesis : interaction with brain-derived neurotrophic factor. (2017).
150. Lewin, G. R. & Barde, Y.-A. Physiology of the Neurotrophins. *Annu. Rev. Neurosci.* **19**, 289–317 (1996).
151. Tanqueiro, S. R. *et al.* Inhibition of NMDA Receptors Prevents the Loss of BDNF Function Induced by Amyloid  $\beta$ . *Front. Pharmacol.* **9**, 237 (2018).
152. Jerónimo-Santos, A. *et al.* Dysregulation of TrkB Receptors and BDNF Function by Amyloid- $\beta$  Peptide is Mediated by Calpain. *Cereb. Cortex* **25**, 3107–3121 (2015).
153. Kemppainen, S. *et al.* Impaired TrkB receptor signaling contributes to memory impairment in APP/PS1 mice. *Neurobiol. Aging* **33**, 1122.e23-1122.e39 (2012).
154. Phillips, H. S. *et al.* BDNF mRNA is decreased in the hippocampus of individuals with Alzheimer's disease. *Neuron* **7**, 695–702 (1991).
155. Morrone, C. D., Thomason, L. A. M., Brown, M. E., Aubert, I. & McLaurin, J. Effects of Neurotrophic Support and Amyloid-Targeted Combined Therapy on Adult Hippocampal Neurogenesis in a Transgenic Model of Alzheimer's Disease. *PLoS One* **11**, e0165393

- (2016).
156. Jin, K., Xie, L., Mao, X. O. & Greenberg, D. A. Alzheimer's disease drugs promote neurogenesis. *Brain Res.* **1085**, 183–188 (2006).
  157. Canas, P. M. *et al.* Adenosine A2A receptor blockade prevents synaptotoxicity and memory dysfunction caused by beta-amyloid peptides via p38 mitogen-activated protein kinase pathway. *J. Neurosci.* **29**, 14741–14751 (2009).
  158. Taupin, P. BrdU immunohistochemistry for studying adult neurogenesis: Paradigms, pitfalls, limitations, and validation. *Brain Res. Rev.* **53**, 198–214 (2007).
  159. Zhang, L. *et al.* Brain-derived neurotrophic factor ameliorates learning deficits in a rat model of Alzheimer's disease induced by Ab1-42. *PLoS One* **10**, 1–14 (2015).
  160. Assi, H., Candolfi, M., Lowenstein, P. R. & Castro, M. G. Rodent Glioma Models: Intracranial Stereotactic Allografts and Xenografts. in *Animal Models of Brain Tumors. Neuromethods* **77**, 229–243 (Humana Press, Totowa, NJ, 2013).
  161. Paxinos, G. & Watson, C. *The Rat Brain in Stereotaxic Coordinates.* Academic Press (1998).
  162. Jacobs, G. H., Fenwick, J. A. & Williams, G. A. Cone-based vision of rats for ultraviolet and visible lights. *J. Exp. Biol.* **204**, 2439–46 (2001).
  163. Prut, L. & Belzung, C. The open field as a paradigm to measure the effects of drugs on anxiety-like behaviors: a review. *Eur. J. Pharmacol.* **463**, 3–33 (2003).
  164. Walf, A. A. & Frye, C. A. The use of the elevated plus maze as an assay of anxiety-related behavior in rodents. *Nat. Protoc.* **2**, 322–8 (2007).
  165. Y Maze Spontaneous Alternation Test. Available at: [http://sbfnl.stanford.edu/cs/bm/lm/bml\\_ymaze.html](http://sbfnl.stanford.edu/cs/bm/lm/bml_ymaze.html). (Accessed: 11th July 2016)
  166. Hughes, R. N. The value of spontaneous alternation behavior (SAB) as a test of retention in pharmacological investigations of memory. *Neurosci. Biobehav. Rev.* **28**, 497–505 (2004).
  167. Spellman, T. *et al.* Hippocampal–prefrontal input supports spatial encoding in working memory. *Nature* **522**, 309–314 (2015).
  168. Quillfeldt, J. A. Behavioral Methods to Study Learning and Memory in Rats. in *Rodent Model as Tools in Ethical Biomedical Research* 271–311 (Springer International Publishing, 2016).
  169. Wolf, A., Bauer, B., Abner, E. L., Ashkenazy-Frolinger, T. & Hartz, A. M. S. A Comprehensive Behavioral Test Battery to Assess Learning and Memory in 129S6/Tg2576 Mice. *PLoS One* **11**, e0147733 (2016).
  170. Batalha, V. L. *et al.* The caffeine-binding adenosine A2A receptor induces age-like HPA-axis dysfunction by targeting glucocorticoid receptor function. *Sci. Rep.* **6**, 31493 (2016).
  171. Tagliabata, G., Hogan, D., Zhang, W.-R. & Dineley, K. T. Intermediate- and long-term recognition memory deficits in Tg2576 mice are reversed with acute calcineurin inhibition. *Behav. Brain Res.* **200**, 95–99 (2009).
  172. Sousa, V. C. *et al.* Maternal separation impairs long term-potential in CA1-CA3 synapses



- and hippocampal-dependent memory in old rats. *Neurobiol. Aging* **35**, 1680–1685 (2014).
173. Gage, G. J., Kipke, D. R. & Shain, W. Whole Animal Perfusion Fixation for Rodents. *J. Vis. Exp.* e3564–e3564 (2012).
  174. Fanselow, M. S. & Dong, H.-W. Are the dorsal and ventral hippocampus functionally distinct structures? *Neuron* **65**, 7–19 (2010).
  175. Gilbert, P. E., Kesner, R. P. & Lee, I. Dissociating hippocampal subregions: A double dissociation between dentate gyrus and CA1. *Hippocampus* **11**, 626–636 (2001).
  176. Wu, C., Scott, J. & Shea, J.-E. Binding of Congo Red to Amyloid Protofibrils of the Alzheimer A $\beta$ 9–40 Peptide Probed by Molecular Dynamics Simulations. *BPJ* **103**, 550–557 (2012).
  177. Bennhold's Congo Red Staining Protocol for Amyloid. Available at: [http://www.ihcworld.com/\\_protocols/special\\_stains/congo\\_red\\_bennhold.htm](http://www.ihcworld.com/_protocols/special_stains/congo_red_bennhold.htm). (Accessed: 14th February 2018)
  178. Schindelin, J. *et al.* Fiji: an open-source platform for biological-image analysis. *Nat. Methods* **9**, 676–682 (2012).
  179. Four Parameter Logistic Curve - data analysis at MyAssays. Available at: <https://www.myassays.com/four-parameter-logistic-curve.assay>. (Accessed: 7th December 2017)
  180. GraphPad QuickCalcs: outlier calculator. Available at: <https://www.graphpad.com/quickcalcs/grubbs1/>. (Accessed: 15th April 2018)
  181. Cunha, G. M. A. *et al.* Adenosine A2A receptor blockade prevents memory dysfunction caused by  $\beta$ -amyloid peptides but not by scopolamine or MK-801. *Exp. Neurol.* **210**, 776–781 (2008).
  182. Martins, M. L. F. Neuroprotective action of a kyotorphin derivative in an animal model of Alzheimer's disease. (2016).
  183. Sousa, N., Almeida, O. F. X. & Wotjak, C. T. A hitchhiker's guide to behavioral analysis in laboratory rodents. *Genes, Brain Behav.* **5**, 5–24 (2006).
  184. Salomons, A. R., Arndt, S. S. & Ohl, F. Impact of anxiety profiles on cognitive performance in BALB/c and 129P2 mice. (2012).
  185. Pellow, S., Chopin, P., File, S. E. & Briley, M. Validation of open : closed arm entries in an elevated plus-maze as a measure of anxiety in the rat. *J. Neurosci. Methods* **14**, 149–167 (1985).
  186. Hånell, A., Marklund, N., Manahan-Vaughan, D. & Pamplona, F. A. Structured evaluation of rodent behavioral tests used in drug discovery research. (2014).
  187. Mouro, F. M. *et al.* Chronic and acute adenosine A2A receptor blockade prevents long-term episodic memory disruption caused by acute cannabinoid CB1 receptor activation. *Neuropharmacology* **117**, 316–327 (2017).
  188. Vorhees, C. V & Williams, M. T. Morris water maze: procedures for assessing spatial and

- related forms of learning and memory. *Nat. Protoc.* **1**, 848–858 (2006).
189. Weiss, E. S. *et al.* Alpha II-Spectrin Breakdown Products Serve as Novel Markers of Brain Injury Severity in a Canine Model of Hypothermic Circulatory Arrest. *Ann. Thorac. Surg.* **88**, 543–550 (2009).
  190. Couillard-Despres, S. *et al.* Doublecortin expression levels in adult brain reflect neurogenesis. *Eur. J. Neurosci.* **21**, 1–14 (2005).
  191. Mullen, R. J., Buck, C. R. & Smith, A. M. NeuN, a neuronal specific nuclear protein in vertebrates. *Development* **116**, 201–211 (1992).
  192. Brown, J. P. *et al.* Transient expression of doublecortin during adult neurogenesis. *J. Comp. Neurol.* **467**, 1–10 (2003).
  193. Zhang, R., He, Z., Jin, W. & Wang, R. Effects of the cannabinoid 1 receptor peptide ligands hemopressin, (m)RVD-hemopressin( $\alpha$ ) and (m)VD-hemopressin( $\alpha$ ) on memory in novel object and object location recognition tasks in normal young and A $\beta$ 1–42-treated mice. *Neurobiol. Learn. Mem.* **134**, 264–274 (2016).
  194. Jimenez, J. C. *et al.* Anxiety Cells in a Hippocampal-Hypothalamic Circuit. *Neuron* **97**, 670–683.e6 (2018).
  195. Colaianna, M. *et al.* Soluble beta amyloid(1-42): a critical player in producing behavioural and biochemical changes evoking depressive-related state? *Br. J. Pharmacol.* **159**, 1704–15 (2010).
  196. Hritcu, L. *et al.* Anxiolytic and antidepressant profile of the methanolic extract of Piper nigrum fruits in beta-amyloid (1-42) rat model of Alzheimer's disease. *Behav. Brain Funct.* **11**, 13 (2015).
  197. Souza, L. C. *et al.* Indoleamine-2,3-dioxygenase mediates neurobehavioral alterations induced by an intracerebroventricular injection of amyloid- $\beta$ 1-42 peptide in mice. *Brain. Behav. Immun.* **56**, 363–377 (2016).
  198. Cho, S. M. *et al.* Correlations of amyloid- $\beta$  concentrations between CSF and plasma in acute Alzheimer mouse model. *Sci. Rep.* **4**, (2014).
  199. Zhu, D. *et al.* M2 Macrophage Transplantation Ameliorates Cognitive Dysfunction in Amyloid- $\beta$ -Treated Rats Through Regulation of Microglial Polarization. *J. Alzheimer's Dis.* **52**, 483–495 (2016).
  200. Walker, J. M., Dixit, S., Saulsberry, A. C., May, J. M. & Harrison, F. E. Reversal of high fat diet-induced obesity improves glucose tolerance, inflammatory response,  $\beta$ -amyloid accumulation and cognitive decline in the APP/PSEN1 mouse model of Alzheimer's disease. *Neurobiol. Dis.* **100**, 87–98 (2017).
  201. Bertoglio, L. J. & Carobrez, A. P. Behavioral profile of rats submitted to session 1-session 2 in the elevated plus-maze during diurnal/nocturnal phases and under different illumination conditions. *Behav. Brain Res.* **132**, 135–143 (2002).

202. Tucci, P. *et al.* Memantine prevents memory consolidation failure induced by soluble beta amyloid in rats. *Front. Behav. Neurosci.* **8**, 332 (2014).
203. Mhillaj, E. *et al.* Celecoxib Prevents Cognitive Impairment and Neuroinflammation in Soluble Amyloid  $\beta$ -treated Rats. *Neuroscience* **372**, 58–73 (2018).
204. Clark, R. E., Broadbent, N. J. & Squire, L. R. Hippocampus and remote spatial memory in rats. *Hippocampus* **15**, 260–272 (2005).
205. Cheng, L. *et al.* A novel antibody targeting sequence 31-35 in amyloid  $\beta$  protein attenuates Alzheimer's disease-related neuronal damage. *Hippocampus* **27**, 122–133 (2017).
206. Balducci, C. *et al.* Synthetic amyloid-beta oligomers impair long-term memory independently of cellular prion protein. *Proc. Natl. Acad. Sci. U. S. A.* **107**, 2295–300 (2010).
207. Mold, M., Ouro-Gnao, L., Wieckowski, B. M. & Exley, C. Copper prevents amyloid- $\beta$ 1–42 from forming amyloid fibrils under near-physiological conditions in vitro. *Sci. Rep.* **3**, 1256 (2013).
208. Ryan, T. M. *et al.* Ammonium hydroxide treatment of A $\beta$  produces an aggregate free solution suitable for biophysical and cell culture characterization. *PeerJ* **1**, e73 (2013).
209. Stine, W. B., Jungbauer, L., Yu, C. & LaDu, M. J. Preparing Synthetic A $\beta$  in Different Aggregation States. in *Methods in molecular biology (Clifton, N.J.)* **670**, 13–32 (2010).
210. Zhang, Z. *et al.* Asiaticoside ameliorates  $\beta$ -amyloid-induced learning and memory deficits in rats by inhibiting mitochondrial apoptosis and reducing inflammatory factors. *Exp. Ther. Med.* **13**, 413–420 (2017).
211. Koh, E.-J. *et al.* Spirulina maxima Extract Ameliorates Learning and Memory Impairments via Inhibiting GSK-3 $\beta$  Phosphorylation Induced by Intracerebroventricular Injection of Amyloid- $\beta$  1–42 in Mice. *Int. J. Mol. Sci.* **18**, 2401 (2017).
212. Tanila, H. The role of BDNF in Alzheimer's disease. *Neurobiol. Dis.* **97**, 114–118 (2017).
213. Gordon, B. A. *et al.* Longitudinal  $\beta$ -Amyloid Deposition and Hippocampal Volume in Preclinical Alzheimer Disease and Suspected Non-Alzheimer Disease Pathophysiology. *JAMA Neurol.* **73**, 1192 (2016).
214. Csernansky, J. G. *et al.* Preclinical detection of Alzheimer's disease: hippocampal shape and volume predict dementia onset in the elderly. *Neuroimage* **25**, 783–792 (2005).
215. Breyhan, H. *et al.* APP/PS1KI bigenic mice develop early synaptic deficits and hippocampus atrophy. *Acta Neuropathol.* **117**, 677–685 (2009).
216. Fletcher, E. *et al.* Staging of amyloid  $\beta$ , t-tau, regional atrophy rates, and cognitive change in a nondemented cohort: Results of serial mediation analyses. *Alzheimer's Dement. Diagnosis, Assess. Dis. Monit.* (2018).
217. Sun, L., Qi, J. & Gao, R. Physical Exercise Reserved Amyloid-beta Induced Brain Dysfunctions by Regulating Hippocampal Neurogenesis and Inflammatory Response via MAPK Signaling. *Brain Res.* (2018).
218. Kiyota, T. *et al.* Presenilin-1 familial Alzheimer's disease mutation alters hippocampal

- neurogenesis and memory function in CCL2 null mice. *Brain. Behav. Immun.* **49**, 311–321 (2015).
219. Garcia-Osta, A. & Alberini, C. M. Amyloid beta mediates memory formation. *Learn. Mem.* **16**, 267–72 (2009).
220. S, B., M, A., G, M., A, A. & H, E. Effect of Aggregated  $\beta$ -Amyloid (1-42) on Synaptic Plasticity of Hippocampal Dentate Gyrus Granule Cells in Vivo. *BiolImpacts* **2**, 189–194 (2012).
221. Selkoe, D. J. Soluble oligomers of the amyloid  $\beta$ -protein impair synaptic plasticity and behavior. *Behav. Brain Res.* **192**, 106–113 (2008).